QUANTIFICATION AND MAPPING OF MANGANESE DEPOSITION AND ASSOCIATED HISTOPATHOLOGICAL CORRELATES IN THE LUNGS OF DECEASED MINEWORKERS IN SOUTH AFRICA

Julian Mthombeni

Supervisor: Prof. Gill Nelson, School of Public Health, Faculty of Health Sciences, University of the Witwatersrand, Johannesburg, South Africa

Co-Supervisor: Prof. Brad Racette, Barrow Neurological Institute, Phoenix, AZ, United States of America

Co-Supervisor: Dr Naseema Vorajee, Department of Histopathology, Lancet Laboratories, Johannesburg, South Africa

A Thesis submitted to the Faculty of Health Sciences, University of the Witwatersrand, Johannesburg, in fulfilment of the requirements for the degree of Doctor of Philosophy.

MARCH 2025

DECLARATION

I, Julian Qedizaba Mthombeni, declare that this thesis is my own, unaided work. It is being submitted for the Degree of Doctor of Philosophy at the University of the Witwatersrand, Johannesburg. It has not been submitted before for any degree or examination at any other university.

_____

Signature of candidate

30 September 2025 in Johannesburg

DEDICATION

I dedicate this work to my departed parents, who first introduced me to education. That first step allowed me to reach the highest level of education I could. Thank you for believing in my academic capacity, even though you did not see me getting my final qualification. I know you would have been proud of me.

I would like to thank the thousands of mineworkers in South Africa who have suffered from diseases due to exposure to mine dust while contributing to the economy of our country. Research into diseases caused by exposure to mining dust goes on.

To my family, thank you for your tireless support and love throughout my academic journey. I know I have taken a lot of your precious time that was supposed to be spent with you. I love you!

ABSTRACT

Background

Occupational manganese exposure is a known health risk for mineworkers in South Africa, where inhalation of manganese dust may lead to neurological health effects. Manganese is a widely used industrial metal, with South Africa being a major global supplier. Many mineworkers in South Africa are chronically exposed to manganese-containing dust through occupational activities. While the neurotoxic effects of manganese are well established, its respiratory impacts remain poorly understood. This study aimed to address the gap by quantifying and mapping manganese deposition in lung tissues, assessing related histopathological differences, and examining their correlation with manganese deposition findings in the brains of deceased mineworkers in South Africa, thereby providing insights into the effects of manganese exposure.

Methods

This cross-sectional study included 16 manganese-exposed mine workers who had worked in mines in the Northern Cape province and 48 platinum (manganese-unexposed mine workers from the Northwest province of South Africa. The data sources were the National Institute for Occupational Health's Pathology Automation (PATHAUT) database and Medical Bureau for Occupational Diseases (MBOD) records. Primary data collection involved quantifying manganese concentrations and assessing lung tissue, as well as histopathology and neuropathology databases. Manganese concentrations in the lungs were measured using Multi Collector Inductively Coupled Plasma Mass Spectrometry (MC-ICP-MS). Histopathological analysis used H&E, MT, PAS, and Reticulin stains. The correlation between lung and brain manganese deposition was analysed. Descriptive statistics were used to summarize manganese concentrations. Correlation analyses, including t-tests, Analysis of Variance, Tukey's Post Hoc test, Pearson correlation coefficient (r) test, Locally Weighted Scatterplot Smoothing (LOWESS), Linear Regression Model, and Generalized Additive Model (GAM) tests were conducted to assess the relationship between manganese levels in the lungs and brain tissues.

Results

All lung tissues showed detectable levels of manganese, confirming chronic inhalational exposure among the study participants. Mapping of manganese deposition revealed non-uniform distributions, with increased concentrations in the upper and lower lobe regions of the lungs, areas that are anatomically predisposed to particle deposition due to lower perfusion and clearance. Histopathological evaluation did not reveal any specific inflammation or fibrosis attributable to manganese exposure, although several samples exhibited pathology related to pneumonia or infectious diseases. Many samples were poorly preserved, which limited the ability to fully interpret subtle histological differences. Correlation analyses showed no significant relationship between manganese concentrations in the lung and brain tissues, suggesting that manganese retention in these organs may be influenced by distinct uptake mechanisms, individual metabolic variability, and duration since last exposure.

Conclusion

These study findings provide novel evidence of manganese accumulation and anatomical deposition patterns in the lungs of deceased mineworkers in South Africa, but there were no histopathological differences specifically linked to manganese. The lack of a significant association supports the null hypothesis and underscores the complex, non-linear toxicokinetics of manganese, suggesting that its distribution is influenced by factors beyond direct occupational exposure.

ACKNOWLEDGEMENTS

I first thank God Almighty for seeing me through all the health challenges I have had throughout my academic life.

I would like to express my sincere appreciation to my supervisors, Prof. Gill Nelson, Prof. Brad Racette, and Dr. Naseema Vorajee, who guided me through the challenging times of my studies. Thank you for your patience and guidance, which contributed to the completion of my thesis.

I extend my sincere gratitude to Prof Jill Murray, the retired head of the Pathology Division of the National Institute for Occupational Health (NIOH), for believing in me. Your encouragement to do my best and excel has paid off. I also thank individual members of the Pathology Division who collect and record the PATHAUT data, which made my study possible. A special thank you to Dr. Lakhoo, who committed herself to professionally assisting me with the pathology objective of my PhD.

Selby Nzou, your loving support has pushed me to break boundaries and reach this far. Ngiyabonga, Gatsheni! To my mentor, Prof. Pilani Nkomozepi, thank you for your guidance and encouragement throughout my research journey. Dr Aminat Olutoyin Adelowotan, you are a mother indeed! Your encouraging words will remain in my ears as long as I live.

My colleagues, Dr. Sumayya Mieta, thank you for holding the department together during my sabbatical leave to complete my lab work. Winnie Kruger, Kapila Bhowan, Brendon Roets, and Bokang Mabece, your support is truly magnificent. To my lab team, Mandla Sibiya, Christevie Mbuyu, Rosy Nxumalo, Cecil Nlandu, and Francina Mokatse, you are just amazing!

Lastly, this work might never have been completed without unconditional love, constant encouragement, and support from my children, Luanda, Danielle, Daniella, and Thando; my sisters, Jabu, Ntathu, Zah, and Fio; ngiyabonga angiqedi. Izandla zedlula ikhanda maKhabazela! I thank you all for walking this journey with me.

TABLE OF CONTENTS

LIST OF FIGURES

LIST OF TABLES

LIST OF ANNEXURES

LIST OF ACRONYMS

ANOVA	Analysis of Variance
BBB	Blood-Brain-Barrier
CCOD	Compensation Commissioner for Occupational Diseases
CRP	C-Reactive Protein
DMT1	**D**ivalent Metal Transporter 1
GAM	Generalized Additive Model
FNEC	Fibrosis Non-Evaluable Cases
H&E	Hematoxylin and Eosin stains
JPEG	Joint Photographic Experts Group
MC-ICP-MS	Multi Collector Inductively Coupled Plasma–Mass Spectrometry
mg/Kg	Milligram per Kilogram
Mn	Manganese
INEC	Inflammation Non-Evaluable Cases
Ki 67	Kiel 67
LOWESS	Locally Weighted Scatterplot Smoothing
MBOD	Medical Bureau for Occupational Diseases
MT	Masson Trichrome stain
ODMWA	Occupational Diseases in Mines and Works Act, 1973
NIOH	National Institute for Occupational Health
PAS	Periodic Acid-Schiff stain
TIBC	Total Iron-Binding Capacity
µg/L	micrograms per liter

LIST OF DEFINITIONS

AUTOPSY: A pathological examination of cardio-respiratory organs

CARDIO-RESPIRATORY ORGANS	Lungs and heart
COMPENSABLE DISEASES	Occupational lung diseases that are compensable under ODMWA, 1973, e.g., silicosis, pulmonary tuberculosis, lung cancer, obstructive lung disease, emphysema, pleural plaques, mesothelioma, or combinations of the above are all compensable diseases
MINEWORKER	A person who works or has worked in a mine
NON-MANGANESE MINER	For this study, non-manganese miners are platinum miners without a history of working in manganese mines
PATHAUT	Pathology Automation System (a database that contains demographic and pathology data of deceased mineworkers
SPECIMEN STORAGE	A collection of cardiorespiratory organs retained from autopsies of deceased mineworkers
SPIROMETRY	A tool to measure the entire volume of air expelled from a full lung (total lung capacity [TLC]) to peak expiration (residual volume [RV]) to evaluate the integrated mechanical performance of the lung, chest wall, respiratory muscles, and airways

CHAPTER ONE – INTRODUCTION

1.1 Background

South Africa is a mineral-rich country with approximately 80% of the world's known high-grade manganese ore, which originates from the rich Kalahari basin of the Northern Cape Province (1) forming the Kalahari manganese belt. Mining in South Africa started in the 1800s with the discovery of gold in what is now Johannesburg, and grew exponentially with discoveries of other mineral deposits, including manganese. Manganese prospecting started in 1922, with the first recorded sale of ore in 1927 (2).

The Northern Cape province is the largest province in South Africa and contains one of the world's largest and highest-grade manganese deposits in the world (3). The province borders Namibia on the northwest and Botswana on the northern boundary as shown in Fig. 1. South Africa has 22 manganese mines: 18 in the Northern Cape province and four in the Northwest, Mpumalanga, and Western Cape provinces (4). The three major current players in manganese production in South Africa are South32, Jupiter Mines, and Assmang. South32, registered on the Australian Securities Exchange with secondary listings on the Johannesburg Stock Exchange and the London market, owns manganese mines in Australia and operates two significant sites (Mamatwan and Wessels mines) situated in the Northern Cape province (1, 4).

Figure 1. *Map of South Africa showing the Northern Cape province*

Source: Map Data@2024 AfriGIS Ltd and The Kalahari Manganese field blog (2017).

South Africa has a wide distribution of manganese deposits, as depicted in the geological deposits map in Figure 2. The locations of some of the top manganese-producing mines (historically and currently active) in the Northern Cape province are shown in Figure 2. The major determinant of the distribution of these mines is the Kalahari basin geology of the area. The basin is a plate-like folded geological structure that has thrust onto the existing geological surface, exposing the seams containing manganese. The fault thrust is aligned in a north-to-south direction. The mines are located along the thrust and within the fold next to the thrust.

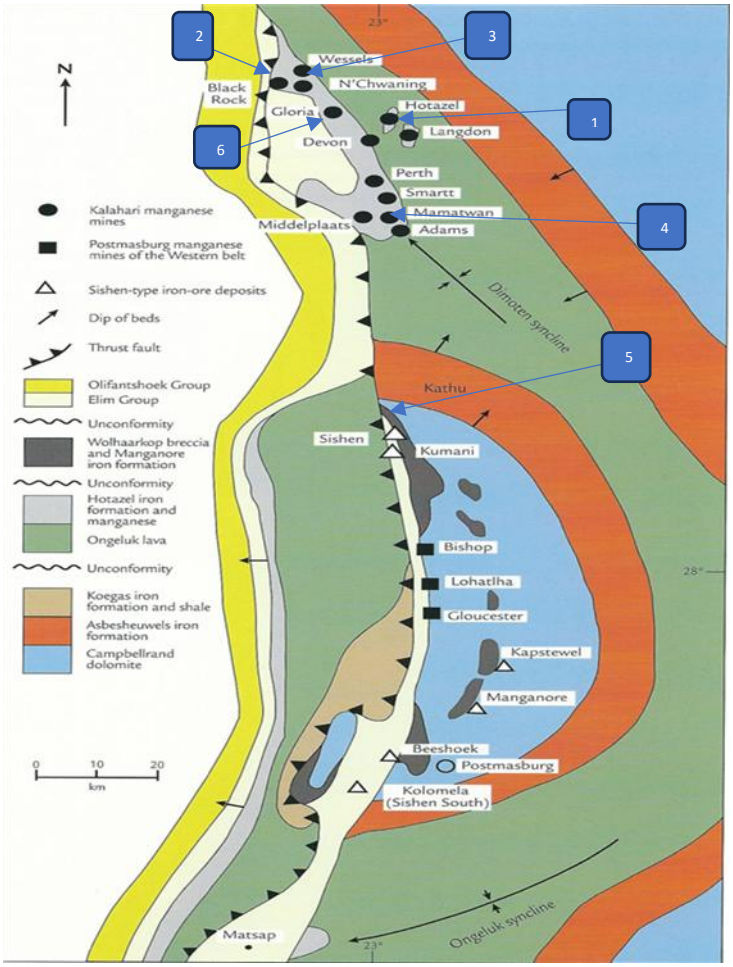

Figure 2. *The Map of Kalahari Basin and the North-South thrust*

Source: The Kalahari Manganese field blog (2017)

1.1.1 The Kalahari manganese field

The Kalahari manganese field is the most significant manganese-producing area in South Africa and the world. The Northern Cape province has several large high-production manganese mines and numerous smaller operations. Major mines in this field include Tshipi Borwa Mine, Mamatwan Mine, Nchwaning Mine, Wessels Mine, and Gloria Mine (5). Other significant current players in the Kalahari manganese field are United Manganese of Kalahari mines (UKM), Kalagadi Manganese, and Kudumane Manganese Resources (KMR), which contribute substantially to the local economy and the global manganese market. A brief bibliography of these leading players in manganese production is presented below:

Tshipi Borwa Mine

Tshipi Borwa is a mine located near Kathu, a small town in the Northern Cape province. The mine is run and owned by Tshipi é Ntle Manganese Mining. Tshipi Borwa's equity is owned by three prominent entities: Ntsimbintle Mining Proprietary Limited, South Africa's foremost black-owned manganese investment holding company; Jupiter Mines Limited, and Ore and Metals Holdings Limited (OM's official name) (6). The mine was established in 2011 and began production in 2012. It quickly became one of the largest manganese mines in South Africa, known for its high-grade manganese ore deposits and modern mining techniques (7). This mine had approximately 100 employees in 2024 (6).

Mamatwan Mine

The Mamatwan Mine, an open-pit operation managed by South32, is known for producing large volumes of manganese ore. It is situated near the town of Hotazel and forms part of the Hotazel Manganese Mines (HMM) consortium, which includes Wessels Mine. Mamatwan mine is one of the oldest manganese mines in the Kalahari basin and has extensive manganese ore reserves. Mamatwan Mine and Wessels Mine combined employed approximately 2000 mineworkers in 2024 (1).

Black Rock Mine

Nchwaning and Gloria mines, collectively known as Black Rock Mine, are located near Hotazel and operated by Assmang. These mines are part of the broader Black Rock Geological Complex. Assmang, on its webpage, describes Black Rock mine as one of

the largest manganese mines in South Africa (8). As of 2024, Black Rock mine had 2,500 permanent employees and 3,500 contractors (8, 9).

Wessels Mine

The Wessels Mine is also situated near the town of Hotazel. It is an integral component of the HMM consortium operated by South32(1, 10). South32 which holds a 44.4% interest in HMM, with the remaining shares owned by Anglo American Public Limited Company and Broad-Based Black Economic Empowerment (B-BBEE) entities (1). The number of employees is not publicly disclosed.

United Manganese of Kalahari Mine

United Manganese of Kalahari mine, a member of the International Manganese Institute, is also located near Hotazel, and jointly owned by Majestic Silver Trading 40 (Pty) Ltd (51%) and Renova Manganese Investments Limited (49%) (10). The mine was founded in 2005 and is 51% black owned, and is the fourth largest manganese producer in South Africa (10, 11). Approximately 1500 mine workers were employed in 2023 (10).

Kalagadi Manganese

Kalagadi Manganese is a large-scale mining operation located near Kuruman. It is a South African mining enterprise run by black women. The mine began production in 2018 and had its peak production in 2019 when it employed 1,250 mine workers. The 2024 employment figure was 960 (12).

Kudumane Manganese Resources

Kudumane Manganese Resources (KMR) manages two primary open-pit mines: York and Hotazel, which are also located near the town of Hotazel in the Northern Cape province. The mine employs approximately 1,000 people to support its mining operations, of which approximately 900 are independent industry contractors (13).

1.1.2 Manganese production in South Africa

South Africa is a leading global producer of manganese ore, with the Northern Cape holding the world's largest deposits. In 2023, the country produced over 19 metric tonnes of manganese ore, exporting more than 18 metric tonnes (14, 15). The

completion of the loop rail link in the Northern Cape in July 2023 significantly boosted transportation capacity, enabling a 12.1% increase in manganese production compared to 2019 (14). This railway expansion facilitated higher exports and improved efficiency in the mining sector. Additionally, the increased transport capacity directly led to more employment opportunities, supporting economic growth (14).

1.1.3 Contribution of mining to the economy and employment in South Africa

The mining industry significantly contributes to South Africa's economy in terms of gross domestic product (GDP), export earnings, corporate tax receipts, and employment (16-18). In 2018, the South African Minerals Council reported minerals sales of about R356 billion (7.3%) towards South Africa's GDP, of which manganese mining contributed about R237 million (0.007%) (19). In 2021, the industry contributed more than R47 billion in export earnings to the country's foreign exchange reserves (1). According to Esau *et al*. (2023), South Africa's mining sector contributed approximately 7.5% to the country's GDP in 2022 and provided more than 475,000 jobs (16).

Many communities in South Africa are dependent on mining for jobs and local businesses (16). The contribution of manganese mining to economic growth and employment in South Africa is well documented (16, 17, 20). In 2018, the manganese mining industry employed an estimated 9,352 people (14). By 2023, the industry had increased its employment to more than 11,503 and generated more than R7 billion in tax revenue (14).

1.1.4 Manganese pathways into the body

There are several pathways of manganese absorption into the human body. Each pathway contributes differently to overall manganese levels in the body. Each route has specific mechanisms for absorption and distribution, with varying health implications (21). Manganese enters the human body primarily through inhalation of dust and fumes, ingestion of contaminated food or water, and, less commonly, through dermal absorption or intravenous exposure (22). Effective regulation and monitoring of manganese exposure are crucial to prevent toxicity and associated health effects.

1.1.4.1 Manganese intake through the ingestion pathway

Manganese is required in small quantities in the human body. Ordinarily, the primary route of manganese into the body is through ingestion from dietary sources (23-27). Manganese is found at low levels in virtually all diets (27). The primary sources of dietary manganese are whole grains and cereals. Manganese is also obtained in green leafy vegetables, brown rice, dried legumes, nuts (hazelnuts, almonds, and pecans), pineapples, and tea (28, 29). The human body cannot produce manganese on its own, but it can store it in the liver, pancreas, bones, kidneys, and brain (30).

1.1.4.1.1 Manganese deficiency in the body

Although there is no recognized syndrome associated explicitly with manganese deficiency, low manganese levels may contribute to symptoms or health issues such as impaired growth and bone health, reduced antioxidant defence, metabolic disruptions (31), to mention a few. Manganese deficiency disrupts the brain's key biochemical and cellular processes, making it more prone to dysfunction and degeneration over time. Though manganese deficiency in humans is rare, deficiency can occur due to malabsorption, poor diet, or chronic illness, particularly in populations with limited access to diverse food sources or those consuming diets low in manganese-rich foods or with specific absorption issues (32). Therefore, ensuring adequate manganese levels is crucial for maintaining optimal brain health and preventing neurodegenerative diseases.

1.1.4.1.2 Excessive intake of manganese through ingestion

While manganese is an essential metal in the body, excessive ingestion can lead to acute toxicity (33, 34). Symptoms may include nausea, vomiting, abdominal pain, and diarrhoea. Manganese ingestion poses a risk to mineworkers, especially in environments with high levels of manganese dust (33). Proper hygiene practices, workplace cleanliness, education, and protective measures are crucial to minimize the likelihood of manganese ingestion and protect the health of mineworkers (33). Regular health monitoring and adherence to safety protocols can help mitigate the potential adverse effects of manganese exposure (33).

1.1.4.2 Manganese exposure through the inhalation pathway

Inhalation is the most important route of manganese exposure for workers in mining and other industrial settings where manganese is processed or utilized (35). Activities such as welding, grinding, smelting, or crushing manganese-containing materials release manganese into the air as dust, fumes, or fine particulates (35, 36). Also, high-temperature processes, like welding, produce manganese fumes, which are more easily inhaled and absorbed due to their particulate nature, which can include nanoparticles. At the same time, mechanical activities generate dust and particulates (37). Manganese particles can be inhaled through the nose and deposited in the nasal cavity. The inhalation of manganese bypasses the body's normal homeostatic mechanisms, leading to accumulation in the brain and other organs (38). Inhaled manganese can be deposited in the nasal cavity and subsequently transported to the brain via the olfactory and trigeminal nerves (39). The deposition and transport of manganese particles are influenced by their size and morphology, with smaller particles being more likely to penetrate deeper into the nasal cavity and reach the brain (40).

1.1.4.2.1 Manganese toxicity through inhalation

Manganese toxicity through inhalation occurs when airborne manganese particles, such as dust or fumes, are breathed in, most commonly in industrial settings like welding, mining, and metal manufacturing (41). Unlike dietary manganese, inhaled particles can bypass the body’s natural barriers by traveling through the olfactory nerve directly into the brain (42). This inhalation can lead to manganese accumulation in brain regions that control movement, causing a neurological condition known as manganism (34).

In another study, in 2009, Flynn and Sussi emphasized that prolonged exposure to high manganese concentrations can cause manganism, a neurodegenerative disorder with symptoms like those of Parkinson's disease (43). This neurodegenerative condition includes motor disturbances such as tremors, rigidity, bradykinesia (slow movement), difficulty walking, and facial muscle spasms (43). Findings from a 2006 study by Bowler, Koller, and Schulz also added that welders exhibited other signs, such as inattention, forgetfulness, and cognitive flexibility deficits, consistent with neurobehavioral impairments (44).

1.1.4.3 Occupational exposure to manganese

The primary route of manganese exposure in occupational settings is inhaling manganese-containing dust and fumes. Manganese exposure primarily occurs in industries such as welding, mining, smelting, and manufacturing manganese compounds. Inhalation of manganese dust in occupational settings can be affected by several factors, such as the type of mining operations, the efficacy of dust control methods, and the ventilation systems employed (33). Workers in manganese alloy production, welding, and battery manufacturing industries are at higher risk due to prolonged exposure to manganese fumes and dust (52). Chronic exposure to high levels of manganese can cause manganism

1.1.4.3.1 Welding

Welding is a significant source of manganese exposure due to manganese in steel and welding electrodes, which leads to elevated levels of manganese in the blood and brain, particularly neurological disorders (45, 46). Manganese levels in welding fumes can vary significantly depending on the welding process, materials used, and ventilation. Welding procedures generate gaseous and aerosol by-products of a complex metal oxide mixture (47). Welders are at risk of inhaling manganese-containing fumes, especially in confined or poorly ventilated spaces (48).

1.1.4.3.2 Smelting

Manganese exposure in smelting primarily occurs through inhaling airborne particles, which can be present in respirable and total particulate forms (49). Smelting involves the high-temperature processing of manganese ores above the melting point, which leads to the release of metallic oxides and other particulates into the air (50) to produce ferromanganese and other alloys, making it a significant source of occupational exposure to manganese. During the smelting of manganese-containing materials, significant emissions of metal fumes and fine particulate matter occur, posing environmental and health risks. Workers easily inhale these fumes. Workers involved in furnace tending, slag handling, and material loading are at a high risk of inhalation due to close contact with emission sources.

Emissions from manganese smelting contribute to environmental pollution, with particulate matter containing hazardous metals being released into the atmosphere.

The dispersion of these particulates can affect air quality and pose long-term environmental health risks (51).

1.1.4.3.3 Mining

Manganese mining is one of the main industrial activities leading to occupational manganese exposure. Workers involved in the extraction, crushing, and processing of manganese ore are at high risk of acquiring severe health issues, primarily affecting the central nervous system. Manganese mining activities pose significant occupational health risks due to the potential for overexposure to manganese dust and fumes. Mining environments often have elevated concentrations of respirable manganese, exceeding recommended occupational exposure limits (52), particularly during dry or high-activity operations (53). Factors such as prolonged exposure, lack of personal protective equipment (PPE), inadequate ventilation, and poor dust control significantly amplify the risk for miners. Without adequate control, manganese exposure in mining can lead to long-term disability, reduced productivity, and increased healthcare costs for affected workers (53).

Mining activities can contaminate the surrounding soil and water, posing additional health risks to nearby communities (54). Due to the close residential proximity of mineworkers to mining sites, continuous environmental exposure to airborne manganese may occur outside of working hours, contributing to prolonged overall exposure. Children and other vulnerable populations living near manganese mines are at high risk of developing health issues due to environmental exposure (55).

1.1.4.3.4 Battery manufacturing and electronics industry

Workers in the battery manufacturing and electronics industries are at risk of manganese toxicity, primarily via inhalation of airborne manganese-containing dust and fumes generated during various production processes. Manganese dioxide (MnO_2), commonly utilized as a cathode material in lithium-ion and alkaline batteries, can become airborne during operations such as mixing, grinding, and handling, increasing the likelihood of respiratory exposure (56). In the electronics sector, manganese is used to fabricate magnetic materials, semiconductors, and electronic components. Occupational exposure may occur during activities such as soldering, component assembly, or chemical processing involving manganese-based substances. Without adequate control measures, repeated inhalation of manganese

particulates may lead to toxic accumulation and associated neurological and respiratory health effects.

1.1.4.4 Manganese regulation in the body

Manganese is tightly regulated through efficient absorption in the intestine and excretion via bile in healthy individuals to maintain physiological levels (29, 57, 58). The human body has several mechanisms to eliminate excess manganese, primarily through its regulation and excretion pathways (59). Manganese ingested through food or water is absorbed in the gastrointestinal tract, particularly in the duodenum and jejunum (59). The body regulates the absorption rate and depends on factors like the form of manganese, the dietary presence of other metals, and the overall manganese status (60). Other metals in the diet, such as iron, can affect the absorption and bioavailability of manganese (59, 61). Manganese absorption is regulated by homeostatic mechanisms that adjust intestinal uptake based on the body's existing manganese levels. When manganese levels are sufficient or elevated, the absorption rate decreases to avert excessive buildup. Conversely, the absorption rate increases when manganese levels are low (62). Excess oral manganese is primarily managed by the body through absorption in the gastrointestinal tract, distribution via the bloodstream, and eventual elimination through biliary and renal routes (29, 63).

The liver plays a critical role in metabolizing and excreting manganese into bile, while the kidneys contribute to its excretion through urine (64). Kidneys play a secondary role in manganese excretion, especially when manganese levels are elevated or if there is liver dysfunction (64), by facilitating the elimination of excess manganese. Manganese obtained from plant sources is typically processed by the liver, with any surplus being eliminated to prevent toxicity. People with liver disease are more susceptible to the buildup of hazardous levels of manganese in their circulation (65) since manganese is normally excreted via the liver.

1.1.5 Types of manganese mining and respiratory exposure to dust

There are two types of manganese mines in South Africa: open-pit and underground mining. Open-pit mining involves removing the surface layers to access manganese ore deposits, such as those found in the Mamatwan and Wessels mines (66). The topsoil covering the ore body is stripped away, and the ore is extracted using heavy machinery, significantly producing dust from drilling, blasting, loading, and hauling

activities (67). Underground mining involves the extraction of ore from below the earth's surface through a network of tunnels and shafts (68). Underground mining is used when the ore body is deeper (68), adding to dust generation during drilling, blasting, and ore handling.

Other sources of manganese dust exposure beyond direct mining activities include ore processing and the processes of transport and handling. Manganese ore undergoes crushing, grinding, washing, and separation to improve its quality and prepare it for further use (69), which produces a significant amount of fine dust particles. Conversely, transporting manganese ore from mining sites to processing plants and shipping points can generate dust during loading, unloading, and transporting, especially if containment measures are inadequate (69).

1.1.6 Mining legislation and regulations

There are several regulatory controls that are aimed at ensuring that mining activities in South Africa are conducted responsibly, minimizing environmental impacts, promoting health and safety, and contributing to sustainable socio-economic development. For example, the Department of Minerals and Resources (DMR) is the custodian of all mineral resources in South Africa. The main regulatory control unique to South Africa's health and safety is the South African Occupational Diseases in Mines and Works Act (70).

1.1.6.1 The South African Occupational Diseases in Mines and Works Act 1973

The Occupational Diseases in Mines and Works Act (70) of 1973 is a unique South African regulatory compensation system that provides compensation for workers certified to have specific occupational lung diseases (71). Mineworkers and ex-mineworkers in South Africa with occupational lung diseases caused by exposure to harmful dust due to their work on the mines can apply for compensation under the ODMWA. Compensable diseases under this Act are respiratory diseases caused by the inhalation of dust and or other hazardous conditions in mines. These include pneumoconiosis, tuberculosis, occupational asthma, chronic obstructive pulmonary disease (COPD), lung cancer, and mesothelioma (71).

During employment, mineworkers undergo regular medical screening examinations organized by employers to check for signs of occupational lung diseases. Ex-

mineworkers are entitled to a free Benefit Medical Examination (BME) at accredited medical facilities every two years to evaluate health conditions linked to their former mining work, especially occupational lung diseases. This program is vital for detecting health issues and ensuring affected individuals receive the necessary compensation and support. Suppose signs of occupational lung disease are found during the BME, the medical practitioner must submit the report and findings to the Medical Bureau for Occupational Diseases (MBOD) as required by the ODMWA. A panel of doctors, known as the Certification Committee and appointed by the MBOD, reviews the medical reports to determine whether the worker suffered from occupational lung disease(s).

When a mineworker dies, a postmortem can be conducted, and cardiorespiratory organs are removed and sent to the National Institute for Occupational Health (72), where autopsy examinations of the organs are performed regardless of the clinical cause of death, on condition that consent is provided by the next of kin (70). A comprehensive autopsy report on each case is sent to the MBOD for possible certification for compensation. Cases certified as having a compensable disease are then referred to the Compensation Commissioner of Occupational Diseases (CCOD) office, where payment for compensation is calculated and effected. The National Institute for Occupational Health (NIOH) collects data on deceased mineworkers during the autopsy process and stores it in a database called the Pathology Automated database (PATHAUT). Additionally, the deceased mineworkers' lungs and hearts (cardiorespiratory organs) are stored in the NIOH specimen storage. Under South Africa's ODMWA autopsy programme, cardio-respiratory organs are retained at NIOH for a maximum of two years after a report has been completed. This interval permits submission of appeals against compensation determinations and enables re-examination of the organs before final adjudication. Upon expiry of the retention period, the organs are disposed of in accordance with institutional policy.

for a specific period as determined by the NIOH policy.

1.1.7 Pathology Automated Database (PATHAUT)

The Pathological Automated system (PATHAUT) database is unique and contains the only comprehensive surveillance data on occupational lung diseases in the South African mining industry (73). Clinical and demographic information, including age at

death, the last mine in which the mineworker was employed, and clinical records with occupational histories, is also documented in the PATHAUT database. The PATHAUT database has been in existence since 1975 and was reported to have more than 115,000 comprehensive pathological records of mineworkers by 2021 (72).

The PATHAUT data gives important information about the deceased mineworkers, including demographic details and pathology reports generated by pathologists based on the analysis of lungs. The pathology report includes diagnoses of diseases, conditions, and abnormalities detected in the lungs and heart of deceased mineworkers during autopsy examination.

In summary, the exploration of manganese entry pathways, its universal presence in mining activities, and the significant economic ramifications for South Africa provide a foundational understanding of the context in which manganese toxicity occurs. This comprehensive background sets the stage for a detailed analysis of the pathological mechanisms and health outcomes associated with manganese exposure, providing insight into how manganese exposure contributes to respiratory pathologies.

1.2 Literature Review

1.2.1 Introduction

This literature review examines the multifaceted health effects associated with chronic occupational exposure to manganese, with a focus on the toxicokinetic processes that follow inhalation. It explores the pathway by which manganese particles enter the pulmonary system, their deposition within the alveolar spaces, subsequent absorption into the bloodstream via the alveolar capillary network, and systemic distribution to vital organs, particularly the brain. The brain is recognised as the primary target organ for manganese accumulation and associated neurotoxic effects (74). Numerous studies have documented the adverse health outcomes linked to manganese exposure, demonstrating that occupational exposure to hazardous substances contributes to a range of work-related diseases and health impairments of exposed individuals (75–78).

1.2.2 Neurological effects due to manganese exposure

Several studies have linked occupational exposure to manganese fumes, especially from welding processes, with adverse neurological effects, which may result in neurobehavioral and cognitive impairments among exposed workers (74-77). Abdel-Rasoul *et al.* recently conducted a comparative cross-sectional study in Egypt (2024) on welders and compared them with non-occupationally exposed controls. The authors found that welders had a significantly higher prevalence of neurological manifestations and lower performance in neurobehavioral tests compared to non-occupationally exposed controls (78), bradykinesia, and movement abnormalities such as tremors and dystonia.

Gonzalez-Cuyar *et al.* (2014) study highlighted an association between high manganese exposure and its accumulation in basal ganglia regions, resulting in neuronal loss within these areas (79).

The central nervous system is susceptible to manganese toxicity due to its mechanisms that allow manganese entry and accumulation. Miah *et al. (*2020) reported an increased accumulation of manganese in specific brain regions, such as the substantia nigra, globus pallidus, and striatum, which triggers neurotoxicity resulting in a neurological brain disorder, termed manganism (80).

Manganese absorbed via inhalation has been shown to bypass systemic excretory and regulatory mechanisms, facilitating its accumulation in the central nervous system (81, 82). Evidence from Curran *et al.* (2009) suggests that even low-level inhalation exposures can lead to manganese deposition in the brain, resulting in neurotoxic and neurobehavioral effects. Although the neurotoxic potential of manganese is well established, emerging evidence also highlights its role in impairing respiratory function, underscoring its multisystem impact (83) (84).

1.2.3 Manganese uptake into the lungs

Several studies have investigated the effects of inhaling manganese on the central nervous system (CNS). Manganese is naturally available and is primarily absorbed through ingestion and inhalation, with inhalation being the most hazardous route of exposure, as evidenced by Dorman *et al.* (2006) in a study of rhesus monkeys. Inhalation of pollutants, including hazardous substances, is recognized as a significant

route for causing human health hazards (85). Dorman *et al.* (2006) further demonstrated direct evidence of manganese transport from the nose to the brain in monkeys. Given the established anatomical and physiological similarities existing between humans and monkeys, it is believed that this route is likewise functional in humans, just as it is in monkeys (86).

Exposure to fine particulate matter [particles which are < 2.5 microns in diameter ($PM_{2.5}$)], including manganese, from mining activities, is associated with adverse health effects, particularly on pulmonary function (87). The negative health impact has been shown by Huang *et al.* (2019) in their study of the impact of $PM_{2.5}$ on the cardiovascular and pulmonary health of individuals employed in the open-pit manganese mines in China (87). Their study suggested that the lung function of these workers had been damaged, with a particular focus on restrictive expiratory complications (87).

1.2.4 Respiratory effects due to manganese exposure

Chronic exposure to manganese dust has been reported to affect respiratory health, leading to bronchitis and pneumonitis (88). Dorman *et al.* (2005) investigated histological alterations in the respiratory system of young male rhesus monkeys following exposure to inhaled manganese sulphate. They support the notion that inhalation of manganese dust has been linked to respiratory issues such as impaired pulmonary function and bronchial hyperreactivity, highlighting the potential for chronic bronchitis due to manganese dust exposure (88). Wang *et al.* (2015) retrospectively investigated the impact of manganese dust exposure on pulmonary functioning in ferromanganese refinery workers in Guangxi, China, using an electronic spirometer on 1658 workers in a ferromanganese refinery. The subjects of the study were selected from a healthy cohort of Guangxi manganese-exposed workers. They found that high manganese dust exposure impaired the pulmonary ventilation function of male workers, particularly in the high exposure group, and this impairment was exacerbated in smokers and concluded that manganese dust can adversely affect the pulmonary ventilation function (89).

Exposure to manganese can also occur through inhalation of manganese fumes in mining or non-mining environments. Welding as an occupation exposes metal workers to welding fumes. Welding fumes are a significant occupational source of manganese

exposure, as manganese is a common component in welding materials, including electrodes and filler rods. During welding, the intense heat vaporises manganese-containing materials, producing fumes containing ultrafine manganese particles (37, 90). These fumes are a complex mixture of different metals, including manganese, which can have significant health implications for welders (90). Welders and workers in industries such as shipbuilding, construction, and manufacturing are at risk of high exposure to manganese, which can lead to various health issues. Manganese exposure has been linked to increased lung inflammation and effects on the immune system (91).

A recent comparative cross-sectional study (2024) of welders exposed to welding fumes was conducted to evaluate the extent of individual exposure to welding fumes and examine the prevalence of chronic respiratory symptoms and related variables among workers in micro and small-scale metal workshops in Akaki Kality Sub-city, Ethiopia. The control group consisted of workers who were not exposed to welding fumes. More than 50% of the samples from the exposed group exceeded the Occupational Exposure Limit (OEL) of 5 mg/m³ (92). These OEL were set by the American Conference of Governmental Industrial Hygienists (ACGIH) and the Occupational Safety and Health Administration (93) (92, 93). The authors reported that welding workers had a notably increased incidence of chronic respiratory problems compared to the control group (92). Furthermore, chronic respiratory problems showed a substantial association with educational status, implementation of safety training, and welding locations (92).

In a cohort study of 484 welders, Hedmer *et al.* (2014) determined the frequency of work-related symptoms among mild steel welders. The occupational exposure to welding fumes was measured repeatedly using respirable dust, respirable manganese, and ozone. Over 50% of the manganese values surpassed the Swedish occupational exposure limit (OEL) of 5 mg/m³ (94). Diseased welders had a greater prevalence of respiratory and ocular symptoms as compared to welders without disease. The authors concluded that the welders were exposed to uncomfortably high levels of manganese (94).

A study was conducted in China in 2022 to assess the concentrations of welding fumes and manganese metal ions in a Wuhan vehicle factory involving welders exposed to

manganese fumes (95). This study assessed the relative risks (hazard ratios) of different levels of welding fumes on the likelihood of workers having lung-related diseases. The subgroup analyses computed risk ratios for pulmonary disorders in welders and compared them to those in individuals who did not engage in welding, while considering various influencing factors (95). The authors concluded that workers with significant exposure to welding fumes are at a considerably higher risk of developing lung-related illnesses (95).

Other studies indicate that manganese exposure can mimic a hypoxia-like response, activating genes associated with angiogenesis and potentially affecting lung susceptibility to respiratory diseases (105, 106). This activation is linked to the upregulation of hypoxia-inducible factor transcription factors, which regulate the expression of genes such as vascular endothelial growth factor (105). The activation of these genes could potentially affect lung susceptibility to respiratory diseases (105).

Many studies suggest the association between metal exposure, particularly manganese in welding fumes, and adverse respiratory manifestations, including decreased spirometric measures and increased prevalence of respiratory symptoms (33, 88, 95). However, it is essential to note that, although the adverse respiratory effects are well-documented, further research is necessary to fully comprehend the mechanisms and potential preventive measures.

1.2.5 Manganese transport into alveolar blood capillaries

Manganese is a necessary nutrient for the alveolar epithelia of the lungs. However, the alveolar epithelia also serve as a pathway for airborne manganese particles that may be neurotoxic to the cells (96). Studies have shown that inhaled manganese can be absorbed into the bloodstream from the lungs, then crosses the Blood-Brain Barrier (BBB) through active transport, thought to involve different mechanisms, including transporter-mediated pathways (97, 98).

In 2006, Fitsanakis et al. (2006) investigated the transport of manganese across a single layer of rat brain endothelial cells to determine if an electromotive permeability mechanism is accountable for the movement of manganese across the BBB. The work confirmed previous discoveries that the transport of manganese across the BBB is facilitated, at least in part, by an active transport mechanism (96).

Heilig *et. al* (2005) compared the pharmacokinetics of pulmonary manganese and iron absorption between control rodents and rodents with iron deficiency. The authors observed that low levels of iron caused significant alterations in the process of removing manganese from the blood, leading to increased levels of manganese remaining in circulation (97). Their observation revealed that blood manganese levels remained high in rats with iron deficiency, due to a buildup of manganese in the cellular fraction. Furthermore, the authors hypothesized that the slow release of manganese from ageing red blood cells with reduced iron might extend and/or alter the effects of exposure to this harmful element (97). Their findings suggest that investigating iron status is necessary to thoroughly assess the risk of neurotoxicity caused by exposure to environmental manganese (97, 99).

Iron deficiency can influence the absorption and toxicity of manganese by altering its pulmonary transport and blood clearance (97). Studies suggest that iron status affects how manganese is absorbed from the lungs into the bloodstream, potentially increasing the neurotoxic effects of manganese (97, 100, 101). However, changes in iron levels do not appear to impact lung DMT1 (divalent metal transporter 1) expression, suggesting that different transporter proteins play distinct roles in manganese absorption across epithelial membranes (97, 98).

Brain *et al.* (2006) conducted a pharmacokinetic study to investigate the influence of iron levels on the transpulmonary transport and tissue distribution of manganese and iron. They hypothesised that manganese and iron, both divalent metals, share common carrier transport systems in the respiratory and gastrointestinal tracts. Their findings supported this hypothesis, revealing that manganese uses the same transporter proteins as other divalent metals such as iron, lead, nickel, copper, and cobalt (102). As a result, the authors concluded that competitive inhibition among these metals, particularly at the level of shared transporter binding sites, plays a central role in limiting the pulmonary uptake and subsequent distribution of manganese to extrapulmonary tissues, including the brain. This competitive interaction effectively suppresses manganese transport from the lungs, thereby modulating its neurotoxic potential (102).

Correlating iron deficiency with manganese deposition could help explain why some individuals may absorb and retain more manganese than others, even at similar exposure levels. This would enhance our understanding of how manganese affects the body, particularly in vulnerable groups, such as mineworkers with low iron levels. It also supports better health monitoring and prevention strategies in occupational settings. To assess the relationship between iron deficiency and manganese deposition in mineworkers, key iron biomarkers such as serum ferritin, serum iron, total iron-binding capacity (TIBC), transferrin saturation, and haemoglobin would be required (103, 104). A study by Kim, Y., *et al*. (2005) evaluated the relationship between blood manganese concentrations and various iron status markers, including serum ferritin, transferrin saturation, and haemoglobin in a population of adults. It was found that individuals with lower iron status had significantly higher blood manganese levels, reinforcing the biological link between iron deficiency and increased manganese absorption. C-reactive protein (CRP) may be included to account for inflammation and respiratory effects. These markers would help determine whether low iron status enhances manganese absorption via shared transport pathways, such as DMT1 and transferrin (103, 104).

Dorman et al. (2005) investigated the effects of high-concentration manganese sulphate inhalation on the lower airways of rhesus monkeys, focusing on histological alterations in the respiratory system, as detailed in section 1.2.6. The authors determined that inhalation exposure to manganese sulfate is associated with higher lung manganese concentrations and small airway inflammation, indicating the potential for manganese to accumulate in the lungs and subsequently enter the bloodstream (88). Furthermore, iron oxide exposure significantly reduces pulmonary transport of manganese and iron, resulting in decreased uptake by other critical organs (88). When individuals are exposed to iron oxide particles, such as those present in mining or welding fumes, these particles can interfere with the normal transport of manganese and iron across the lungs into the bloodstream. As a result, less manganese and iron are absorbed from the lungs and distributed to other vital organs, such as the brain, liver, or heart. This effect likely occurs because iron oxide particles saturate or block shared transport mechanisms (e.g., DMT1 and transferrin receptors), leading to competitive inhibition that limits the uptake of both metals. Essentially, the lungs act as a barrier under iron oxide exposure, reducing systemic availability of these essential (and potentially toxic) metals.

Brain et al. (2006) investigated the effect of iron levels on the transport of Mn and iron across the lungs and the distribution in body tissues. Using a rat lung model, they found that iron deficiency increases manganese absorption through the lungs due to the upregulation of shared transporters, such as DMT1 and transferrin receptors. Conversely, normal or high iron levels reduced Mn uptake. The study highlighted that individuals with low iron stores may be more vulnerable to manganese accumulation and toxicity following inhalation exposure (102).

1.2.6 Lung tissue inflammation due to manganese overexposure

Manganese exposure can negatively impact the blood-air barrier by inducing oxidative stress and inflammation, which in turn damages the alveolar epithelium and capillary endothelium (103). The blood-air barrier, also known as the alveolar-capillary barrier, is a crucial interface in the lungs where gas exchange occurs (80). This barrier consists of the alveolar epithelium, the capillary endothelium, and the interstitial space between them. Manganese exposure can affect this barrier in several ways, potentially compromising respiratory function and overall lung health (33).

In 2013, Zhang and others conducted a study where they demonstrated that manganese triggers caspase-9-mediated cell death in human bronchial epithelial cells (104). The authors further reported that high levels of airborne manganese can cause pulmonary oedema and impaired lung function (104). In addition, Dorman et al. (2006) added that inhaled manganese can lead to pulmonary inflammation, bronchiolitis, and alveolar duct inflammation, affecting lung function (88).

Zhang et al. (2013) further demonstrated that manganese exposure can induce oxidative stress and inflammation, leading to damage of the alveolar epithelium and capillary endothelium (104). Oxidative stress exacerbates inflammation and can contribute to neuronal damage. The overabundance of reactive oxygen species can further trigger ferroptosis, a form of regulated cell death (104). Moreover, the activation of the cyclic guanosine monophosphate (cGMP) - adenosine monophosphate (AMP) synthase stimulator of interferon genes pathway (cGAS−STING) by manganese exposure suggests a potential link to inflammation (104). Furthermore, persistent

activation of the cGAS−STING pathway due to manganese exposure may contribute to chronic neuroinflammation and neurodegenerative processes (104).

Based on the above studies of manganese overexposure, manganese may cause inflammation and oxidative stress in the lung tissue, potentially leading to damage of the alveolar epithelium and capillary endothelium.

1.2.7 Lung Microscopic Anatomy and Histopathological Changes in Mn Toxicity

The microscopic structure of the lung tissue is mostly maintained by collagen and elastin fibres, which are woven into an uninterrupted network throughout the lung and greatly enhance its flexibility and mechanical qualities (105). The mechanical characteristics and structural integrity of lung tissue are largely dependent on collagen and reticular fibres (106). Reticular fibres sustain the structure of the alveoli, whereas collagen fibres give flexibility and prevent over-stretching. Their significance in lung health and illness is shown by the notable alterations that both fibre types experience with ageing and in pathological states like fibrosis (107). Chronic manganese exposure induces oxidative stress and inflammation, promoting the activation of fibroblasts and the excessive deposition of collagen fibres. This can lead to pulmonary fibrosis, impairing lung elasticity and gas exchange (108).

Manganese toxicity adversely affects the microarchitecture of the lungs by promoting fibrosis (collagen overproduction) and degrading reticular fibres (109). A recent study by Choi *et al.* (2024) demonstrated that lead or PM2.5 exposure caused fibrotic alterations and apoptosis in human lung fibroblasts in alveolar epithelial cells (110). The authors assessed the adverse impacts of four heavy metals, including manganese, found at high concentrations in the ambient air of South Korea, and examined their paracrine effects on alveolar epithelial cells. They found that long-term exposure to heavy metals adversely impacted the proliferation, migration, and survival of lung fibroblasts (109). Manganese markedly increased the expression of fibrotic markers (109).

Inhalation exposure to manganese sulphate has been associated with higher lung manganese concentrations and small airway inflammatory abnormalities, which were reversible upon cessation of exposure (88, 111). In a 2006 study by Dorman and others, the levels of manganese in the tissues of rhesus monkeys were assessed after

exposure to manganese sulphate by inhalation. A group of monkeys was subjected to either air or manganese sulphate for 65 days before their tissues were analysed. The brain and bile exhibited the most significant relative increase in manganese content after being exposed to manganese sulphate (86). The authors reported a recovery of manganese levels in the tissues of animals exposed to sub-chronic manganese sulphate. Manganese levels in exposed animals returned to the same levels as those in animals exposed to air after 90 days (86). These findings enhanced the understanding of the circumstances under which manganese sulphate exposure results in elevated manganese concentrations in the brains and other tissues of non-human primates (88). Furthermore, high-dose inhalation of manganese sulphate over a prolonged time was associated with minor inflammation in the bronchioles and alveolar ducts, indicating an impact on the trachea and air passages (88).

A study by Huang *et al.* (2019) on the study of inhaled fine particulate matter of 2.5 microns ($PM_{2.5}$) particles demonstrated that fine manganese dust can enter the bronchioles down to terminal alveoli, where they can be engulfed by macrophages and remain in bronchial and alveolar cells for an extended period (87). The prevalent forms of lung function impairment observed in workers exposed to dust typically manifest as restricted ventilatory dysfunction (87). This can further lead to the narrowing and blockage of the bronchial and alveolar passages, as well as inflammation (87). Additionally, it can damage the bronchial smooth muscle and elastic fibres (87).

Exposure to soluble manganese in mice can stimulate angiogenic gene expression in pulmonary epithelial cells, potentially increasing the lungs' susceptibility to respiratory diseases. A study by Bredow *et al.* (2007) found that brief exposures to industrially relevant concentrations of soluble manganese altered the expression of genes associated with lung hypoxia, which may serve as mediators of manganese toxicity. These changes in gene expression could make the lungs more vulnerable to developing respiratory diseases in environments with manganese exposure (112).

Bredow *et al.* (2007) using adult mice models defined manganese exposure explicitly as inhalation of aerosolized soluble Manganese Chloride ($MnCl_2$). This inhalation route mimics occupational and environmental inhalation exposures in humans (e.g., miners, welders, or industrial workers), where airborne Mn dust or fumes are the primary

concern. The route of exposure shapes deposition, clearance, and tissue responses which was considered in this study for the translation of results.

1.2.8 Techniques to evaluate manganese in tissue

1.2.8.1 Multi Collector Inductively Coupled Plasma Mass Spectrometry (MC-ICP-MS)

Date and Gray presented advancements in atomic spectroscopy at the 1982 United Kingdom (UK) National Atomic Spectroscopy Symposium, leading to the development of a commercial Multi Collector Inductively Coupled Plasma source Mass Spectrometry (MC-ICP-MS) instrument (113). In 1983, Date introduced the MC-ICP-MS, a revolutionary new method of analysis, combining the speed and convenience of sample introduction into the MC-ICP-MS with the high sensitivity and isotope ratio capability of atomic mass spectrometry (114). Researchers have since preferred the MC-ICP-MS for quantifying trace elements, including manganese, in biological tissues due to its superior sensitivity, accuracy, and capacity for efficient multi-elemental analysis. Although there are other techniques, such as Atomic Absorption Spectroscopy (115). Inductively Coupled Plasma Optical Emission Spectroscopy (ICP-OES) and X-ray Fluorescence (XRF), which possess distinct benefits, these techniques often lack the sensitivity and multi-element capacity of MC-ICP-MS (116, 117).

1.2.8.2 Histochemistry stains for inflammation and fibrosis

To identify toxicity caused by manganese exposure in the lungs, specific special stains can be used to detect changes in lung tissue structure, fibrosis, and cellular damage. Staining with H&E is fundamental in histopathology due to its ability to distinctly outline cellular and tissue architectures, facilitating the identification and examination of several disorders (118). The H&E stain is usually used as a routine stain to visualize general tissue morphology (119), highlighting general structural changes, including inflammatory cells and cellular damage. Therefore, H&E staining can be used to identify areas of necrosis, inflammation, and overall lung architecture affected by manganese toxicity. There are also specialised stains, such as Masson's Trichrome, Periodic Acid-Shiff (PAS), and Reticulin, which can provide insight into fibrosis and specific tissue alterations.

Masson's Trichrome staining (MT) is a predominantly used histological method for detecting and measuring fibrosis in many tissues, including pulmonary tissue. This

staining technique is especially effective in highlighting collagen fibres, which are indicative of fibrotic alterations (118, 120).

While PAS is not a direct marker of inflammation, such as H&E or immunostains (e.g., CD45, CD68), it is a valuable supportive stain for assessing structural and mucopolysaccharide-related changes that occur during inflammation. Suvarna *et.al* (2018) highlight PAS application in inflammatory and pathological conditions such as glomerulonephritis, chronic bronchitis, and fungal infections (121).

Gordon and Sweet's silver stain for reticulin fibres (Retic) is a histological technique used to highlight reticular fibres, a type of thin collagen fibre found in various tissues like the liver, lungs, and spleen (122). Reticulin fibres appear black, aiding in the detection of structural changes in the extracellular matrix, particularly in fibrosis or the early stages of tissue scarring. In pulmonary fibrosis, the distribution and architecture of reticular fibres might indicate the severity of the condition. The transition from a normal reticular network to its depletion is associated with advanced stages of fibrosis (107). These stains can provide insights into the structural and cellular changes in lung tissues resulting from heavy metal toxicity and could help in the diagnosis and study of manganese-induced pulmonary damage.

1.3 Gaps in Current Knowledge

While much is known about manganese toxicity's neurological effects, the localised pulmonary impacts and histopathological alterations due to manganese deposition in the lungs of manganese-exposed mineworkers remain poorly understood. There is limited data on how manganese concentrations vary across different lung lobes and how these correlate with manganese deposition concentrations in the brain.

1.4 Problem Statement

The South African manganese mining industry is expanding; consequently, the number of workers employed in the industry is increasing, thereby expanding the number of people exposed to manganese dust. Despite extensive research on manganese neurotoxicity and its concentrations in the brain, a significant knowledge gap remains regarding manganese deposition in the lungs of mineworkers, particularly in South Africa. This study aims to fill this gap by quantifying and mapping manganese deposition in the lungs and correlating these findings with pathological findings in the

brains of deceased mineworkers in South Africa. The outcomes of this study will provide critical insights that may ultimately contribute to the improvement of occupational health standards in the manganese mining industry.

1.5 Justification

Pathological tissue is very difficult to obtain from workers worldwide. South Africa has a long-standing formal statutory autopsy programme for examining deceased workers for occupational diseases. The availability of autopsy data and samples of organs of deceased mineworkers allows studying manganese toxicity in the various human body systems, such as the respiratory and the central nervous system.

Furthermore, there are no human studies that have investigated the histopathological effects of manganese on lung tissue or the relationship between manganese concentrations in the lungs and brain tissue following long-term exposure to manganese dust. Moreover, there is limited knowledge of the human health effects on the respiratory system from chronic manganese exposure. Understanding the health effects of chronic exposure and the relationship between manganese concentrations in the brain and lungs will help elucidate the mechanism of manganese toxicity. This research aimed to quantify and map manganese deposition, along with its associated histopathological correlates, in the lungs and brains of deceased mineworkers in South Africa.

1.6 Research Question

What are the histologic changes, and how are manganese concentrations distributed and correlated between the lungs and brain in deceased manganese-exposed mineworkers compared to non-manganese-exposed mineworkers in South Africa?

Hypotheses

- There are higher manganese concentrations in the lungs of manganese-exposed mineworkers than in those of manganese-unexposed mineworkers.
- The histopathological patterns (inflammation and fibrosis) in the lungs of manganese-exposed mineworkers differ from those of manganese-unexposed mineworkers.

- The concentration of manganese in the lungs of deceased manganese-exposed mineworkers correlates with the concentration levels in the brain [cerebellum and the basal ganglia regions (Caudate, Putamen, Globus pallidus externus and Globus pallidus internus)].

1.7 Study Aim and Objectives

This study aimed to identify histologic changes, quantify, map, and correlate manganese deposition in the lungs with that in the brains of deceased manganese-exposed mineworkers in South Africa.

1. To compare the concentrations of manganese in the lungs of deceased manganese-exposed and manganese-unexposed mineworkers in South Africa, using a Multi Collector Inductively Coupled Plasma–Mass Spectrometry (MC-ICP-MS).
2. To map the deposition of manganese in the lungs of deceased manganese-exposed and manganese-unexposed mineworkers in South Africa.
3. To compare the histological features due to manganese in the lungs of deceased manganese-exposed and manganese-unexposed mineworkers in South Africa using H&E and Masson Trichrome (MT), and Gordon and Sweet's silver stain for reticulin fibres histochemistry stains.
4. To correlate the manganese concentrations in the lungs and the brains of deceased manganese-exposed mineworkers in South Africa.

CHAPTER TWO – MATERIALS AND METHODS

2.1 Introduction

This chapter describes the methods used to quantify and map manganese deposition and associated histopathological changes, and correlate the findings with the manganese concentrations in the brains of deceased manganese-exposed mineworkers in South Africa. The chapter starts by giving a detailed flowchart of the study methodology. The study design, study population, study setting, power calculations, sampling methods, and data collection procedures are described. The tools used for data collection are also described. The chapter ends by describing data management, analysis, and ethical considerations.

2.2 Flowchart of study methodology

The flow chart of the study methodology begins with the death of a manganese-exposed mineworker in the Northern Cape, after which the lungs and brain are removed, fixed in 10% buffered formalin, and sent to the National Institute for Occupational Health (NIOH) for analysis (Figure 3). The NIOH supplies pre-prepared 10% buffered formalin to undertakers and mortuaries nationwide for the preservation of post-mortem organs retrieved for occupational disease compensation purposes. This formalin solution, produced by Merck Industrial Chemicals, is stored in labelled plastic containers at room temperature.

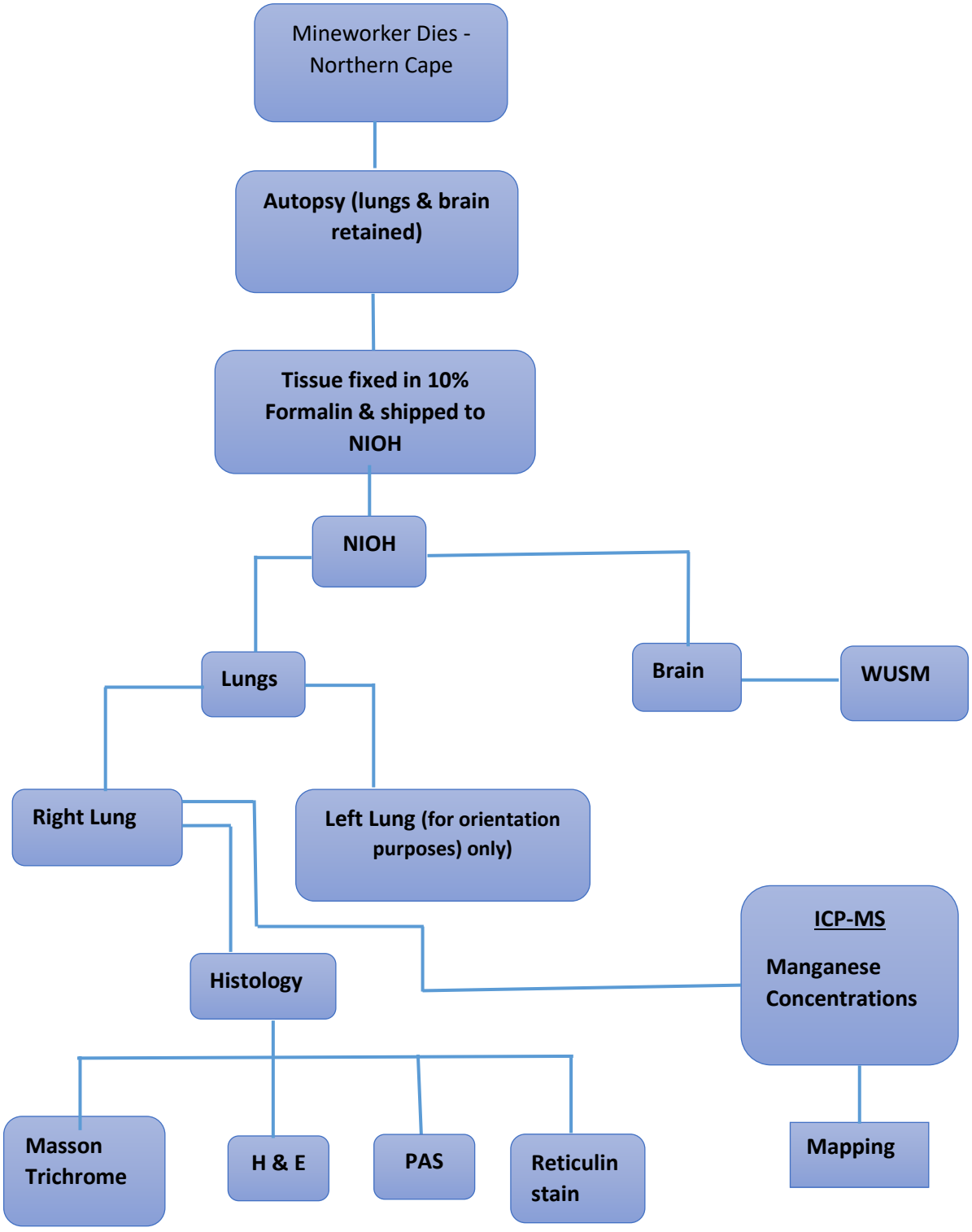

Figure 3. *Schematic flowchart of study methodology*

Key: NIOH – National Institute of Occupational Health.

WUSM – Washington University School of Medicine.

H&E – Haematoxylin and Eosin.

PAS – Periodic Acid-Schiff

2.3 Study Design

A cross-sectional study was conducted.

2.4 Study Population

Two populations were included in this study. The first population comprised all deceased manganese-exposed mineworkers whose lungs were removed at autopsy, examined, and stored at the NIOH specimen storage, and whose brains were removed for the neuropathological study, in the period January 2010 to December 2020. A neuropathology study is being conducted by my supervisors, Professors Gill Nelson and Brad Racette, using brains collected from deceased manganese-exposed mineworkers from the Northern Cape province of South Africa, where manganese is mined.

The second study population comprised all deceased platinum mineworkers without a history of working in manganese mines, whose lungs were removed at autopsy, examined, and stored at the NIOH specimen storage in the same period.

Platinum-exposed mineworkers served as a control group for this study because platinum is a heavy metal, similar to manganese, but without the expected toxicity associated with manganese. Having this scientific control helps to isolate the toxic effects specific to manganese by comparing the outcomes to a group exposed to a different, less toxic metal. In addition, using platinum-exposed mineworkers ensured that both the manganese-exposed and the control group consisted of mineworkers who may share similar occupational settings, demographic characteristics (age, smoking habits, physical activity), and occupational histories, improving the validity of the study.

From this point onwards, platinum-exposed mineworkers will be referred to as manganese-unexposed mineworkers.

2.4.1 Inclusion criteria

All cases of deceased manganese-exposed and manganese-unexposed mineworkers whose lungs were removed at autopsy, examined, and stored at the NIOH specimen storage for the period January 2010 to December 2020 were included in the study.

Since there were few cases of manganese-exposed lungs, smoking was not excluded as a confounding factor; however, care was taken in reporting histological analysis by involving a registered anatomical pathologist experienced in pulmonary pathology to avoid over-interpretation of inflammation and fibrosis.

2.4.2 Exclusion criteria

Cases from the NIOH specimen storage with lungs that were poorly preserved or diseased (reported to have tuberculosis, lung cancer, emphysema, coal worker's pneumoconiosis, silicosis, or a combination thereof, on pathological examination) were excluded. Poorly preserved or autolysed organs are referred to as biological tissues or organs that have degraded, deteriorated, or sustained damage due to inadequate preservation methods or adverse conditions. This could be due to insufficient or no preservation, improper use of formalin preservative, or delayed preservation, leading to autolysis. The general protocol for the neuropathology study on manganese-exposed mineworkers is that lungs and brain should be removed not more than 5 days from the date of death and immediately preserved in 10% buffered formalin before it can be shipped to the NIOH.

2.5 Sample Size Estimation

The sample size was calculated using the only study that used human post-mortem tissue sampled from deceased mineworkers from South Africa by Gonzalez-Cuya et al. (2014). The current study quantifies manganese concentrations in the lungs of deceased manganese-exposed mineworkers whose brains were removed for neuropathology studies and correlates these concentrations with those found in the brains of the same subjects, which were also used by Conzalez-Cuya *et al.* (2014). The same authors reported quantitative histopathology with immuno-histochemistry in manganese-exposed and manganese-unexposed mineworkers in South Africa (79). The minimum sample size was calculated using a power of 80%. The effect size is an integral part of the sample size calculation. The effect size was defined as the difference in mean manganese levels between the manganese-exposed and manganese-unexposed groups.

The sample size was calculated based on the comparison of means using Stata 17 software. From the study of Gonzalez-Cuyar *et al.* (2014), the mean of the microglial

densities in the external segments of the globus pallidus in the brains of people exposed to manganese was 1.33 (SD 0.55), while the mean of those who were not exposed to manganese was 0.87 (SD 0.34). Assuming a power of 80% confidence level, a statistical significance level of 0.05, and a ratio of 1:3 for the population of manganese-exposed and manganese-unexposed, the sample size for this study was calculated to be 60 (15 manganese-exposed and 45 manganese-unexposed mineworkers) (Table 1). A ratio of 1:3 was used based on the small number of available manganese-exposed lungs compared to manganese-unexposed lungs at the NIOH.

The study used the general formula for sample size calculation for comparing two independent groups (manganese-exposed vs manganese-unexposed) as shown below:

$$n_1 = \frac{(Z_{\alpha/2} + Z_{ß})^2 . [p_1 (1-p_1) + r . p_2(1 - p_2)]}{\Delta^2}$$

$$n_2 = r. n_1$$

Where:

- n_1: Sample size for manganese-exposed mineworkers
- n_2: Sample size for manganese-unexposed mineworkers
- r: Ratio of control to exposed group (r = 3 for a 1:3 ratio)
- $Z_{\alpha/2}$: Z-value for the significance level (two-tailed, $Z_{\alpha/2}$ = 1.96 for α = 0.05)
- Z_{β}: Z-value for the power (80% power corresponds to Z_{β} = 0.84)
- p_1: Expected proportion or mean in the exposed group.
- p_2: Expected proportion or mean in the control group.
- Δ: Minimum detectable difference between p_1 and p_2 (effect size)

***Table 1**. Study sample size calculation**

Study Parameters		
Alpha = 0.0500 Power = 0.8000 Delta = -2.9681		
Miners (estimated sample sizes)		
Manganese-exposed (N1 = 15)		Manganese-unexposed (N2 = 45)
Mean	1.3300	0.8700
SD	0.5500	0.3400
N total = 60		
N2/N1 = 3.0000 (estimated ratio)		

*based on the mean of the microglial densities by Gonzalez-Cuyar *et al.* (2014).

2.6 Study Sample

Manganese-exposed mineworkers were matched on period of exposure (within five-year exposure intervals). The sample size was calculated to examine a minimum of 15 manganese-exposed and a minimum of 45 manganese-unexposed mineworkers on a ratio of 1:3; thus, a minimum total of 60 lungs were to be used for the study. Subsequently, a total of 64 lungs (16 manganese-exposed and 48 manganese-unexposed) were available and used for the study. Purposive sampling was selected based on the characteristics of the population and the study's objectives.

2.7 Study Site

In South Africa, platinum mines and manganese deposits occur in different regions. The Kalahari manganese fields are located in the Northern Cape province, whereas platinum mines are situated in the Northwest province of South Africa, known as the platinum province. Lungs of deceased manganese-exposed mineworkers were removed by a doctor appointed by Professors Nelson and Racette for their neuropathology study in the manganese mining areas in the Northern Cape province and by prosectors in the platinum mining areas in the Northwest province of South Africa. The lungs were macro- and microscopically examined at the NIOH, and analytical chemistry and histological processes were performed at the University of Johannesburg.

2.8 Data Collection

2.8.1 Data sources

The study used the following four data sources:

i) PATHAUT database

The PATHAUT database managed by the NIOH in South Africa is a valuable resource for research on occupational diseases. PATHAUT includes data on autopsies of deceased mineworkers and ex-mineworkers, focusing on cardiorespiratory tissue analysis. This database is particularly useful for investigating the histopathological impacts of various occupational exposures, including manganese dust in the mining industry and demographic data of deceased mineworkers (sex, date of birth, date of death, age at death, mining period of exposure, cause(s) of death, as well as autopsy pathology findings). Demographic data were extracted from the PATHAUT database, described, and summarized onto an Excel spreadsheet.

ii) The MBOD records

The MBOD is an organization in South Africa that plays a crucial role in recognizing and addressing occupational diseases. The MBOD is underpinned by the Occupational Diseases in Mines and Works Act (1973) (70). The MBOD is responsible for identifying, assessing, and formally acknowledging occupational disorders through conducting in-depth medical evaluations and generating detailed reports addressing causation for confirmed cases of occupational diseases (123). The MBOD maintains detailed medical records of mineworkers, including those related to respiratory diseases, which are prevalent in the mining industry.

The MBOD provided detailed hard copy files of deceased mineworkers' medical records from their archives, which were reviewed to extract comprehensive work histories.

iii) Lungs of manganese-exposed and manganese-unexposed deceased mineworkers (primary data).

The researcher generated two spreadsheets: one for manganese concentrations found in the lungs and another for histology data of the lungs of deceased mineworkers, for this study.

iv) Neuropathology database

A neuropathology database (secondary data) was provided by Professors Nelson and Racette, which was generated from a neuropathology study. This database includes manganese concentration data from the brains of deceased mineworkers from South Africa. The sections sampled for manganese concentrations in the brain comprised the cerebellum, caudate, putamen, globus pallidus externus, and globus pallidus internus. These sections were selected based on their vulnerability to manganese accumulation, functional relevance to manganese toxicity, and pathophysiological insights into phenomena such as Parkinson's disease, to provide an understanding of the broader implications of neurotoxicity and its impact on health. The data were generated using the MC-ICP-MS technique, which was subsequently used for the analysis of manganese concentrations in the lungs of the same deceased mineworkers. This database was used to compare and correlate manganese concentrations in the brains and those found in the lungs of deceased manganese mineworkers.

2.8.2 Tools used for data collection

The study used spreadsheets to collect data for manganese-exposed and manganese-unexposed cases.

2.8.2.1 Spreadsheet for manganese-exposed cases

The spreadsheet from the neuropathology study database contained critical information useful for this study. Information provided on manganese concentrations included the specific NIOH case numbers, date of birth, date of death, age at death, sex, race, clinical cause of death, NIOH autopsy clinical findings, and the total number of years exposed to manganese per mineworker. The database comprised 92 cases spanning the period from 2008 to 2022.

This information was verified against the list extracted from the NIOH PATHAUT database. Part of the verification included checking whether samples were still available at the NIOH specimen storage or if they had been routinely discarded. The available cases were then selected and set aside for the study. Pathology reports of

the available manganese-exposed cases were downloaded from the PATHAUT database, and files were extracted from the MBOD to further validate their exposure history.

2.8.2.2 Spreadsheet for manganese-unexposed cases

A list of deceased manganese-unexposed mineworkers exposed exclusively to platinum was extracted from the PATHAUT database using Stata 17 software. A spreadsheet was then formulated to transfer information from the PATHAUT database. Information on the manganese-unexposed cases also provided important details, as described above for the manganese-exposed cases, which were useful for the study. Hard copy files of the deceased manganese-unexposed mineworkers whose lungs were available at the NIOH specimen storage were retrieved from the MBOD, also to verify against the PATHAUT extracted list and to review records to exclude other diseased lungs with any or a combination of tuberculosis, lung cancer, emphysema, coal mineworkers' pneumoconiosis, and silicosis. Comprehensive work histories were also retrieved from the MBOD hard copy files.

2.8.3 Grouping of cases

Cases were grouped according to period of exposure. Fifteen-year exposure intervals were implemented for both the manganese-exposed and the manganese-unexposed mineworkers. These were grouped for matching at a ratio of 1:3, with manganese-exposed and manganese-unexposed groups for comparison.

2.8.4 Lung tissue preparation

Cases selected for the study were removed from the NIOH specimen storage.

2.8.4.1 Lung tissue wash up

Routinely, lungs that have been examined to determine compensable diseases at the NIOH are further preserved in 10% formalin and stored, awaiting a prescribed NIOH period before being discarded. During autopsy examination, the lungs were sliced into thin pieces to further examine for occupational lung diseases. To prepare these lungs for the study, the researcher individually removed the lung slices from the storage buckets and thoroughly washed the lungs in running tap water for over 24 hours to remove formalin before separating slices of the right lung from slices of the left lung.

The separation of the lung slices subsequently allowed sampling of specific lobe tissue sections for analytical chemistry and histological analysis.

2.8.4.2 Selection of lung slices

The right lung was used for the study. The right lung tends to receive slightly more ventilation and perfusion than the left, because the right main bronchus is wider, shorter, and more vertical than the left main bronchus, making it a better indicator of the overall exposure in occupational lung diseases due to its size and position (124). Many occupational pathology and forensic protocols recommend using the right lung to maintain consistency and comparability between cases and across studies. Slices of the right lung were selected for each case, separating a right lung slice from the left by matching the number of lobes. Normally, the right lung is identified by three lobes and the left by two lobes, as described in the Human Anatomy Colour Atlas and eBook Textbook (125). The right lung slices were distinguished from the left by the number of lobes and primary bronchi entering the hilum. On the right lung, the bronchus is parallel to the pulmonary artery, whereas in the left lung, the main/primary bronchus is below the pulmonary artery (125), as shown in Figure 4 A & B.

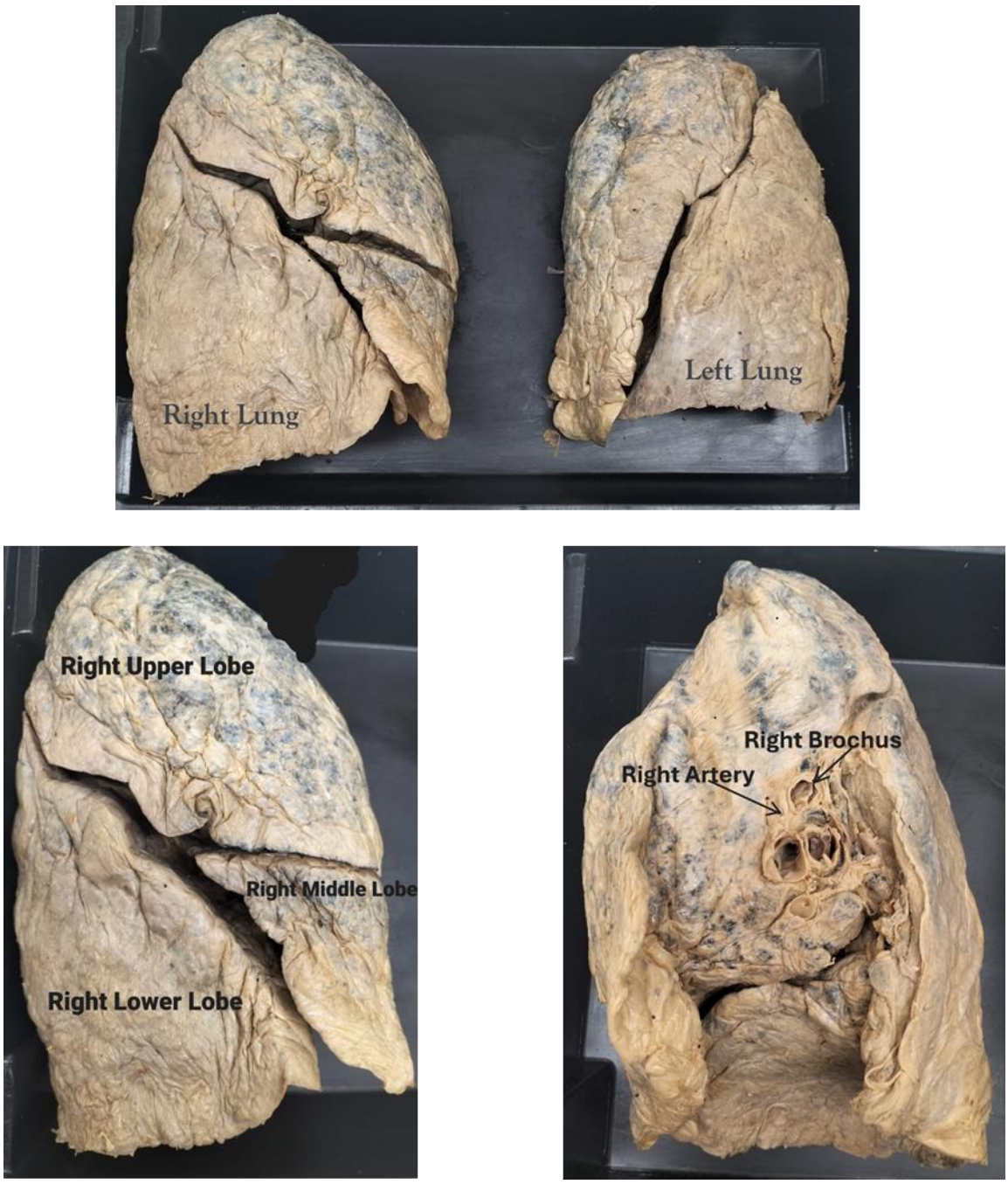

Figure 4. *Gross pulmonary anatomy of the right lung*

Photo credit: Julian Mthombeni (2025)

2.9 Lung Tissue Sampling

Right lung slices with three lobes (Fig. 5) were selected for tissue sampling. Two sections were sampled from the upper lobe, one from the middle lobe, and three from the lower lobe, totalling six sections per lung. All sampled sections were cut using ceramic scissors and knives. Sampled sections were preserved in 10% buffered formalin for subsequent processing. These sections were used for the quantification of manganese concentrations (objective 1), mapping of manganese deposition (objective 2), and for histopathological analysis *(*objective 3*).*

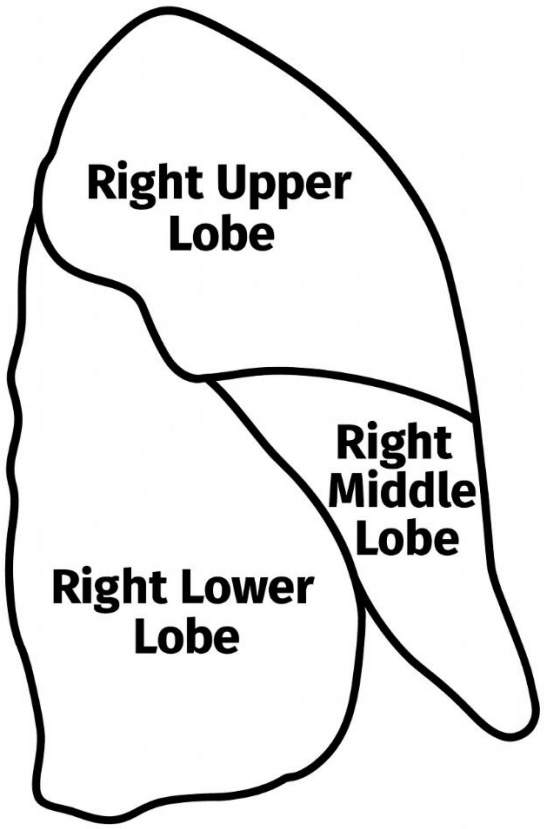

Figure 5*. Schematic diagram of the right lung showing three lobes*

Schematic credit: Julian Mthombeni (2025)

2.10 Tissue Treatment and Processing

Tissue samples were further fixed in 10% buffered formal saline for 24 hours in the laboratory. After 24 hours, samples were subdivided into two groups each. One section was used to quantify the manganese content (objectives 1 and 2), and the other for histological analysis (objective 3).

For objectives 1 and 2, the manganese concentration in formalin-fixed lung tissue was analysed using a Multi-Collector inductively coupled plasma–mass spectrometry (MC-ICP-MS), a rapid and powerful analytical multi-element technique for determining trace elements in biological samples and their concentrations. (126). MC-ICP-MS is a versatile analytical technology that has revolutionized trace element analysis across various scientific disciplines. Its great sensitivity, multi-element capabilities, and flexibility to varied sample types make it a vital method in modern analytical laboratories. (114). MC-ICP-MS is a preferred technique due to its exceptional sensitivity, minimal detection thresholds, and capacity to manage intricate matrices (127), rendering it a vital instrument in several scientific research areas, in life sciences, clinical diagnostics, and industrial fields (128). Manganese concentrations were then mapped for the different lobes. The equipment was supplied by PerkinElmer South Africa (Pty) Ltd.

2.10.1 Tissue preparation and processing for MC-ICP-MS

Sampled pieces of lung tissue (64 cases x 6 sections) selected were freeze-dried using an OLB-FD 10/12/18 series version AO 202108 freeze dryer, supplied by Lasec Group, South Africa, following a protocol by Molnar *et al.* (2021). Samples were labelled following the sampling scheme, which matched the numbers allocated for each case. Freeze-drying is widely used to preserve cells and tissues in the dry state. Freeze-drying involves both freezing and drying phases, each of which imposes distinct physicochemical stresses on biomaterials. Collected tissue samples were cut into small (~20 mm^3) pieces and stored at −80 °C for 24 hours, optimally arranged in 2 mL plastic tubes to maximize the surface area. Tubes remained open throughout the entire drying process. Sublimation of the samples was monitored using a Pt100 temperature sensor placed in the centre of a chosen piece of tissue. A Pt 100 temperature sensor was also supplied by Lasec Group, South Africa. Dried tissue products were manually smashed with 5 mm ceramic balls into powder. Powdered tissue samples were

subsequently relabelled and taken to an analytical chemistry laboratory for MC-ICP-MS analysis. Ultra-cleaning of the microwave vessels was crucial to ensure the purity of the samples.

2.10.1.1 Ultra cleaning of the microwave vessels

Cleaning of microwave vessels using nitric acid (HNO_3) and 18.2 Mohm/cm ultrapure water, both supplied by Merck (Pty) Ltd, was a crucial step that ensured that previous debris did not interfere with the concentrations of trace elements in the incoming samples. Cleaning of microwave vessels was carried out by first rinsing the 24 x 100 mL vessels that fit into one microwave carousel with tap water. A portion of 10 mL of concentrated HNO_3 was added to each vessel. Vessels were loaded into a MARS 6 one-touch technology Microwave Oven digestor supplied by SpectraLab Scientific, and an Xpress clean program was run at 153°C for approximately 25-30 minutes. After the cleaning phase, the vessels were allowed to cool to room temperature, and the acid was disposed of in an acid waste container. It was essential to ensure that the acid fumes were released slowly, in the opposite direction to the researcher's face, under a fume cupboard upon opening the vessels. Thereafter, the vessels were thoroughly washed with ultra-purified water and air-dried before being used for solid digestion.

2.10.1.2 Solids digestion

Approximately 0.25g of powdered tissue from each sample was weighed accurately to the nearest 0.1 mg using a MetterToledo XP205 analytical balance supplied by Microsep (Pty) Ltd, and each sample was transferred to microwave digestion vessels. A 10 mL volume of suprapure HNO_3 was measured and added to each sample. Labelled vessels were placed in a MARS 6 one-touch technology Microwave Oven digester, where the vessels were ramped to 200 °C for 25 minutes and allowed to cool for an additional 10 minutes.

Samples (640 in total) were then quantitatively transferred to labelled 50mL volumetric flasks; rinsed the remaining content of the vessels with 18.2 Mohm/cm ultrapure water and gradually added to the flask, followed by gently swirling the flask to mix the solution thoroughly to make up to the 50 mL mark of stock solution. The flasks were stoppered and inverted several times to ensure the solution was homogenously mixed. A 1000 µL of each stock solution was pipetted into labeled 15 mL tubes and made up to the

10 mL mark with 1% suprapure HNO_3. Every tube used was labelled with a corresponding number initially issued for correlation samples.

A control for the trace elements was measured using a PerkinElmer Nexion 300 MC-ICP-MS with calibration standards at 0, 0.1, 1, and 10 µg/L, prepared from certified stock solutions purchased from Accutrace standards. The calibration standards produced a linear regression line (Instrument response against concentration), which was used to determine the concentrations of elements in the samples. The instrument calibration was verified by preparing and analysing INTCL plant Certified Reference Material (CRM) (Annexure 1).

The 15 mL tubes containing 10 mL of the final samples were then transferred to an MC-ICP-MS vial for concentration analysis. The autosampler used with the MC-ICP-MS instrument had a maximum capacity of 60 vials at a time for analysis. Analysis took approximately 4 hours per batch of 60 samples to completion. Thereafter, manganese concentrations were estimated from each of these samples taken from each lobe.

2.10.2 Data handling and processing for MC-ICP-MS

2.10.2.1 Manganese concentration calculations

Manganese raw intensities were downloaded from the MC-ICP-MS-linked computer to calculate manganese concentrations for all samples. After sample analysis, raw signal intensities corresponding to ^55Mn were obtained from the MC-ICP-MS system software. These intensities were converted to concentrations and initially expressed in micrograms per Liter (µg/L), representing the manganese concentration in the liquid digestate of each sample.

A unit conversion was performed to express concentrations in milligrams of manganese per kilogram of dry tissue weight (mg/kg), normalising manganese concentrations relative to the original solid tissue mass. The conversion formula applied was:

Mn (mg/kg) = Mn (µg/L) × 0.05 / sample weight (g), where 0.05 L represents the total volume of acid used for digestion (typically 50 mL), and the sample weight refers to the dry mass (in grams) of lung or control tissue weighed prior to digestion.

This conversion enables standardized comparisons of manganese content across different samples, regardless of initial volume or mass discrepancies. All calculated

manganese concentrations were tabulated and exported for downstream statistical analyses, including correlation and regression modelling. Furthermore, the data were geocoded and used in the spatial mapping of manganese distribution patterns in lung tissue sections.

2.10.2.2 Manganese depositions mapping

The spatial deposition and distribution of manganese content and concentrations in the lobes of the lung tissue of deceased mineworkers in South Africa were mapped using manganese concentrations generated for Objective 1. Manganese mean concentrations were discussed and described in terms of their weight per unit area of the lung. Diagrams of the outlines of the right lung were produced using Mind the Map scientific image and illustration software.

2.10.3 Tissue preparation for histology

Three stains were employed for histology techniques. H&E is used for general lung architecture, MT is used for collagen deposition, and Reticulin is used for reticulin fibres. Slides for H&E were stained using the Thermo Scientific Gemini AS automatic stainer, supplied by Thermo Fisher Scientific. The other stains were conducted manually according to the staining protocol outlined in Annexure 2. The H&E technique was employed to demonstrate tissue structures and cellular details, while the MT stain was valuable for highlighting collagen fibre structures and quantifying vascular density per mm^2 in tissue samples of the lungs of the manganese-exposed and manganese-unexposed deceased mineworkers, whereas the Reticulin stain helped in evaluating the distribution and architecture of reticular fibres, which can serve as a potential tissue marker of fibrosis severity (107).

Sections of the lobes were further micro-dissected (10 by 10 mm) and processed for histology in an automatic tissue processor (HistoCore PEARL Tissue Processor) and embedded in paraffin wax using a Leica EG1150 Tissue Embedding machine to form blocks, both of which were supplied by Leica Biosystems. A total of six blocks, representing three lobes per lung (3 upper lobes, 1 middle lobe, and 2 lower lobes), were prepared per case. For the 64 cases, 384 blocks were embedded with paraffin wax. Blocks were sectioned to prepare slides for staining. For the 64 cases, 2304 slides were generated, of which half (1152 slides) were stained with H&E, MT, and Reticulin stains, and the other half (1152 slides) were set aside for spares. Annexure 2

represents the protocol used for each of the histochemistry stains. Histochemistry reagents used were purchased from Labotec (Pty) Ltd.

Blocks representing sections of each lobe were sectioned at 3 microns (μ) using a Leica RM2125 RTS rotary microtome, also supplied by Leica Biosystems.

2.10.4 Masking of histology slides

After staining with histochemical stains (H&E, MT, and Retic), the slides were sent to the study co-supervisor, a registered pathologist, for relabelling to blind the researcher. Blinding mitigates the potential for intentional or inadvertent bias in outcomes, thereby enhancing the reliability of study conclusions. (129). Slides were relabelled with random numbers generated by the pathologist to eliminate bias. Case numbers were only revealed after the analysis was complete.

2.10.5 Assessment of histochemistry slides

For histochemistry (H&E, MT, and Reticulin stains), an independent, registered pathologist specialised in anatomical pathology assessed the slides and assisted with interpreting the findings. The pathologist's area of expertise is pulmonary pathology, which aligns with the study's objectives. Stained slides were assessed for inflammation and collagen deposition using a Leica ICC50 W microscope supported by a scoring card (Annexure 3).

The classification of inflammation and fibrosis was designed to incorporate both severity and extent of tissue involvement. Severity was graded according to established histopathological criteria and described using a quantitative four-level scale, where 0 = absent or <10% involvement, 1 = mild (10–30%), 2 = moderate (30–60%), and 3 = severe (>60%). The extent was defined as the proportion of the tissue section affected and evaluated using a descriptive categorisation, where focal denoted pathology confined to a single lobe, and diffuse indicated involvement of more than one lobe. This combined framework allowed for a nuanced assessment, capturing both the intensity and distribution of pathological changes. This dual-parameter framework provided a comprehensive assessment, enabling differentiation between cases with limited but intense pathology and those with more widespread but comparatively milder alterations. The fibrosis classification applied in this study followed the standardized histopathological grading system proposed by Ashcroft *et al.* (1988) (130).

The pathologist utilized her expert knowledge in pulmonary pathology to identify inflammation, which may have been related to an infection or smoking, and fibrosis, which may have been related to smoking or any of the pneumoconioses (silicosis, coal workers' pneumoconiosis, mixed dust fibrosis, and asbestosis). A total of 43 cases were removed from the study.

Quantitative data collected during slide review (Annexure 3) were computed onto a spreadsheet for statistical analysis, and qualitative analysis was documented and subsequently discussed.

2.10.6 Other data

Additional data for covariates were obtained from the NIOH and MBOD autopsy records. These included clinical characteristics and detailed records of mining exposure. Mining exposure records showed the period during which individual mineworkers had worked in the mines, in years and months. Mineworkers typically work 45 hours per week, with a maximum of nine hours per day for a five-day work week and 8 hours per day for a six-day work week, as per the Mine Health and Safety Act (No. 29 of 1996) (131).

2.11 Data Management

A total of five Excel spreadsheets of datasets were compiled for this study. These included: (132) PATHAUT data detailing and summarizing demographic characteristics of deceased mineworkers; (1) MBOD records provide comprehensive occupational histories of study participants. (1) primary analytical data from manganese concentration measurements obtained using an MC-ICP-MS; (133) Primary histopathological data for inflammation and fibrosis assessment, and (5) secondary neuropathological data on regional brain manganese concentrations, sourced from the Washington University neuropathology study.

Histological photomicrographs were captured during tissue analysis and stored as Joint Photographic Experts Group (JPEG) files. All electronic data, including images and Excel spreadsheets, was securely stored in a password-protected cloud-based repository. Access was restricted to the primary researcher, who granted access to supervisors as needed to maintain data privacy and security.

2.12 Data Analysis

For objective 1, the demographic characteristics of the mineworkers were described using frequencies and percentages for categorical variables, while continuous variables, such as age, were described using means and standard deviations. The means of manganese concentrations for the sampled portions of the lobes were calculated and recorded on a spreadsheet. Average manganese concentrations were calculated for each lobe (upper, middle, and lower).

The Shapiro-Wilks test was used to check if the manganese concentrations in the lungs were normally distributed. ANOVA was used to compare the means, followed by Tukey's post hoc test. Data for the full lung was computed by finding the averages of the lobes for all cases. A t-test was used to compare the means of the lungs for the two groups to test for significant differences in their means.
For objective 2, the Mind the Map software was used to illustrate and map manganese concentrations in the lung and produced diagrams.

For objective 3, an Olympus BX43 light microscope was used to review histopathology slides to produce data, which was subsequently analysed using Pearson's Chi-square test. Histopathology data were used to explore the relationship between manganese exposure and inflammation and manganese exposure and fibrosis. Histology photomicrographs were taken using a Leica DM1000 LED microscope with a camera. Photomicrographs were produced, and images were converted into high-contrast, binary (black and white) images, which were used for Threshold analysis.

For objective 4, manganese concentrations in the brains were also tested for normality using the Shapiro-Wilks normality test. Pearson's correlation test was conducted. Manganese concentrations in the brains of deceased manganese-exposed mineworkers and manganese concentrations in the lungs of the same mineworkers were correlated using primary data from objective one and secondary data from the neuropathology study. A relationship between manganese in the brain and manganese in the lungs was explored using Locally Weighted Scatterplot Smoothing (LOWESS) and a generalization of linear regression, the Generalized Additive Model (GAM).

2.13 Ethical Considerations

Ethical clearance was obtained from the University of the Witwatersrand Human Research Ethics Committee (Medical), Clearance certificate no. M210401 (Annexure 4) before data collection. Permission letters from the custodians of the PATHAUT database and access to the lungs of the deceased subjects were obtained from the head of the Pathology department at the NIOH (Annexure 5). Permission to access files at the MBOD was also obtained from the MBOD Director (Annexure 6). Furthermore, the study supervisors provided permission to use the neuropathology study results for the fourth objective (Annexure 7). Generally, for all deceased mineworkers, the next-of-kin signs an NIOH-informed consent for the autopsy procedure (Annexure 8). In addition, specifically for manganese-exposed deceased mineworkers, a second autopsy consent form (INFORMATION LEAFLET AND INFORMED CONSENT for the next-of-kin of manganese-exposed mineworkers) is signed to allow removal of the brain for the neuropathology of chronic manganese exposure study. Next-of-kin provided informed consent for the autopsy procedure, and a neuropathology of chronic manganese exposure family questionnaire was conducted, giving health and lifestyle information, including medical history, alcohol consumption, smoking history, and any other relevant medical information (Annexure 9).

All data was kept confidential. The researcher and the supervisors had sole access to data kept in a password-protected file. The pathology material will be stored for two years following the completion of the study, after which it will be destroyed using the standard University of Johannesburg waste disposal procedure.

CHAPTER THREE – RESULTS

3.1 Introduction

This chapter presents a detailed narrative, along with supporting tables and figures, that illustrate the findings of this study. Results are presented according to the study's objectives, starting with a description of the demographic characteristics of the study participants. The concentrations and areas in the lungs in which manganese was found (depositions) are presented. This is followed by a comparison of the histological features in the lungs of manganese-exposed and -unexposed mineworkers included in the study. Lastly, the outcome of the correlation of the manganese concentrations in the lungs and the brains of deceased manganese-exposed mineworkers is also described.

3.2 Demographic Characteristics of Study Participants

3.2.1 Manganese-exposed mineworkers

There were 92 cases of deceased mineworkers who were autopsied from 2008 to 2022 on the neuropathology database. Since this study concentrated on the period 2010 to 2020, 13 (14%) cases fell outside the study period. The cases outside the study period comprised one case from 2008, 11 (12%) cases from 2009, and another case from 2022. A pool of 79 (86%) cases was within the study period and available for the study. Of the 79 cases of deceased mineworkers, 46 (58%) were exposed to manganese only, therefore meeting the selection criteria. The other 33 (42%) had mixed exposures. At the time of this research, 16 (35%) cases of lung were available at the NIOH specimen storage, and they met the selection criteria. All 16 lungs were sampled for the study as per Annexure 9. Thirty (65%) lungs had already been discarded following NIOH routine procedures. Based on the sample calculation in Table 1, a comparison of one manganese-exposed versus three manganese-unexposed lungs was used in this study, with a sample of 16 manganese-exposed and 48 manganese-unexposed lungs.

3.2.2 Demographic characteristics of the manganese-exposed mineworkers

Demographic data of the manganese mineworkers included in the study are tabulated in Annexure 9. This demographic data included the mineworkers' age at death, year of death, work histories, causes of death, and autopsy findings. The study participants

were all men who died between 2010 and 2020. The study participants' characteristics are summarized in Table 2. The mean age of manganese-exposed mineworkers was 54 ± 9.879 years, ranging from 33 to 71 years, with a median of 56.0 years. The manganese mineworkers were exposed for an average of 22.83 ± 10.81 years, with a minimum exposure of 4.4 years and a maximum exposure of 39.7 years, and a median of 25.5 years.

Table 2. *Demographic and work characteristics of study participants*

	Mn-exposed (n=16)		**Mn-unexposed (n=48)**	
	Mean ± SD	Median	Mean ± SD	Median
Age at death (years)	54.0 ± 9.880	56.0	53.2 ± 6.410	53.0
*Years worked	22.8 ± 10.810	25.5	20.9 ± 8.170	21.7
Cause of death				
	n	%	n	%
Natural	15	94	37	77
Unnatural	**1**	6	10	21
Under investigation	0	-	1	2
Age distribution (years)				
	n	%	n	%
30 - 45	3	19	6	13
46 - 60	9	56	24	50
61+	4	25	18	47
Duration of exposure (years)				
	n	%	n	%
1 - 15	5	31	12	25
16 - 30	4	25	17	35
31+	7	44	19	40

*Number of years and months exposed to mining dust

Clinical causes of death were according to information extracted from the PATHAUT database. In contrast, NIOH findings were the findings of the pathologist after the examination of the heart and lungs at autopsy. Most 15 out of 16 (94%) of the clinical causes of death were reported as “Natural causes”, with two having a specific pathologic cause of death (Hyperglycaemia and Varicella). Only one manganese-

exposed mineworker died of unnatural causes (6%) (a wound on the right temporal area with possible depressed fracture of the skull), Annexure 9. Whereas for platinum-exposed deceased mineworkers, there were more incidences of unnatural death, including blunt force, multiple injuries, and carbon monoxide poisoning, amongst others, Annexure 10.

3.2.3 Manganese-unexposed mineworkers

There were 1295 platinum-only exposed cases of mineworkers on the platinum-only exposed spreadsheet who died and were autopsied at the NIOH from 2010 to 2020. Some cases from 2010 to 2013 (526 cases, 41%) had already been discarded as per the NIOH processes. This left 769 (59%) platinum-only exposed lungs of mineworkers for the period 2010 to 2020 available at the NIOH specimen storage for the study. Of the 769 cases, 438 (57%) had tuberculosis, 24 (3%) had emphysema, and 13 (1.7%) had lung cancer as per the NIOH pathology findings. These cases were excluded, leaving 294 (38%) cases to select from for the study. A systematic sampling method was used to select 48 (16%) cases of platinum-only exposed lungs from the 294 lungs available at the NIOH specimen storage for the study. The 294 cases of lungs were given a randomly generated number from 1 to 294. A total of 48 lungs were randomly selected using a Google number generator software tool. This was double-checked by verifying the total count to ensure that exactly 48 lungs were selected, which validated proportionality and randomness. This systematic approach ensured unbiased selection while adhering to the desired sample proportion.

3.2.4 Demographic characteristics of the manganese-unexposed mineworkers

The demographic characteristics of the manganese-unexposed mineworkers included in the study are presented in Annexure 10. This data included the mineworkers' age at death, year of death, work histories, causes of death, and autopsy findings. The study participants were all black men who died in the period 2010 - 2020. The mean age of manganese-unexposed mineworkers was 53.2 ± 6.350 years, ranging from 35 to 68 years of age, with a median of 53.0 years (Table 2). The manganese-unexposed mineworkers were exposed to platinum dust for an average of 20.9 ± 8.170 years, with the minimum exposure being 3.8 years and the maximum being 39.9 years. The median exposure time for this group was 21.7 years, as shown in Table 2.

Similar to the manganese-exposed group, the majority of clinical causes of death in this cohort, 37 out of 48 cases (77%), were recorded as "natural causes," with seven cases specifying pathologic causes such as cardiovascular, respiratory, infectious, or other organ-specific/systemic diseases. Additionally, 10 out of 48 individuals (21%) died from "unnatural causes". However, there was one case contributing 2% that did not have a cause of death and was reported as under investigation (Annexure 10).

3.2.5 Lung pathologies in manganese-exposed vs unexposed groups

Lung pathology was more than twice as common in the manganese-exposed group (87.5%) compared to the manganese-unexposed group (39.6%). Both groups showed similar lung conditions (e.g., pneumonia, emphysema, pulmonary oedema), but the frequency of these pathologies was higher in the manganese-exposed group.

3.2.6 Groups of cases based on age (15-year intervals)

The ages of manganese-exposed and unexposed mineworkers ranged from 35 to 75 years (Table 2) and were grouped in 15-year intervals. Both groups showed a peak in frequency within the 46–60-year age range, representing the most common interval for age at death. The frequency distribution then declined gradually in older age categories. Across all intervals, the manganese-unexposed group generally had a higher case count than the exposed group. Despite differences in absolute numbers, the overall age distribution pattern was similar between the two groups, with a central peak followed by a tapering decline.

3.2.7 Groups of cases based on duration of years worked (15-year intervals)

The comparison of the duration of years worked between manganese-exposed and -unexposed mineworkers, grouped by years worked (in intervals of 15 years), is displayed in Table 2. The periods of exposure ranged from 4.4 to 39.9 years for the eight interval groups. The highest peak for both the manganese-exposed and unexposed groups was in the range of 31+ years of work. The distribution pattern in the two groups was slightly skewed to the right (Table 2).

3.3 Mapping of Manganese Concentrations in the Lungs

The manganese concentrations in the total lung tissue were normally distributed in both groups, as determined by the Shapiro-Wilk test ($p = 0.146$ and $p = 0.957$ for the

manganese-exposed and unexposed groups, respectively); the concentrations were also normally distributed in the individual lobes (Table 3).

Table 3. *Distribution of manganese concentrations in the lungs**

	Manganese-exposed (n-16)			**Manganese-unexposed (n=48)**		
Full lung p-value	0.146			0.957		
LUNG REGIONS	UL	ML	LL	UL	ML	LL
Actual concentration values (µg/g) (Mean±SD)	1.580 ±0.363	1.160 ±0.590	1.105 ±0.411	1.100 ±0.568	1.040 ±0.605	0.965 ±0.400
Lobe p-value	0.579	0.611	0.085	0.061	0.230	0.156

UL: upper lobe, ML: middle lobe, LL: lower lobe

*Test of normality: Shapiro-Wilk test

3.3.1 Lung manganese concentration comparison

The right lungs were tested for manganese content. Total lung manganese concentrations were computed and compared between the manganese-exposed and the manganese-unexposed groups using a student t-test at a 0.05 confidence level. Manganese concentrations in the lungs of deceased manganese-exposed mineworkers (1.263 ± 0.343) were statistically significantly different from those in manganese-unexposed mineworkers (1.033 ± 0.413) at p =.0.049. However, the manganese mean distribution pattern showed similarities between the two groups.

*Table 4. Mapping of manganese concentration by lung lobe**

Lobe		Manganese-exposed (n=16)	Manganese-unexposed (n=48)
	No. of samples	Mean±SD	Mean±SD
Upper	3	1.580 ± 0.363	1.100 ± 0.658
Middle	1	1.160 ± 0.590	1.040 ± 0.605
Lower	2	1.050 ± 0.411	0.965 ± 0.400
Total lung	6	1.263 ± 0.260	1.033 ± 0.042

*Analysis of variance (68)

3.3.2 Lobar manganese concentration comparison

A comparison of the distribution of manganese in the lungs, broken down by lobes and mapped, is shown in Table 4. Since data were found to be normally distributed, total lobar manganese concentrations were computed and compared among lobes (upper, middle, and lower) for the manganese-exposed vs the manganese-unexposed using one-way ANOVA followed by Tukey's multiple comparison, post hoc test to find significant differences of the means for the lobes. Data were reported as mean ± standard deviation, with significant differences indicated by p-values, showing where the manganese deposition was notably higher in exposed individuals.

In the manganese-exposed group, the mean manganese concentration was highest in the upper lobe (1.580 ± 0.363 mg/kg), compared to the middle (1.160 ± 0.590 mg/kg) and lower lobes (1.050 ± 0.411 mg/kg), as shown in Table 4. However, these differences were not statistically significant at the 95% confidence level (p = 0.357), indicating no significant variation in manganese concentrations across the lung lobes.

Whereas, for the manganese-unexposed group, the upper lobe showed a similar pattern with the highest mean (1.100 ± 0.568) from the middle (1.040 ± 0.605) and the lower lobes (0.965 ± 0.400) at (p = 0.357). The lower lobe showed the lowest mean amongst the three lobes in both manganese-exposed (1.050 ± 0.411) and manganese-unexposed (0.965 ± 0.400) groups, Table 4.

Further analysis using Tukey's multiple comparison post hoc test, Table 5 compares each mean of manganese-exposed lobes against the means of other manganese-

exposed lobes and manganese-unexposed lobes. Tukey's test showed that the most significant mean difference was in the upper lobe (1.580 ± 0.363) of the manganese-exposed group in comparison with the lower lobe (0.965 ± 0.400) for the manganese-unexposed group at *p*= 003, Table 5. The results showed statistically significant differences in a few comparisons, notably between Mn-e UL and Mn-u UL (p = 0.036), Mn-e UL and Mn-u ML (p = 0.009), and Mn-e UL and Mn-u LL (p = 0.003).

Table 5. *Multiple comparisons of manganese concentrations by lung lobe**

Comparisons pair	Summary	*P*-value
Mn-e vs Mn-e		
Mn-e LL vs Mn-e ML	ns	0.992
Mn-e LL vs Mn-e UL	ns	0.991
Mn-e ML vs Mn-e UL	ns	0.176
Mn-e vs Mn-u		
Mn-e LL vs Mn-u LL	ns	0.995
Mn-e LL vs Mn-u ML	ns	0.948
Mn-e LL vs Mn-u UL	ns	1.000
Mn-e ML vs Mn-u LL	ns	0.872
n-e ML vs Mn-u ML	ns	0.676
Mn-e ML vs Mn-u UL	ns	0.985
Mn-e UL vs Mn-u LL	**	0.003
Mn-e UL vs Mn-u ML	**	0.009
Mn-e UL vs Mn-u UL	*	0.036
Mn-u vs Mn-u		
Mn-u ML vs Mn-u LL	ns	0.999
Mn-u LL vs Mn-u UL	ns	0.998
Mn-u ML vs Mn-u UL	ns	0.963

*Tukey's post-Hoc test

Mn-e = Manganese-exposed; Mn-u = manganese-unexposed; UL = Upper Lobe; ML = Middle Lobe, and LL = Lower Lobe. Superscripts show significant differences where *p<0.01, **p<0.001, and ns (no statistically significant differences) p>0.05.

Lastly, the remaining groups showed no significant differences, as indicated by a p-value greater than 0.05 (Table 5).

3.3.3 Lobar manganese mapping in exposed lungs

The distribution of manganese concentration within the right lung was mapped using mean and standard deviation, and then colour-coded according to a key. Similar patterns of manganese concentrations are mapped as shown in Figure 7, indicating that there were similar trends of manganese concentrations as in the manganese-exposed group with high (1.580 ± 0.363) µg/g depositions in the upper lobe followed by the middle (1.16 ± 0.590) µg/g and the least in the lower lobes (1.050 ± 0.411) µg/g.

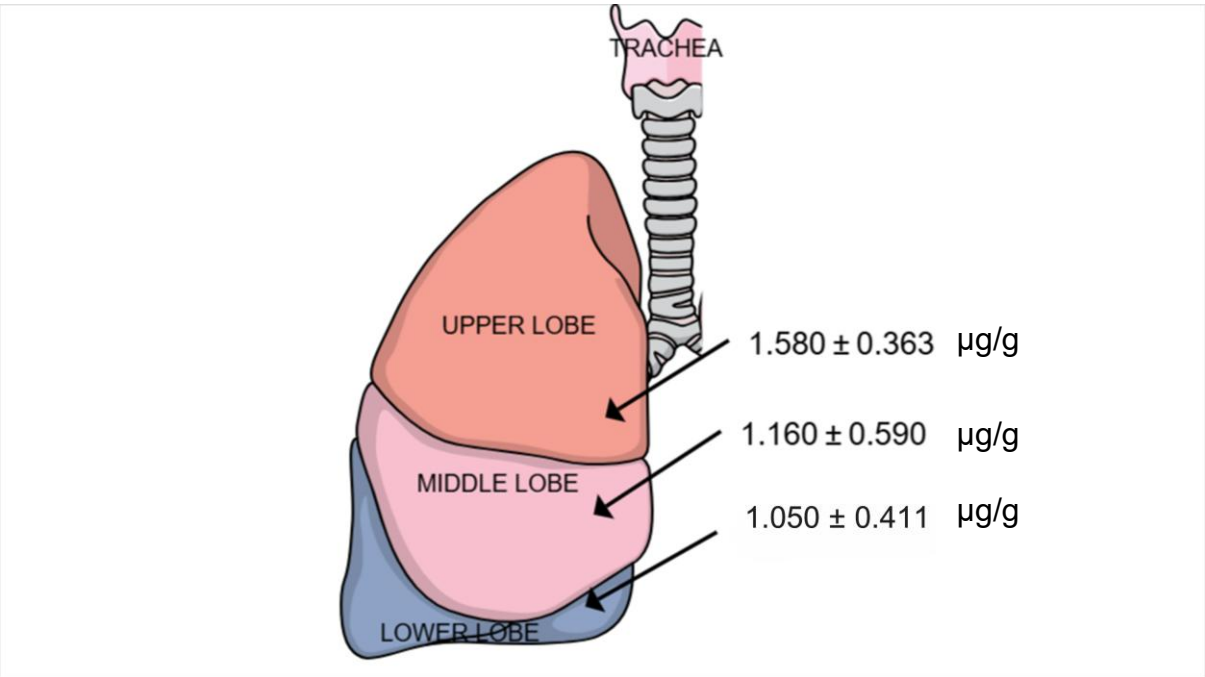

Figure 6. *Manganese concentration mapping by lobe for exposed mineworkers*

Schematic diagram created by J. Mthombeni

3.3.4 Lobar manganese mapping in unexposed lungs

The manganese concentration distribution within the right lung was mapped, providing the mean and standard deviation, and was color-coded according to a key. The map (Figure 7) showed that there were similar patterns of manganese concentrations as in the manganese-exposed group, with high (1.100 ± 0.568) µg/g depositions in the upper lobe, followed by the middle (1.040 ± 0.605) µg/g and the least in the lower lobes (0.965 ± 0.400) µg/g.

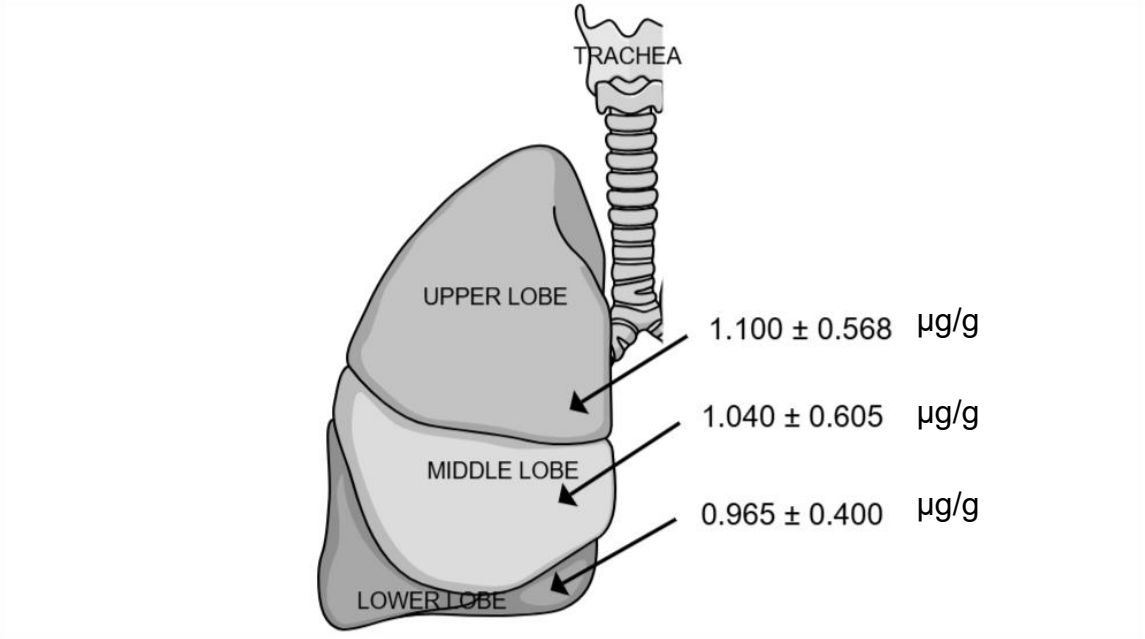

Figure 7. *Manganese concentration mapping by lobe for unexposed mineworkers*
Schematic diagram created by J. Mthombeni

3.4 Histopathological Comparison of Lungs

Objective three was to compare the histological features and investigate the effects of manganese exposure on lung tissue of deceased manganese-exposed and manganese-unexposed mineworkers, using histological staining techniques, H&E, MT, PAS, and Reticulin staining histochemistry. The focus was on inflammation and fibrosis development due to exposure to manganese dust. These staining methods allowed for a detailed examination of tissue architecture, collagen deposition, and fibre network alterations, providing comprehensive insights into the structural impact of manganese toxicity.

3.4.1 Inflammation assessment

Of the 64 cases analysed for inflammation, 21 (33%) were classified as Inflammation Non-Evaluable Cases (INEC) due to specific pathological conditions. Most cases had some features suggestive of suboptimal preservation, although histological assessment remained feasible for all except three (7%), which were too poorly preserved for assessment, leaving 40 cases.

Of these 40 cases, nine (23%) had severe pneumonia, one case (3%) had tuberculosis, four cases (10%) had congestion and haemorrhage, four cases (10%)

had mixed dust fibrosis and pneumonia, and a tumour was present in one case (3%). These conditions disqualified the reliable assessment of inflammation, necessitating their exclusion from the analysis.

A total of 21 cases were assessed for inflammation using H&E staining. Among them, 18 cases (86%) showed <10% inflammation in all three lobes; therefore, they were graded as 0. Three of the 21 cases (14%) showed varying severity and distribution of inflammation. Of the three, one case (33%) presented with mild diffuse inflammation across all three lobes, another had mild inflammation confined to the upper lobe, and the third showed moderate inflammation localized to the lower lobe.

3.4.2 Comparison of inflammation in the lungs

Among the 16 manganese-exposed cases, moderate inflammation was observed in one case (6%), localised to the lower lobe. Periodic acid–Schiff (PAS) stain confirmed the presence of numerous fungal yeasts morphologically consistent with Histoplasmosis, leading to the exclusion of this case from further analysis. In contrast, inflammation was identified in two of the 48 manganese-unexposed cases (4%). Of these, one case presented with less than 10% inflammation, which was subsequently excluded, whereas the other demonstrated mild inflammation, which was focal to the upper lobe. Following exclusion of the fungal-positive case, none of the manganese-exposed cases demonstrated inflammation.

3.4.3 Fibrosis assessment in the lungs

Of the 64 cases assessed for fibrosis, five (8%) were classified as Fibrosis Non-Evaluable Cases (FNEC) due to specific pathological conditions. Of the five cases, two (40%) showed evidence of asbestos bodies with severe asbestosis, and three (60%) were too poorly preserved, therefore, not assessable.

A total of 59 (92%) cases were assessed for fibrosis using MT and Reticulin stains, of which five cases (8%) showed interstitial fibrosis with alveolar wall expansion. The pattern is consistent with chronic interstitial lung disease. Among the five cases, one (20%) showed mild fibrosis across all three lobes, while three (60%) had mild fibrosis localised to the upper and middle lobes. The remaining case (20%) revealed mild fibrosis restricted to the lower lobe.

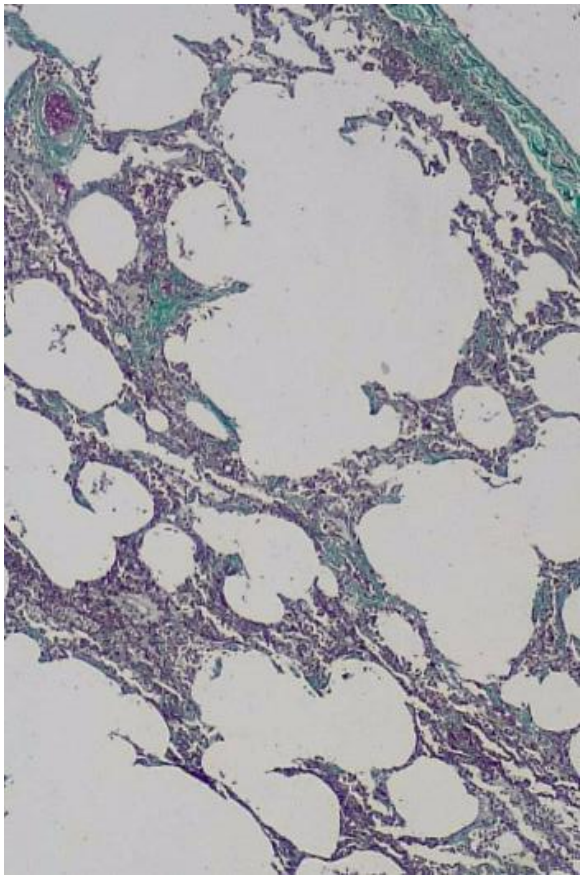

A. Micrograph MT

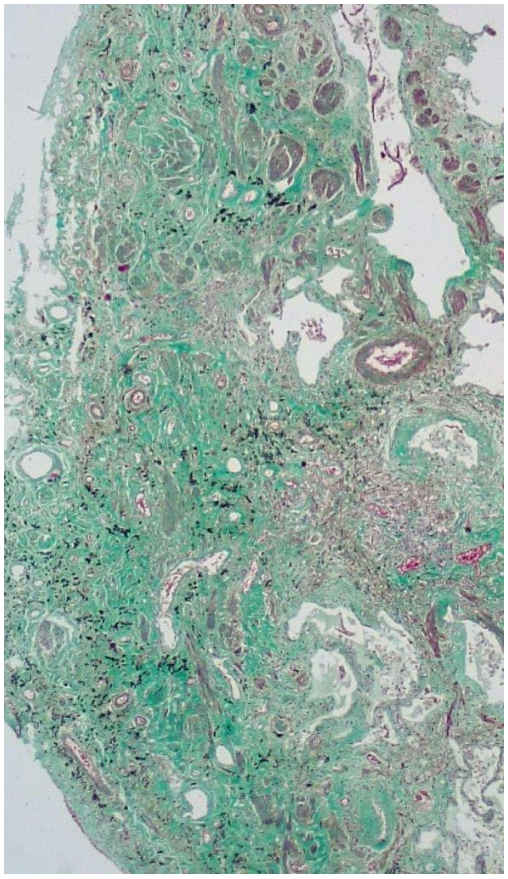

B. Micrograph MT Fibrosis UL

C. Micrograph Threshold Image of B

Figure 8. *High-resolution photomicrographic images stained with Masson Trichrome*

Histological tissue sections taken at a low-power magnification (x2.5). A: Representative tissue section of a normal lung; B: Representative lung tissue section showing mild fibrosis (11 - 30%). Green/blue colour represents collagen fibres deposited within the tissue. The fibrotic tissue appears dense and interwoven, replacing much of the normal parenchymal architecture. C: Representative micrograph cell threshold of image B showing fibrosis in approximately 23% of the tissue section. Photo credit: Dr N. Vorajee.

Image 8A. A micrograph image representing normal lung tissue, which was used as a control to measure fibrosis in this study.

Image 8B. A micrographic image demonstrating mild fibrosis with mild collagen deposition (Fibrosis) in the interstitium, with expansion of the alveolar walls. There is increased blue-green staining in the interstitium, indicating collagen deposition. The collagen appears patchy and mild, not uniformly dense, which is an indication of mild interstitial fibrosis. This micrograph shows fibrotic changes compared to normal lung tissue (Image 8A).

Image 8C. A thresholded image of micrograph B. The black regions correspond to fibrotic collagen, while the white background represents alveolar spaces, non-collagen tissue, and empty spaces. The black-stained regions are interwoven through the lung parenchyma, particularly around alveolar septa, indicating interstitial fibrosis. Despite collagen deposition, many alveolar spaces remain open and distinguishable, indicating that fibrosis has not yet progressed to the point of architectural distortion.

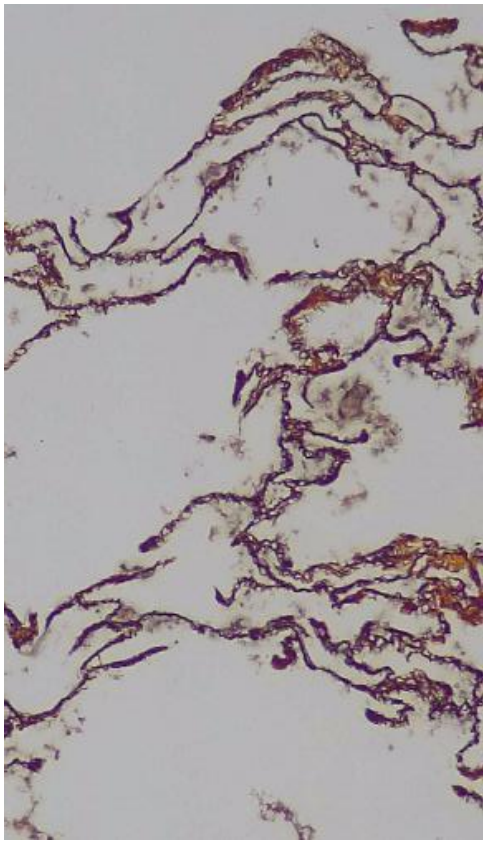

A. Micrograph Retic stain

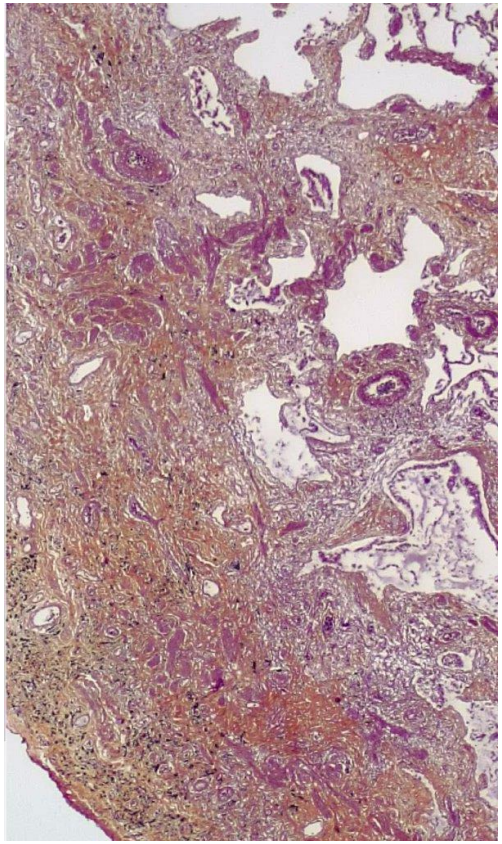

B. Micrograph Retic Fibrosis

C. Micrograph Threshold Image of B

Figure 9. *High-resolution photomicrographic images stained with Reticulin Stain*

Histological tissue sections taken at a low-power magnification (x2.5). A: Representative tissue section of a normal lung. B: Representative lung tissue section showing mild fibrosis (UL) (11 - 30%). Reddish-pink areas represent collagen fibres, which are abundant and widely distributed throughout the tissue. Their dense presence confirms fibrotic remodelling. C: Representative micrograph cell threshold of image B. Photo credit: Dr N. Vorajee

Image 9A. A micrograph image representing normal lung tissue, which was used as a control to measure fibrosis in this study. The normal reticulin framework of the lung is represented by a single layer of reticulin fibres in the alveolar walls.

Image 9B. A micrographic image demonstrating mild fibrosis with mild collagen deposition (Fibrosis). The presence of golden-brown fibres highlights the fibrosis in the interstitium with expansion of the alveolar wall. The alveolar walls appeared thickened compared to normal lung tissue.

Image 9C. The thresholded image isolated fibrotic areas by highlighting reticulin fibres, which indicated structural remodelling and early-stage fibrosis.

These micrographs, stained with Reticulin stain, reveal the reticulin fibre network and deposition of fibrosis. The black areas represent regions with dense reticulin fibre deposition, typically marking areas of fibrosis. Whereas the white areas are alveolar spaces and regions with minimal or no staining.

3.4.4 Comparison of fibrosis in the lungs

Among the 16 manganese-exposed cases, 2 (13%) showed interstitial fibrosis with alveolar wall expansion, with one case (6%) showing mild fibrosis across all three lobes and the other (6%) only displaying mild diffuse fibrosis in the upper and middle lobes. In contrast, among the 48 manganese-unexposed cases, three (6%) demonstrated mild to moderate interstitial fibrosis with alveolar wall expansion. Of the three cases, two (67%) had mild diffuse fibrosis in the upper and middle lobes, with one of them also exhibiting moderate fibrosis in the lower lobe, while the third case (33%) showed mild fibrosis focal to the lower lobe.

3.4.5 Quantification of inflammation and fibrosis

For the analysis of inflammation, a Pearson Chi-square test of independence was conducted to examine the relationship between manganese exposure (exposed and unexposed) and inflammation occurrence across different lung lobes (UL, ML, LL) with two categorical variables across a 3 × 3 contingency table. The results showed no significant association between manganese exposure and inflammation, $p = 0.323$.

Again, for the analysis of fibrosis, a Pearson Chi-square test of independence was conducted to examine the relationship between manganese exposure (exposed and

unexposed) and fibrosis occurrence across different lung lobes (UL, ML, LL) with multiple categories. The *p-value* of 0.809 indicated that there was no significant association between manganese exposure and fibrosis occurrence.

3.5 Correlation of Manganese Levels in Lungs and Brain

This section focused on exploring the correlation between manganese concentrations in the lungs of manganese-exposed mineworkers and the concentrations found in the brains of the same manganese-exposed mineworkers.

3.5.1 LOWESS analysis of manganese concentrations in lungs and brain

The Locally Weighted Scatterplot Smoothing (LOWESS) plot of manganese concentrations in the brains and lungs was used to provide a non-parametric visualisation of the comparison of the relationship between concentrations in the brains and lungs, Figure 10. The LOWESS curves illustrate the trend in the data without assuming a specific linear model.

A smoothed trend through the scatterplot using LOWESS is shown in Figure 10, comparing manganese concentrations in the lungs and brains. Both trends increased gradually around the midpoint of the sample range and slightly declined toward the end. Brain concentrations were consistently lower than lung levels, but followed the same directional changes. The curve showed a nonlinear relationship between lung and brain manganese concentrations. Outliers with unusually high lung and brain manganese concentrations (lung =1.75 µg/g and brain = 1.95 µg/g) noticeably skewed the upper right section of the LOWESS curve upward. This data point disproportionately affected the trend. Therefore, these outliers were removed in Figure 10.

We formally analysed the relationship between manganese concentrations in the lung and brain using a Generalised Additive Model (GAM) and extension of linear regression, adjusting for age, duration of exposure, and time since last exposure Figure 11. Understanding this correlation was critical for determining the mechanisms influencing the distribution of manganese in the lungs and the brain and the subsequent health risks. Since inhalation of manganese particles is likely the most important route of exposure in manganese mining, we hypothesized that there would

be a strong linear association between lung manganese and brain manganese concentrations, with the caveat that in those removed from exposure, the association may diminish Figure 11.

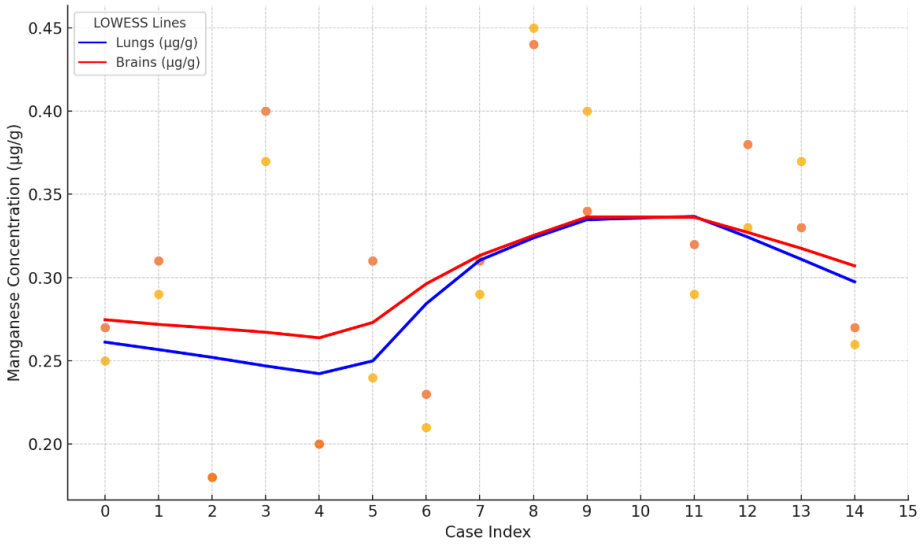

Figure 10. *LOWESS manganese concentrations comparison of the lungs vs the brains*

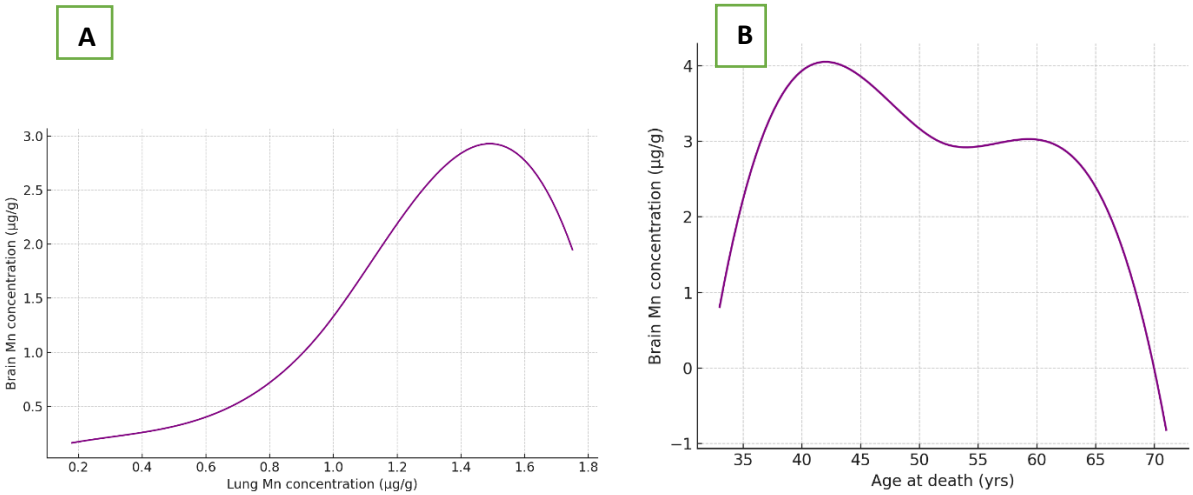

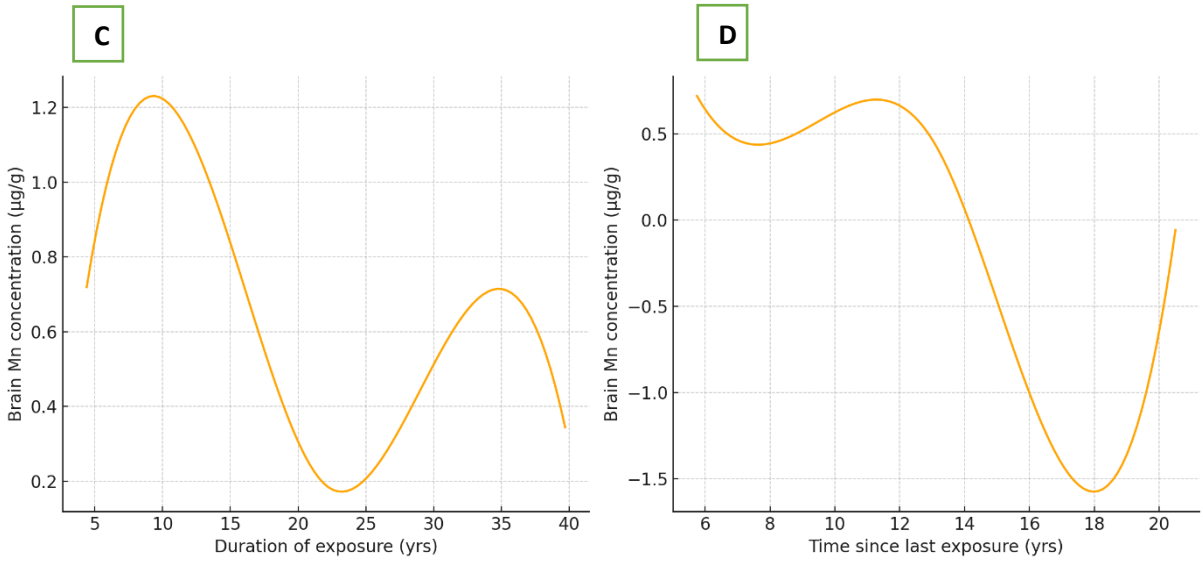

Figure 11. *Modelled effects of predictors on brain manganese concentration*

Graph A. Total lungs (lung manganese concentration)

The curve showed a non-linear, upward trend that steeply ascended after ~1.4 units of lung manganese concentration.

Graph B. Age at death (years)

The effect showed a nonlinear trend, peaking around age 45–50, beyond which the brain manganese levels declined with older age.

C. Duration of exposure

The curve began at a higher concentration for short exposures (~4–7 years) and showed a declining trend up to ~20–25 years, and the trend rose again slightly around 30–35 years.

D. Time since last exposure

A non-linear relationship between duration since last exposure and brain manganese concentration is shown in Graph D. Initially, manganese levels in the brain remained relatively stable with a mild increase up to approximately 12–13 years post-exposure, followed by a marked decline and a subsequent resurgence around the 20-year mark.

For individuals beyond the standard retirement age of 63 years (134); the date of last manganese exposure was estimated as the date of retirement.

3.5.2 Average manganese levels in the lungs and the brains

Lung manganese concentrations were consistently higher than brain levels across all exposure durations, with an average of 1.23 µg/g and low variability, showing a slight decline over time, as shown in Table 6. In contrast, brain manganese averaged 0.46 µg/g with greater variability and with no clear trend. Similar patterns of manganese concentrations in both organs occurred in the different exposure groups, with the highest concentration in the lung (1.393 µg/g) in the 1–15 years and the lowest was in the brain (0,267 µg/g) in the 16-30 years groups.

The Pearson correlation coefficient between lung and brain manganese concentrations was 0.43, indicating a moderate positive linear relationship between the two variables across the exposure groups.

Table 6. *Mean manganese concentrations in lungs and brain by years of exposure*

TOTAL YEARS OF MN EXPOSURE	FREQUENCY	LUNG ($\mu g_{Mn}/g$)	BRAIN ($\mu g_{Mn}/g$)
1-15	5	1.393	0.667
16-30	4	1.047	0.267
31+	7	1.270	0.420

n = 16

Summaries of average manganese concentrations in the lungs and globus pallidus (GP) across different durations of occupational exposure are displayed in Table 7. The data indicated that lung manganese concentrations remained relatively high and stable over time, with no clear linear trend. In contrast, globus pallidus concentrations showed greater variability. A Pearson correlation between total lung and total globus pallidus concentrations yielded r = 0.43, indicating a moderate positive relationship.

Table 7. Average manganese levels in the lung and globus pallidus by duration of exposure (N = 16)

TOTAL YEARS OF MN EXPOSURE	FREQUENCY	LUNG ($\mu g_{Mn}/g$)	GLOBUS PALLIDUS ($\mu g_{Mn}/g$)
1-15	5	1.393	0.857
16-30	4	1.047	0.270
31+	7	1.270	0.450

3.5.3 Association between lung and brain manganese concentrations

Further to finding that the distribution of manganese deposition within the brain followed a normal pattern, the Pearson's correlation coefficient test was used to assess the strength and direction of the linear relationship between lung manganese concentrations and the concentrations in the brain regions, Table 8.

The correlation test between total lungs and various brain regions showed generally weak positive correlations across the board. None of the relationships were statistically significant (all p-values > 0.05). The highest correlation was with the cerebellum ($r \approx 0.28$), followed by the olfactory bulb ($r \approx 0.27$), but neither reached statistical significance.

Table 8. *Associations between manganese levels in brain regions and lungs*

Brain region	r	P-value
Cerebellum	0.280	0.290
Caudate	0.090	0.740
Putamen	0.127	0.638
Globus pallidus ext.	0.112	0.680
Globus pallidus int.	0.087	0.748
Olfactory bulb	0.270	0.312

r: Pearson’s correlation coefficient, (n=16)

A combined plot was used to provide a comprehensive and balanced visualization of the relationship between the manganese concentration in the basal ganglia structures

and the lung, helping to uncover potential complexities that a linear model alone might have missed. The combined LOWESS analysis showed a nonlinear association between lung manganese concentration and manganese accumulation across basal ganglia structures (caudate, putamen, and globus pallidus), Figure 12. The globus pallidus (green) showed the strongest increase in manganese levels with rising lung concentrations, while the putamen (orange) and caudate (blue) demonstrated comparable but more gradual upward trends.

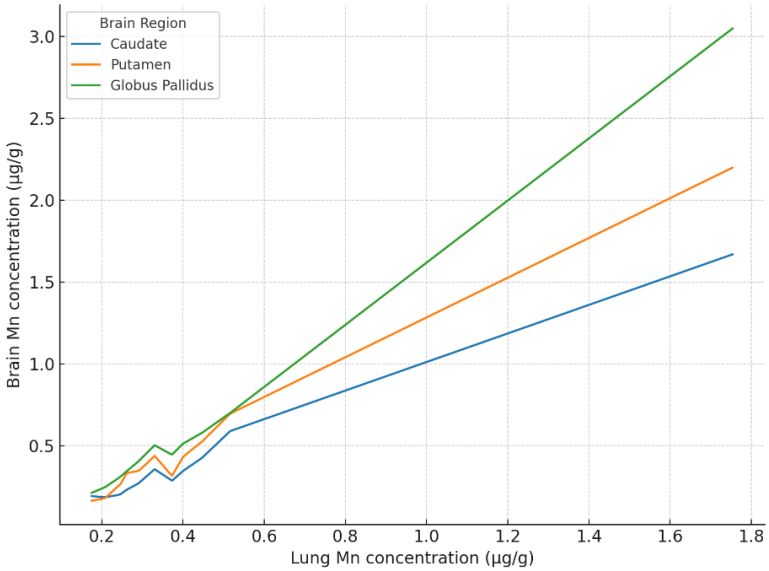

Figure 12. *LOWESS comparison: Manganese concentrations in the basal ganglia structures vs the lung*

Generalized Additive Model (GAM) plots showing the nonlinear relationships between lung manganese concentrations and manganese levels in each basal ganglia region, Figure 13. The purple dots represent individual cases, and the orange lines show the regression trend, with shaded areas representing 95% confidence intervals.

Graph A (Caudate vs Lung Mn): Showed a strong linear trend with positive correlation.

Graph B (Putamen vs Lung Mn): Slightly steeper slope, indicating a stronger response to increasing lung Mn.

Graph C (Globus Pallidus vs Lung Mn): The steepest slope with the highest correlation, aligning with its known role in manganese deposition.

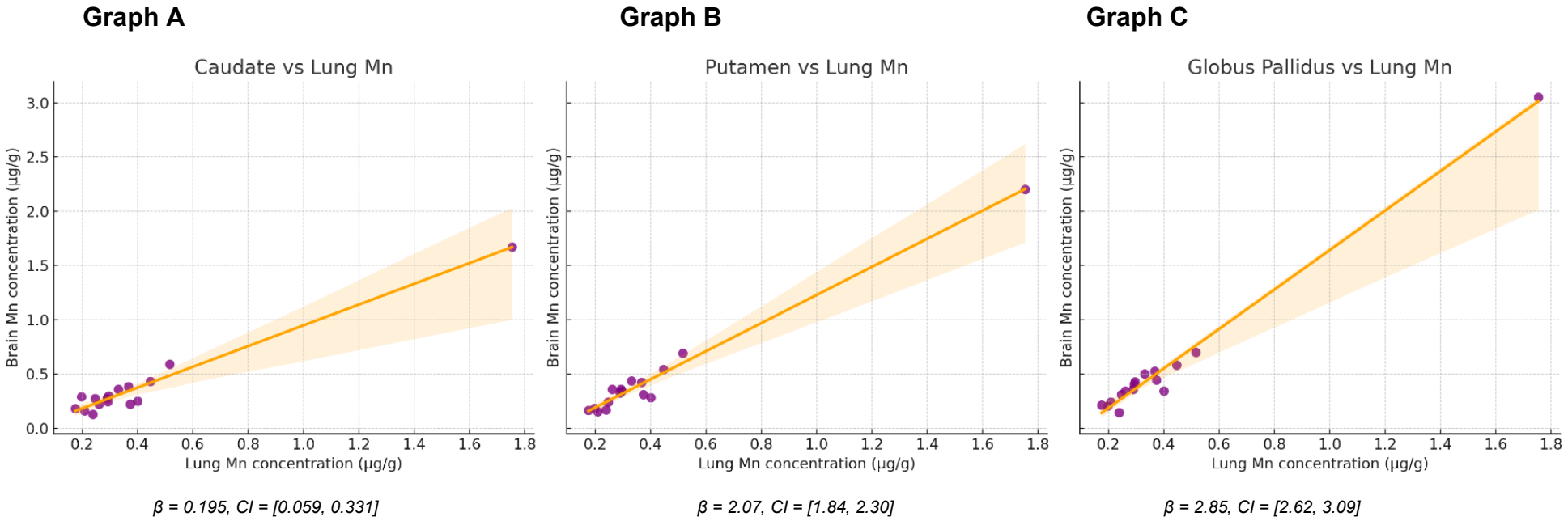

Figure 13. *GAM plot for manganese concentrations in the basal ganglia structures vs the lung*

CHAPTER FOUR – DISCUSSION

4.1 Introduction

This discussion chapter provides an in-depth analysis of the research findings in relation to manganese accumulation and its impact on the lungs of manganese-exposed mineworkers. This section interprets the data gathered on demographics of the study participants, the levels and distribution of manganese depositions in the mineworkers' lungs, and explores the histopathological changes observed, offering insights into how manganese exposure may have contributed to lung diseases in this occupational setting. Furthermore, the chapter discusses the findings of the correlation between the manganese deposition in the lungs and the brains of manganese-exposed mineworkers. The chapter closes by discussing the strengths, limitations, and recommendations for future study.

The chapter contextualizes the findings within existing literature on occupational manganese exposure and respiratory health and also examines the broader implications for mineworkers exposed to manganese dust. Additionally, the chapter acknowledges the study's limitations and proposes areas for future research.

4.2 Key Demographic Insights of the Study Sample

The demographic profile of the manganese-exposed study participants revealed a slightly older median age at death (56 years) and a high proportion of natural-cause mortality (94%). While these patterns may reflect chronic health trajectories, there is no conclusive evidence that manganese exposure directly contributed to delayed health effects or increased risk of non-accidental death. Nonetheless, these observations are consistent with prior findings, such as those by Bouchard *et al.* (2008), who reported persistent neurotoxic symptoms in alloy workers years after exposure cessation. Data from annexures 9 and 10 show consistent manganese-related deaths across 2010–2018, though younger age group fatalities could not be conclusively linked to occupational exposure. Variability in individual susceptibility due to factors such as health status, lifestyle, and co-exposures likely influenced outcomes.

4.3 Implications of Manganese Deposition on Pulmonary Health

The manganese-exposed group had higher levels of manganese in the upper, middle, and lower lobes of the lungs compared to the unexposed group. These significant differences indicate that manganese deposition in the lungs is much higher in exposed individuals, particularly in the upper lobe. The *p*-values below 0.05 reinforce that this is not a random variation but a clear impact of occupational exposure.

The findings of the ANOVA statistical analysis suggest some significant differences, primarily in the upper lobe measurements, while the middle and lower lobes showed fewer notable differences. The higher mean measurement results for the manganese-exposed group suggest that exposure may have been associated with changes in the upper lobe size or density, possibly due to inflammation, fibrosis, or structural adaptations to exposure. The significant difference in the upper lobe of the manganese-exposed group could indicate that manganese particles preferentially accumulated or induced changes in this upper region of the lung, potentially leading to more localized effects in exposed individuals. West J.B, in 2012 discusses the concepts of ventilation-perfusion matching in the lungs, explaining how the gravitational pull influences perfusion and how the apex of the lung receives less blood flow compared to the bases. However, for mineworkers, the long-term mining posture tends to promote deposition of particulate matter in the apical region of the lung (135) which opposes the natural flow of blood in the lungs. The apical part of the lung differs anatomically and functionally from other lung regions.

During drilling, mineworkers often work in crouched or kneeling postures, which can limit overall lung expansion and alter ventilation–perfusion relationships. In such constrained respiratory mechanics, inhaled dust particles may be more likely to deposit in proximal or upper lung regions due to reduced ventilation in dependent zones. This concept is consistent with known effects of posture on regional ventilation and particle deposition (136)

Due to mineworkers' posture and response to gravity and ventilation dynamics, the apical regions in mineworkers receive more blood flow compared to lower lung regions, where blood is supposed to pool due to gravity. This creates ventilation-perfusion imbalances in the apical region, with a relatively higher air-to-blood ratio. The middle and lower lobes have a higher perfusion rate, which matches ventilation more closely

and enhances efficient gas exchange (137). This suggests that the upper lobes are more affected by dust exposure in manganese mineworkers

The middle lobe appeared less affected by manganese exposure, which may be due to differences in particle deposition and clearance dynamics across lung regions. This indicates that manganese exposure might have a less pronounced effect on this region, which could be related to airflow patterns that limit particle deposition in the middle lobe or tissue differences that are less susceptible to manganese-induced changes. Although the basic histological structure of the lung lobes, such as alveoli, bronchioles, and vasculature, is largely uniform, regional differences exist at the functional and physiological level. The study by Churg & Brauer (2000) provides indirect evidence of such variation, particularly in particle clearance and macrophage activity, implying functional differences across lobes (138). These differences may contribute to lobar-specific patterns of disease, including variable responses to inhaled toxins such as manganese. This finding supports the idea that manganese exposure does not lead to substantial deposition or changes in the middle lobe, possibly due to the anatomical and physiological factors outlined above.

In summary, the middle lobe's unique anatomical position and functional characteristics likely protect it from significant manganese deposition. Its balanced ventilation-perfusion ratio, efficient lymphatic drainage, and intermediate structural complexity seem to reduce the susceptibility to manganese accumulation, making it less affected by occupational exposure compared to the upper and lower lobes. Weibel, Cournand, and Richards in 1963 described variations in alveolar surface area and branching among different lung lobes. Their findings support the idea that the middle lobe’s structural attributes, such as smaller surface area and branching, contribute to reduced particle deposition compared to the more complex structures of the upper and lower lobes (139). This insight highlights the need to focus on the upper and lower lobes for manganese exposure assessments, as these areas are more prone to deposition and subsequent tissue changes.

Whereas the lower lobe measurements lacked a significant difference, which might reflect lesser manganese particle deposition or resistance to exposure effects in this region. This consistency across lobes could imply that manganese exposure predominantly affected the upper lung region, potentially due to the deposition patterns of manganese particles or anatomical airflow dynamics. A further pairwise analysis

using Tukey's post hoc test showed areas of specific statistical differences, primarily in the upper and lower lobes, with marked differences between exposed and unexposed groups in these areas. Additionally, the data underlined that the impact of manganese exposure is localized to certain lobes, possibly due to anatomical and airflow characteristics unique to these areas.

Heyder and Svartengren (1987) explain how gravitational forces influence particle deposition within the respiratory system, with heavier particles more likely to settle in the lower lobes. The authors outline how the lower lung regions tend to collect particulates due to sedimentation, especially during prolonged exposure to airborne particles (140). The findings of this study are also supported by Schlesinger (1995), who reviewed comparative deposition of inhaled aerosols in experimental animals and humans. In this review, Schlesinger discussed how lung anatomy and particle dynamics affect deposition patterns in different lobes, with airflow and gravity playing key roles in determining particle location (141). This review study supports the observation that gravity and airflow direct particles to the upper or lower lobes more frequently than the middle lobe.

Lymphatic drainage in the apical region is generally limited compared to the basal regions. This could affect how fine particles such as manganese are cleared in the apical region, which might lead to more prolonged exposure to any inhaled particulates. Whereas lower lung regions have a more extensive lymphatic drainage network, aiding in the efficient removal of particulates and other foreign matter from the lung tissue. Furthermore, lower lung regions typically have higher macrophage activity to counteract the increased particulate load due to gravitational deposition, especially in the lower lobes, where inhaled particles are more likely to settle (140). Airways in the apical portion tend to be smaller and less branched than those in the lower lobes, creating variations in airflow and particle deposition patterns. The airways in the lower lung regions are more extensive, with greater branching to accommodate higher airflow and better distribution across the lung tissues (140).

Given these anatomical and functional differences, manganese and other inhaled particles might accumulate more in the upper lobe region, where they may be less efficiently cleared due to lower lymphatic drainage and perfusion. This can lead to higher manganese tissue concentrations, potentially explaining why manganese-

exposed individuals showed more pronounced changes in the upper lobe region compared to other lung areas. These factors may contribute to a higher risk of inflammation and structural changes specific to the upper lobe, as seen in some occupational lung diseases. These findings support the idea of targeted structural or functional assessment in the upper and lower lobes when evaluating the respiratory effects of manganese exposure in occupational settings.

4.4 Clinical Relevance and Implications for Manganese Toxicity

The significant manganese accumulation in the vulnerable upper lobe raises concerns about potential lung damage, including inflammation, fibrosis, and respiratory impairment, which are commonly reported in manganese-exposed workers. Increased manganese deposition could contribute to chronic lung diseases such as bronchitis, pneumoconiosis, or fibrosis. The lack of statistical significance in lobar analysis does not diminish the broader significance of manganese accumulation, particularly where there was higher deposition, which could impair lung function over time. Since the lungs serve as a portal for manganese entry into the bloodstream, higher manganese deposition could increase the risk of systemic effects, such as neurotoxicity (manganism), which has been linked to prolonged exposure to manganese dust (142).

The increased manganese concentrations in the lungs of exposed workers, especially in the upper lobes, could have significant health implications for the mineworkers. Chronic manganese inhalation is associated with a range of pulmonary and neurological issues, and the higher deposition in specific lung regions suggests the potential for localized damage. According to Tyler and Plopper (1985), monkeys and humans possess similar lung structure, with their respiratory bronchioles and other minor airways exhibiting comparable susceptibility to inhaled toxins, including cigarette smoke, coal dust, and ozone (143). Dorman *et al.* (2005) conducted studies on rhesus monkeys investigating the respiratory effects of manganese exposure, focusing on its impact on the lower airways of these rhesus monkeys (144). They found that rhesus monkeys exposed to high levels of manganese sulfate developed significant lower airway pathology, including inflammation, cellular damage, and fibrosis, particularly in bronchioles and alveoli (145, 146). These findings can also apply to the situation in humans. However, there is a dire shortage of studies on the effects of manganese exposure on human lungs. The current study did not find any correlation between manganese exposure and pathology found in the lungs.

4.5 Tissue Pathology Insights into Manganese-Related Health Effects

The autopsy findings provided a more detailed picture of the health effects related to manganese exposure, particularly regarding lung pathology. A common theme across many of the cases was the prevalence of respiratory conditions, including various forms of pneumonia, asbestosis, fibrosis, and other lung pathologies.

Pneumonia is common in individuals with weakened immune systems or pre-existing lung damage (147), which may have been exacerbated by long-term manganese exposure in this cohort. Excessive manganese exposure has been shown to impair immune function. For instance, in a study by Qi *et al.* (2024) of expression levels of critical immunological markers and immune checkpoints in rats exposed to manganese, in 2024, manganese exposure in rats led to decreased levels of immunoglobulins and complement proteins, indicating suppressed humoral immune function (147).

Additionally, an earlier study by Qi *et al.* (2023) suggested that manganese exposure may alter immune responses, potentially contributing to inflammation or immune suppression in affected workers, suggesting immune system damage (148). Workers with compromised lung health due to years of inhaling manganese and other particulate matter may be more susceptible to lung infections, leading to higher rates of pneumonia (149) as was seen in this cohort. Chronic exposure to particulate matter can impair the immune response, making the lungs more susceptible to infections (150). This has been particularly evident in environments with high levels of organic dust and other particulates, which can exacerbate respiratory conditions and increase the risk of pneumonia (149). Furthermore, manganese exposure has been linked to pulmonary inflammation and vascular changes (151).

Histopathological analysis of lung tissue using H&E staining did not reveal evidence of inflammation attributable to manganese exposure. While some slides displayed inflammation, these were associated with concurrent conditions such as pneumonia and other infectious diseases, rather than occupational exposure. Additionally, the quality of many lung specimens was suboptimal due to poor preservation, which limited the ability to draw definitive conclusions in some cases. Some tissue appeared structurally disorganized, showing areas of immune cell infiltration, necrosis, and possible edema, findings suggestive of an ongoing inflammatory process that may be

associated with manganese exposure. These features are consistent with acute or chronic inflammation, potentially caused by infection, injury, or autoimmune activity, similar to findings of Qi et al., (2023).

Asbestosis was present in several cases reported at autopsy and in the assessment of histopathology slides of manganese-exposed and manganese-unexposed individuals, suggesting co-exposure to asbestos fibers alongside manganese dust.
While manganese and asbestos have not been extensively studied in tandem, their shared ability to induce oxidative stress, inflammation, and fibrosis suggests that co-exposure could result in greater pulmonary damage than either alone. This warrants further investigation, particularly in occupational health settings such as mining, where such exposures may co-occur.
This is particularly concerning because, according to Weis in 1999, asbestosis is a known risk factor for lung cancer and other severe respiratory conditions (152). The combination of asbestosis and manganese exposure likely compounded the damage to the lungs, leading to increased morbidity and mortality in these workers. In summary, prolonged exposure to manganese and other particulate matter in occupational settings can compromise lung health, increasing susceptibility to lung infections and higher rates of pneumonia.

Severe mixed dust fibrosis, as seen in histopathology analysis, indicated chronic lung damage due to the inhalation of various dusts over a long period. Fibrosis is irreversible scarring of lung tissue, severely impairing lung function and often leading to respiratory failure over time (153). The histology analysis of MT stained slides showed mild pulmonary fibrosis, with excess collagen deposition and alveolar wall thickening leading to disrupted lung function. Although the fibrosis observed in this study was classified as mild, it represented established fibrotic changes, which are irreversible and carry pathological significance. Such changes are commonly seen in interstitial lung diseases (ILDs), post-infectious fibrosis, or chronic environmental exposure to lung irritants. Micrograph stained with Retic also suggested chronic pulmonary fibrosis, with extensive collagen deposition, alveolar wall thickening, and altered lung structure. The findings indicate a late-stage fibrotic process, which is irreversible, leading to lung stiffness and restricted function. The presence of fibrosis in mineworkers' lungs suggested long-term exposure to harmful substances in the mine, with manganese likely playing a significant role in the development of these conditions.

Pulmonary and intra-alveolar edema were observed in the lung tissue histology, indicating fluid accumulation within the alveolar spaces, findings that may result from infections, cardiovascular dysfunction, or chronic exposure to toxic agents. Additionally, the presence of small foci of tumor seen at autopsy and confirmed by histological analysis in one case, though not fully characterized, raises questions about the potential carcinogenic effects of manganese exposure in conjunction with other mining-related hazards.

4.6 Inflammation, Fibrosis, and Clinical Relevance

This section discusses the histopathological findings comparing inflammation and fibrosis prevalence in manganese-exposed versus manganese-unexposed individuals, by closely analysing the histopathology slides to find the possible effects of manganese in the lungs. This section further provides a critical assessment of how the results contribute to scientific knowledge.

Studies on occupational manganese exposure have reported varying inflammatory responses, often associated with concurrent exposure to other particulates, such as silica and asbestos (154). Histopathological findings of this study indicated a low prevalence of inflammation in only 7% of the total cases, suggesting that manganese exposure alone may not be the main cause of inflammatory responses in the lungs. Inflammation in the lungs is frequently influenced by multiple environmental and occupational factors, and while manganese exposure has been implicated in oxidative stress and neurotoxicity, its direct impact on pulmonary inflammation remains less conclusive since studies have suggested a potential reversibility upon cessation of exposure (88). The absence of inflammation in most cases could be atributted to the reversal of inflammation post exposure due to withdrawal from the mining environment whereby the mineworkers could have been hospitalised, retired, or off sick away from the mine dust environment, as shown in the rhesus monkey studies by Dorman *et., al,* 2005 where their findings showed that signs of inflammation had been reversed after 45 days post exposure to chronic manganese dust levels (88).

The presence of pre-existing conditions, such as tuberculosis and pneumonia, in several cases could have complicated the interpretation, as these conditions independently contribute to inflammation and may have overshadowed the specific

effects of manganese; therefore, these cases were excluded from the histopathology slide analysis.

A slightly higher prevalence of fibrosis was observed among manganese-exposed individuals compared to manganese-unexposed cases. However, the lack of a statistically significant association (p = 0.809) suggested that manganese exposure alone did not strongly correlate with the development of fibrosis. Previous research has indicated that chronic exposure to manganese-containing dusts may contribute to fibrotic lung changes, often in conjunction with other inhaled toxicants. Although animal models have demonstrated the profibrotic potential of manganese through mechanisms involving oxidative stress and inflammatory cytokine release (Dorman *et al.* 2006), the current findings suggest that other occupational hazards or individual susceptibility factors may play a more substantial role in fibrosis development. Furthermore, the presence of asbestosis in some cases highlighted the confounding role of mixed dust exposure, which has been extensively linked to lung fibrosis in mining populations (155).

In summary, the demographic trends, duration of manganese exposure, clinical causes of death, histopathological and autopsy findings collectively suggest a high burden of respiratory diseases and early mortality among manganese-exposed mineworkers. The prevalence of conditions like pneumonia, asbestosis, and fibrosis points to the severe health impacts of long-term dust inhalation and co-exposure to other toxic substances in the mining environment. However, the presence of these pulmonary conditions could not be directly attributable to manganese toxicity, as shown by histopathological correlation analysis in this study. These findings suggest that any differences observed in fibrosis frequency across different lobes and exposure conditions were likely due to random variation rather than a true effect of manganese exposure.

The results of this study suggest no statistically significant relationship between manganese exposure and the occurrence of either inflammation or fibrosis in the assessed lung lobes. However, given the limited sample size, further investigation with a larger dataset would be necessary to draw more definitive conclusions. These results underscore the need for stricter occupational health measures, including improved

ventilation, personal protective equipment, and regular health screenings to prevent or mitigate the long-term effects of manganese exposure in mineworkers.

4.7 Correlation of Manganese Distribution in the Lungs and Brains

Statistical analyses were conducted to assess the potential correlation between manganese concentrations in the lungs and brain tissues. Pearson correlation test, followed by LOWESS and GAM, was applied to determine linear and non-linear associations. These tests demonstrated weak, non-significant correlations, indicating that manganese accumulation in the brain does not reliably correspond with levels of manganese concentrations found in the lungs.

The absence of a strong correlation between manganese concentrations in lung and brain tissues suggests that manganese uptake and retention in the brain may be governed by additional physiological and biochemical factors beyond direct pulmonary exposure. Individual metabolic variability, including differences in manganese absorption, distribution, and excretion, could significantly influence systemic manganese levels and tissue-specific accumulation. Furthermore, manganese transport into the brain is regulated by active mechanisms, such as the divalent metal transporter 1 (DMT1) and calcium channels, which facilitate passage across the blood–brain barrier (156). These transport systems may be selectively upregulated or downregulated depending on individual homeostatic needs or prior exposure history.

A smoothed trend derived from LOWESS analysis revealed a moderate, positive monotonic relationship between lung and brain manganese concentrations, characterized by a nonlinear trend that reflected the biological complexity of manganese movement. This observation is consistent with previous research indicating that manganese accumulation patterns can differ significantly between pulmonary and neurological tissues due to differences in uptake, clearance, and regulation mechanisms (82, 156, 157). The Pearson correlation coefficient ($r \approx 0.43$) further supported a moderate strength of association, suggesting that while increases in lung concentrations generally correspond to increases in brain concentrations, the relationship was not strictly proportional. This partial decoupling is likely influenced by organ-specific transporters, such as the divalent metal transporter-1 (DMT1) and ZIP8, which play roles in regulating manganese entry into the brain (99, 158). Moreover, the blood-brain barrier exerts an additional level of regulation, potentially limiting

manganese transfer at higher systemic levels (159, 160). Thus, although brain concentrations broadly mirror trends in lung tissue, the brain appears to modulate manganese accumulation more tightly, particularly at elevated exposure levels, highlighting the nonlinear and compartmentalized nature of manganese distribution.

LOWESS analysis of manganese concentrations in the brain and lungs relative to duration of exposure revealed a nonlinear trend, with an initial rise followed by a plateau phase, indicating the attainment of a steady state. This plateau reflected biological regulation mechanisms, such as blood-brain barrier control and metal transporters, e.g., Solute Carrier Family 30 Member 10 (SLC30A10), which controls the eflux of manganese in the brain, as well as pulmonary clearance pathways that limit excessive accumulation. While these systems help maintain manganese homeostasis, prolonged exposure may still lead to cumulative effects, particularly in individuals who are vulnerable. These findings are supported by previous studies highlighting saturation kinetics and neuroprotective transport processes.

The LOWESS plot analysis of time since last exposure versus brain manganese concentration reveals a nonlinear trend, suggesting a dynamic pattern of manganese clearance and retention in neural tissues. In the early years following exposure cessation (0–10 years), brain Mn concentrations appear relatively stable or even slightly elevated, potentially reflecting residual manganese retained in deep brain structures, such as the basal ganglia. Around 10–13 years post-exposure, the LOWESS curve shows a decline, indicating gradual manganese clearance mechanisms at work, likely mediated by neuronal and astrocytic metal transporters such as SLC30A10 and SLC39A14, which regulate Mn efflux and uptake, respectively (158, 161).

Interestingly, a late resurgence in brain manganese levels is observed approximately 15–20 years after last exposure in some individuals. This could be attributed to several factors, including age-related decline in manganese clearance capacity, genetic variability in metal transporters, or cumulative effects from undiagnosed or secondary exposures. Studies have shown that manganese can remain sequestered in brain tissue for extended periods, particularly in individuals with compromised hepatic or renal clearance (82). Furthermore, manganese has a long biological half-life in the brain, and redistribution from peripheral tissues may contribute to delayed increases

post-exposure (162). Aschner also noted that redistribution from peripheral compartments, such as bone or liver, may lead to delayed or prolonged manganese elevations in the brain due to its slow clearance rate(162)

Lastly, the time elapsed since the last occupational exposure may have influenced manganese concentrations in tissue at the time of death, particularly due to the potential for redistribution or clearance of manganese from specific organs over time. This consideration is supported by findings from Dorman *et al.* (2005), who demonstrated in rhesus monkeys that signs of manganese-induced inflammation were reversible, with notable resolution observed 45 days after cessation of chronic manganese dust exposure (88). These results highlight the dynamic nature of manganese kinetics and suggest that tissue manganese concentration levels may decline following cessation of exposure, potentially obscuring exposure-related effects in postmortem analyses.

These results further suggest that other additional factors beyond direct pulmonary exposure, such as individual metabolic variation, transport mechanisms across the blood-brain barrier, or duration since last exposure, may have influenced manganese uptake and retention in the brain.

The lack of a statistically significant relationship supports the null hypothesis and highlights the complexity of manganese toxicokinetics in occupational settings. Although manganese was present in both organ systems, no clear dose-response pattern could be established. These findings emphasise the need for more comprehensive studies incorporating larger sample sizes, better-preserved tissue specimens, and longitudinal exposure data to fully understand the distribution dynamics and health implications of manganese in mining populations.

4.8 Implications and Limitations of Findings

The absence of a statistically significant link between manganese exposure and histopathological changes in the lungs aligns with previous epidemiological studies that suggest manganese primarily affects the central nervous system rather than the respiratory system (163). However, the limited sample size and the exclusion of non-evaluable cases reduce the power to detect subtle associations. The high proportion of cases with suboptimal preservation may have further impacted the assessment of

inflammatory and fibrotic changes. Future studies with larger cohorts, controlled exposure assessments, and molecular biomarkers of lung injury may provide a more definitive understanding of manganese's pulmonary effects. Additionally, longitudinal studies tracking mineworkers over time could help distinguish between acute and chronic lung pathologies associated with manganese exposure.

4.9 Strengths of the Study

This study is one of the first to compare manganese deposition between lung and brain tissues in mineworkers, bridging knowledge gaps in understanding how manganese toxicity may affect multiple organs differently. Exploring the correlation between manganese in the lungs (where exposure is direct) and the brain (where neurological effects occur) adds significant value to occupational health research.

Examining manganese toxicity in mineworkers from the Northern Cape, South Africa, is highly relevant given their unique exposure risks. The study sheds light on an underserved population, providing valuable insights into the specific occupational health risks this population may face.

South Africa has a unique PATHAUT database that serves primarily as an administrative tool for compensation. This database facilitates the recording of disease data, along with supplementary information on demographics and exposure to mining dust. It is essential to note that this database is the primary resource for conducting trend analyses related to occupational respiratory diseases, one of the few, if not the only, similar databases worldwide.

The use of stored tissue material allows for comprehensive tissue analysis in deceased individuals, providing access to both lung and brain tissues that would not typically be available from living participants. This enabled the study to assess the cumulative, long-term effects of manganese exposure at a tissue level. This study utilized the PATHAUT database, along with materials stored in the specimen storage at the NIOH. The use of postmortem tissue samples offered significant advantages for evaluating the long-term effects of manganese exposure. It provided direct access to both lung and brain tissues, which are not ethically or practically accessible in living individuals. This facilitated a comprehensive tissue-level analysis, enabling the study of cumulative exposure and pathological changes that developed over time.

This approach enabled a detailed investigation of manganese distribution in target organs, including specific brain regions and lung tissue, thereby helping to link occupational exposure with potential neurotoxic and respiratory outcomes.

Furthermore, the application of reticulin fibre staining in lung tissues enabled the study to accurately detect and map fibrotic changes resulting from manganese exposure. This accurate detection strengthened the study by providing structural evidence of the effects of manganese on lung tissue.
In addition, reticulin fibres analysis carried out in the study effectively documented inflammation and fibrosis progression amongst the manganese-exposed cohort. This helps to establish a relationship between manganese levels and structural changes.

4.10 Limitations

This study quantified and mapped manganese concentrations in the lungs of mineworkers in South Africa. The study is groundbreaking, marking a significant advancement, as no study has quantified manganese concentrations in human lungs. Only a few studies have previously focused on manganese depositions in brain tissue, and these have not been correlated with any other parts of the human body. As a novel study, there was limited data directly comparing manganese deposition between lung and brain tissues. This lack of a benchmark makes it challenging to contextualize findings or validate the methodologies used for measuring and correlating manganese concentrations between these organs.

Several limitations still applied, even in the context of such a pioneering approach, as the study aimed to contribute new insights to occupational health, manganese toxicity, and its biological deposition patterns.

4.10.1 Number of samples used for the study

Since this study was retrospective and utilised samples stored at the NIOH, lung samples were not consistently available for all deceased individuals, which limited the number of participants in the study and potentially impacted its statistical power. The researcher utilised all the available lungs for the study. Many deceased mineworkers had comorbid conditions (e.g., tuberculosis, chronic obstructive pulmonary disease,

pneumonia, asbestosis, or other lung conditions) that may have confounded manganese deposition results, complicating the assessment of manganese concentrations, which may have been caused by manganese exposure only, as well as considering the limited samples available for the study.

4.10.2 Lung sampling (loss of anatomical orientation)

Once the lungs are dissected and randomly positioned, as is the case at the NIOH, following sectioning of the lungs for histopathological analysis, ascertaining the original anatomical orientation becomes challenging. It is challenging to determine which slice comes after another when attempting to reconstruct the lung. An attempt was made to reconstruct the lung and sample the bronchopulmonary segments using a bronchopulmonary segment scheme developed by Pinkert et al. (2000). The sampling method presented a major challenge, specifically the reproducibility of the same lung construction for different lungs. Therefore, accurately sampling the 10 bronchopulmonary segments would be a challenge, as one would need to reconstruct the dissected lung to align the three-dimensional bronchopulmonary tree. Subsequently, tissue sections were selected from the 3 lobes (upper, middle, and lower) of the right lung.

Ideally, to take samples from the bronchopulmonary segments, the lungs should be preserved by inflating them with 10% buffered formalin using a perfusion infiltration technique immediately after removal. In addition, the lungs should be removed as a complete, intact unit, without separating them from the bronchus, and samples should be taken while the lung is still intact. However, this process is complex and cumbersome, and it would be impossible for the NIOH to conduct this technique since manganese mines are in the Northern Cape. Moreover, the NIOH does not routinely check heavy metal concentrations in the lungs of deceased mineworkers.

Furthermore, there are high chances that mineworkers die around where they live and work, which is far away from Johannesburg, where NIOH is based. The current protocol involves the removal of the lungs closer to where the mineworker has died. Logistically, it usually takes 4-8 weeks for the lungs of manganese mineworkers to reach NIOH in Johannesburg. Manganese-unexposed lungs are commonly removed, separated from the bronchus, preserved in 10% formalin, and shipped to the NIOH days or sometimes even months after death.

4.10.3 Disruptions in the supply chain

The researcher had planned to conduct immunohistochemistry stains to reveal the specific cellular structures or molecular pathways involved in manganese accumulation. The disruptions in the supply chain caused by the COVID-19 pandemic impacted the procurement of antigens and sera for immunohistochemistry used in this investigation. However, the study was strengthened by conducting extensive histochemistry with the addition of reticulin fibre stain. As manganese exposure often induces inflammatory responses, which are crucial for understanding manganese's long-term impact, the use of a reticulin fibre stain in studying fibrosis and inflammation is scientifically significant because it specifically highlights structural changes in tissue architecture, particularly in the context of fibrosis, a key pathological feature in response to toxic exposures.

Reticulin stains are highly effective in highlighting reticular (type III collagen) fibres, which are typically located around blood vessels and support connective tissues in the lungs. Reticulin staining can reveal early fibrotic changes before the development of dense fibrotic tissue, making it a sensitive tool for detecting the onset of fibrosis. As fibrosis progresses, reticular fibres increase in density and arrangement, a structural change readily visible with reticulin staining. This provides a valuable measure for assessing the severity and stage of fibrosis related to manganese exposure, which can be particularly relevant in tissues exposed to chronic manganese levels, such as the lungs of mineworkers.

Manganese exposure often triggers inflammation, which in turn promotes fibrotic responses as the tissue attempts to repair itself. Reticulin staining can help identify areas where inflammation has led to changes in reticular fibre organization, thus supporting an understanding of how manganese exposure leads to chronic inflammation and fibrotic damage over time. Reticulin fibre staining specifically targets structural changes associated with fibrosis, enabling researchers to distinguish these from other potential tissue alterations caused by manganese exposure, such as necrosis or oedema. This specificity helps clarify the direct relationship between manganese exposure, inflammation, and fibrosis.

4.11 Recommendations for Further Research

Future longitudinal cohort studies of living manganese-exposed workers to assess clinical outcomes over time and investigate early signs of manganese-related pulmonary or neurological impairment using biomarkers, imaging, and functional tests. Future comparative tissue distribution studies across organs could explore manganese distribution in other organs (e.g., liver and kidneys) to better understand systemic absorption and accumulation patterns.

Further histochemical and molecular studies should be conducted to examine the cellular changes induced by manganese, utilising advanced techniques such as electron microscopy and molecular imaging.

These studies could provide insights into the impact of manganese on cellular structure, function, and oxidative stress markers in various cell types.

CHAPTER FIVE – CONCLUSION

These study findings offer important insights into manganese concentrations in the lungs of manganese-exposed mineworkers from the Northern Cape province of South Africa, a population with unique and prolonged exposure to manganese through the mining of manganese ore.

Quantitative analysis revealed detectable levels of manganese deposition in the lung tissues of deceased South African mineworkers, indicating long-term inhalational exposure in the occupational setting. Mapping of manganese concentrations in lung tissue revealed a distinct pattern of manganese deposition, with concentrations tending to accumulate in the upper lung region.

Manganese deposition was not correlated with chronic inflammatory responses or fibrotic alterations in lung tissues. Even though manganese was detected in lung tissue, no specific histopathological alterations were directly attributed to manganese deposition.

While no clear correlation was observed between manganese levels in lung and brain tissues, the detection of manganese in both organs indicates that manganese is taken up following prolonged exposure.

In conclusion, this study underscores the importance of enhanced health monitoring among workers exposed to manganese. The presence of manganese in both lung and brain tissues raises the question of whether exposed workers should be assessed for corresponding neurological and/or respiratory health effects. These findings support targeted medical evaluations to identify and manage potential long-term outcomes.

REFERENCES

1. South32. South Africa Manganese: South32; 2024 [Available from: https://www.south32.net/what-we-do/our-locations/southern-africa/south-africa-manganese.
2. Minerals C. The Kalahari Manganese Fields: Cape Minerals; 2017 [Available from: https://www.capeminerals.co.za/the-kalahari-manganese-fields.
3. Ntsimbintle. The Kalahari Manganese field: Ntsimbintle Holdings; 2024 [Available from: https://www.ntsimbintle.co.za/our-business/the-kalahari-manganese-field.
4. CREAMER M. South Africa has 22 operating manganese mines – AmaranthCX. Mining Weekly. 2020 28 September 2020.
5. Minerals C. The Kalahari Manganese Fields Johannesburg: Cape Minerals; 2024 [Available from: https://www.capeminerals.co.za/the-kalahari-manganese-fields.
6. Mining TeNM. Tshipi e' Nhle Johannesburg, South Africa: Tshipi e Nhle; 2024 [Available from: https://www.tshipi.co.za/.
7. Mining TéNM. Tshipi é Ntle Manganese Mining: Tshipi é Ntle Manganese Mining; n.d. [Available from: https://www.tshipi.co.za/.
8. Assmang. Manganese Ore: Assmang; n.d. [Available from: https://www.assmang.co.za/assmang-manganese-ore/.
9. Mine A. Black Rock Mine operations: Assmang Mine; 2024 [Available from: https://assmang.ci.hr/applicant/index.php.
10. UMK. Key role of manganese for South Africa Johannesburg, South Africa: United Manganese of Kalahari; 2024 [Available from: https://www.umk.co.za/potential-of-manganese/.
11. Kalahari UMo. History: International Manganese Institute; 2024 [Available from: https://www.umk.co.za/about-us/.
12. IMni. The Kalagadi Manganese Mine Paris, France: International Manganese Institute; 2024 [Available from: https://www.manganese.org/en/tech-tours/kalagadi-mine.
13. Joshua M. Kudumane Manganese Resources : The Core of Kalahari Mining United Kingdom2024 [Available from: https://www.mining-outlook.com/corporate-stories/kudumane-manganese-resources-the-core-of-kalahari-mining#investment-and-the-future.
14. MCSA. Facts and Figures 2023 Datasheets South Africa: Minerals Council South Africa; 2023 [Available from: https://www.mineralscouncil.org.za/industry-news/publications/facts-and-figures.
15. Steenkamp JD, Bam W, Ringdalen E, Mushwana M, Hockaday S, Sithole N. Working towards an increase in manganese ferroalloy production in South Africa-a research agenda. Journal of the Southern African Institute of Mining and Metallurgy. 2018;118(6):645–54.
16. Esau M, Cole MJ, Broadhurst JL, Chimbganda T, Abrams A, editors. Developing a national mine closure risk and opportunity atlas for South Africa. Proceedings of the International Conference on Mine Closure; 2023.
17. Rossouw M, Baxter R. Subject concepts and issue outline. Journal of the Southern African Institute of Mining and Metallurgy. 2011;111(7):511–6.
18. Schmidt-Whitley J, Sutorius-Lavoie N. Mining and mineral processing remains vital for African economy. Engineering and Mining Journal. 2004;205(5):21–3.
19. Africa MCS. Facts and Figures Johannesburg: Mineral Council South Africa; 2018 [Available from: http//www.facts-and-figures-2018/pdf.
20. Tholana T, Musingwini C, Njowa G. An algorithm to construct industry cost curves used in analysing cash cost performance of operations for selected minerals in South Africa. Journal of the Southern African Institute of Mining and Metallurgy. 2013;113(6):473–84.
21. Inoue N. Occupational neurotoxicology due to heavy metals-especially manganese poisoning. Brain and Nerve. 2007;59(6):581–9.
22. Santamaria AB, Sulsky SI. Risk assessment of an essential element: manganese. J Toxicol Environ Health A. 2010;73(2):128–55.
23. Aschner JL, Aschner M. Nutritional aspects of manganese homeostasis. Molecular Aspects of Medicine. 2005;26(4-5 SPEC. ISS.):353–62.
24. Aschner M, Dorman DC. Manganese: pharmacokinetics and molecular mechanisms of brain uptake. Toxicological reviews. 2006;25(3):147–54.

25. Gad SC. Manganese. Encyclopedia of Toxicology, Fourth Edition: Volume 1-9. 62023. p. V6–17.
26. Gad SC, Pham T. Manganese. Encyclopedia of Toxicology: Third Edition2014. p. 150–2.
27. Szentmihályi K, Vinkler P, Fodor J, Balla J, Lakatos B. The role of manganese in the human organism. Orvosi Hetilap. 2006;147(42):2027–30.
28. Costa LG, Aschner M. Manganese in health and disease: Royal Society of Chemistry; 2014.
29. Freeland-Graves JH, Mousa TY, Sanjeevi N. Nutritional Requirements for Manganese. In: Costa L, Aschner M, editors. Manganese in Health and Disease: The Royal Society of Chemistry; 2014. p. 0.
30. Soares MV, Quines CB, Ávila DS. Manganese. Essential and Toxic Trace Elements and Vitamins in Human Health2020. p. 141–52.
31. Hospitals M. Manganese Deficiency: Symptoms and Treatments India2024 [Available from: https://www.medicoverhospitals.in/diseases/manganese-deficiency/.
32. Sachse B, Kolbaum AE, Ziegenhagen R, Andres S, Berg K, Dusemund B, et al. Dietary Manganese Exposure in the Adult Population in Germany—What Does it Mean in Relation to Health Risks? Molecular Nutrition and Food Research. 2019;63(16).
33. Williams M, Todd GD, Roney N, Crawford J, Coles C, McClure PR, et al. Toxicological profile for manganese. 2013.
34. Dobson AW, Erikson KM, Aschner M. Manganese neurotoxicity. Annals of the New York Academy of Sciences. 2004;1012:115–28.
35. Karyakina NA, Shilnikova N, Farhat N, Ramoju S, Cline B, Momoli F, et al. Biomarkers for occupational manganese exposure. Critical Reviews in Toxicology. 2022;52(8):636–63.
36. Mehrifar Y, Pirami H, Farhang Dehghan S. The relationship between exposure to manganese in welding fumes and incidence of migraine headache symptoms. Tehran University Medical Journal. 2018;76(2):135–41.
37. Sriram K, Lin GX, Jefferson AM, Stone S, Afshari A, Keane MJ, et al. Modifying welding process parameters can reduce the neurotoxic potential of manganese-containing welding fumes. Toxicology. 2015;328:168–78.
38. Hałatek T, Sinczuk-Walczak H, Szymczak M, Rydzynski K. Neurological and respiratory symptoms in shipyard welders exposed to manganese. International Journal of Occupational Medicine and Environmental Health. 2005;18(3):265–74.
39. Dorman DC, McManus BE, Parkinson CU, Manuel CA, McElveen AM, Everitt JI, editors. Nasal toxicity of manganese sulfate and manganese phosphate in young male rats following subchronic (13-week) inhalation exposure. Inhalation Toxicology; 2004.
40. Hernandez-Pellón A, Fernandez-Olmo I, Ledoux F, Courcot L, Courcot D. Characterization of manganese-bearing particles in the vicinities of a manganese alloy plant. Chemosphere. 2017;175:411–24.
41. Asildağ MA, Sari G, Koyuncu A, Şimşek C. Manganism due to occupational welding fume exposure: a case report. Industrial Health. 2024;62(5):334–7.
42. Moberly AH, Czarnecki LA, Pottackal J, Rubinstein T, Turkel DJ, Kass MD, et al. Intranasal exposure to manganese disrupts neurotransmitter release from glutamatergic synapses in the central nervous system in vivo. NeuroToxicology. 2012;33(5):996–1004.
43. Flynn MR, Susi P. Neurological risks associated with manganese exposure from welding operations–a literature review. International journal of hygiene and environmental health. 2009;212(5):459–69.
44. Bowler RM, Koller W, Schulz PE. Parkinsonism due to manganism in a welder: Neurological and neuropsychological sequelae. NeuroToxicology. 2006;27(3):327–32.
45. Antonini JM, Santamaria AB, Jenkins NT, Albini E, Lucchini R. Fate of manganese associated with the inhalation of welding fumes: Potential neurological effects. NeuroToxicology. 2006;27(3):304–10.
46. Flynn MR, Susi P. Manganese, iron, and total particulate exposures to welders. Journal of Occupational and Environmental Hygiene. 2009;7(2):115–26.
47. Zimmer AT, Biswas P. Characterization of the aerosols resulting from arc welding processes. Journal of Aerosol Science. 2001;32(8):993–1008.
48. Lucchini RG, Aschner M, Kim Y. Manganese. Handbook on the Toxicology of Metals: Fifth Edition. 22021. p. 501–38.

49. Hanley KW, Andrews R, Bertke S, Ashley K. Manganese Fractionation Using a Sequential Extraction Method to Evaluate Welders Shielded Metal Arc Welding Exposures during Construction Projects in Oil Refineries. Journal of Occupational and Environmental Hygiene. 2015;12(11):774–84.
50. Ma Y, Kero I, Gates SJF, Tranell G, editors. Trace elements behavior during the oxidation of liquid SiMn alloy. Minerals, Metals and Materials Series; 2017.
51. Mirmohammadi S, Moghaddasi Y, Yazdani J, Yousefinejad R, Esfandyari Y, Gorgani M, et al. Correlation between airborne manganese concentration at the workstations in the iron foundry and manganese concentration in workers' blood. Medycyna Pracy. 2017;68(4):449–58.
52. Roels H, Ghyselen P, Buchet J-P, Ceulemans E, Lauwerys R. Assessment of the permissible exposure level to manganese in workers exposed to manganese dioxide dust. Occupational and Environmental Medicine. 1992;49(1):25–34.
53. Utembe W, Faustman EM, Matatiele P, Gulumian M. Hazards identified and the need for health risk assessment in the South African mining industry. Human and Experimental Toxicology. 2015;34(12):1212–21.
54. Ewusi A, Sunkari ED, Seidu J, Coffie-Anum E. Hydrogeochemical characteristics, sources and human health risk assessment of heavy metal dispersion in the mine pit water–surface water–groundwater system in the largest manganese mine in Ghana. Environmental Technology and Innovation. 2022;26.
55. Nascimento S, Baierle M, Göethel G, Barth A, Brucker N, Charão M, et al. Associations among environmental exposure to manganese, neuropsychological performance, oxidative damage and kidney biomarkers in children. Environmental Research. 2016;147:32–43.
56. Bader M, Dietz MC, Ihrig A, Triebig G. Biomonitoring of manganese in blood, urine and axillary hair following low-dose exposure during the manufacture of dry cell batteries. Int Arch Occup Environ Health. 1999;72(8):521–7.
57. Mercadante CJ, Herrera C, Pettiglio MA, Foster ML, Johnson LC, Dorman DC, et al. The effect of high dose oral manganese exposure on copper, iron and zinc levels in rats. BioMetals. 2016;29(3):417–22.
58. Baj J, Flieger W, Barbachowska A, Kowalska B, Flieger M, Forma A, et al. Consequences of disturbing manganese homeostasis. International Journal of Molecular Sciences. 2023;24(19):14959.
59. Shirina LI, Mazo VK. Mineral substance in human nutrition. Manganese: Absorbtion and bioavailability. Voprosy Pitaniia. 2006;75(5):4–14.
60. Chen P, Bornhorst J, Aschner MA. Manganese metabolism in humans. 2018.
61. Moshtaghie AA, Badii AA, Hassanzadeh T. Investigation of manganese and iron absorption by rat Everted Gut Sac. Pakistan Journal of Biological Sciences. 2006;9(7):1346–9.
62. Cousins RJ, Liuzzi JP. Trace metal absorption and transport. Physiology of the Gastrointestinal Tract: Elsevier; 2018. p. 1485–98.
63. Evans GR, Masullo LN. Manganese Toxicity: StatPearls Publishing, Treasure Island (FL); 2023 2023.
64. Gurol KC, Aschner M, Smith DR, Mukhopadhyay S. Role of excretion in manganese homeostasis and neurotoxicity: a historical perspective. American Journal of Physiology-Gastrointestinal and Liver Physiology. 2022;322(1):G79–G92.
65. Krieger D, Krieger S, Theilmann L, Jansen O, Gass P, Lichtnecker H. Manganese and chronic hepatic encephalopathy. The Lancet. 1995;346(8970):270–4.
66. Pienaar P, Smith W. A case study of the production of high-grade manganese sinter from low-grade Mamatwan manganese ore. INFACON 6. 1992;1:131–8.
67. Bustillo Revuelta M, Bustillo Revuelta M. Mineral resource extraction. Mineral resources: from exploration to sustainability assessment. 2018:311–421.
68. Ghorbani Y, Nwaila GT, Zhang SE, Bourdeau JE, Cánovas M, Arzua J, et al. Moving towards deep underground mineral resources: Drivers, challenges and potential solutions. Resources Policy. 2023;80:103222.
69. Baba AA, Ibrahim L, Adekola FA, Bale RB, Ghosh MK, Sheik AR, et al. Hydrometallurgical processing of manganese ores: a review. Journal of minerals and materials characterization and engineering. 2014;2(3):230–47.
70. ODMWA. OCCUPATIONAL DISEASES IN MINES AND WORKS ACT. In: minister P, editor. Cape Town, South Africa: Government Gazette; 1973.
71. Occupational Disease in Mines and Works Act No. 78 (1973).

72. NIOH. Pathology Division Surveillance Report. Johannesburg, South Africa: National Institute for Occupational Health; 2021. Report No.: NIOH Pathology Report 2/2023.
73. Nelson G. Occupational respiratory diseases in the South African mining industry. Global Health Action. 2013;6(1):19520.
74. Mohammadyan M, Babanezhad E, Charati JY. Evaluation of neurobehavioral symptoms in welders exposed to welding respirable particles containing manganese. Iran Occupational Health. 2022;19(1):200–14.
75. Park RM, Berg SL. Manganese and neurobehavioral impairment. A preliminary risk assessment. Neurotoxicology. 2018;64:159–65.
76. Mehrifar Y, Bahrami M, Sidabadi E, Pirami H. The effects of occupational exposure to manganese fume on neurobehavioral and neurocognitive functions: An analytical cross-sectional study among welders. EXCLI Journal. 2020;19:372–86.
77. Cecil R. Neurotoxicity following exposure to manganese-containing welding fumes. Journal of Health Safety and Environment. 2011;27(4):249.
78. Abdel-Rasoul GM, Abu-Salem MES, Salem EAA, Allam HK, Abdel-Monaem AM, Younis FE. Neurological and neurobehavioral effects of welders in Egypt exposed to manganese containing welding fumes. International Archives of Occupational and Environmental Health. 2024.
79. Gonzalez-Cuyar LF, Nelson G, Criswell SR, Ho P, Lonzanida JA, Checkoway H, et al. Quantitative neuropathology associated with chronic manganese exposure in South African mine workers. Neurotoxicology. 2014;45:260–6.
80. Miah MR, Ijomone OM, Okoh CO, Ijomone OK, Akingbade GT, Ke T, et al. The effects of manganese overexposure on brain health. Neurochemistry international. 2020;135:104688.
81. Curran CP, Park RM, Ho Sm, Haynes EN. Incorporating genetics and genomics in risk assessment for inhaled manganese: From data to policy. NeuroToxicology. 2009;30(5):754–60.
82. Aschner M, Guilarte TR, Schneider JS, Zheng W. Manganese: recent advances in understanding its transport and neurotoxicity. Toxicology and applied pharmacology. 2007;221(2):131–47.
83. Roels H, Bowler RM, Kim Y, Henn BC, Mergler D, Hoet P, et al. Manganese exposure and cognitive deficits: a growing concern for manganese neurotoxicity. Neurotoxicology. 2012;33(4):872–80.
84. Lucchini RG, Guazzetti S, Zoni S, Donna F, Peter S, Zacco A, et al. Tremor, olfactory and motor changes in Italian adolescents exposed to historical ferro-manganese emission. Neurotoxicology. 2012;33(4):687–96.
85. Gwiazda R, Lucchini R, Smith D. Adequacy and consistency of animal studies to evaluate the neurotoxicity of chronic low-level. Info: Postprints, Multi-Campus. 2007.
86. Dorman DC, Struve MF, Wong BA, Dye JA, Robertson ID. Correlation of brain magnetic resonance imaging changes with pallidal manganese concentrations in rhesus monkeys following subchronic manganese inhalation. Toxicological Sciences. 2006;92(1):219–27.
87. Huang Y, Bao M, Xiao J, Qiu Z, Wu K. Effects of PM2.5 on cardio-pulmonary function injury in open manganese mine workers. International Journal of Environmental Research and Public Health. 2019;16(11).
88. Dorman DC, Struve MF, Gross EA, Wong BA, Howroyd PC. Sub-chronic inhalation of high concentrations of manganese sulfate induces lower airway pathology in rhesus monkeys. Respiratory research. 2005;6:1–10.
89. Wang F, Zou Y, Shen Y, Zhong Y, Lv Y, Huang D, et al. Synergistic impaired effect between smoking and manganese dust exposure on pulmonary ventilation function in guangxi manganese-exposed workers healthy cohort (GXMEWHC). PLoS ONE. 2015;10(2).
90. Kazi TG, Baloch S, Baig JA, Afridi HI, Arain MB. Evaluate the adverse impact of metal oxide on workers of different age groups that engage with gas metal arc welding process: health risk assessment. Environmental Science and Pollution Research. 2021;28(7):8652–61.
91. Antonini JM, Zeidler-Erdely PC, Young S-H, Roberts JR, Erdely A. Systemic immune cell response in rats after pulmonary exposure to manganese-containing particles collected from welding aerosols. Journal of immunotoxicology. 2012;9(2):184–92.
92. Badima H, Kumie A, Meskele B, Abaya SW. Welding fume exposure and prevalence of chronic respiratory symptoms among welders in micro-and small-scale enterprise in Akaki Kality sub-city, Addis Ababa, Ethiopia: a comparative cross-sectional study. BMC Pulmonary Medicine. 2024;24(1):147.

93. Jafari N, Shoaibinobarian N, Dehghani A, Rad A, Mirmohammadali SN, Alaeian MJ, et al. The effects of purslane consumption on glycemic control and oxidative stress: A systematic review and dose–response meta-analysis. Food Science & Nutrition. 2023;11(6):2530–46.
94. Hedmer M, Karlsson JE, Andersson U, Jacobsson H, Nielsen J, Tinnerberg H. Exposure to respirable dust and manganese and prevalence of airways symptoms, among Swedish mild steel welders in the manufacturing industry. International Archives of Occupational and Environmental Health. 2014;87(6):623–34.
95. Li G, Jiang J, Liao Y, Wan S, Yao Y, Luo Y, et al. Risk for lung-related diseases associated with welding fumes in an occupational population: Evidence from a Cox model. Frontiers in public health. 2022;10:990547.
96. Fitsanakis VA, Piccola G, Aschner JL, Aschner M. Characteristics of manganese (Mn) transport in rat brain endothelial (RBE4) cells, an in vitro model of the blood-brain barrier. NeuroToxicology. 2006;27(1):60–70.
97. Heilig E, Molina R, Donaghey T, Brain JD, Wessling-Resnick M. Pharmacokinetics of pulmonary manganese absorption: Evidence for increased susceptibility to manganese loading in iron-deficient rats. American Journal of Physiology - Lung Cellular and Molecular Physiology. 2005;288(5 32-5):L887–L93.
98. Thompson K, Molina R, Donaghey T, Brain JD, Wessling-Resnick M. The influence of high iron diet on rat lung manganese absorption. Toxicology and Applied Pharmacology. 2006;210(1-2):17–23.
99. Thompson KJ, Kim J, Wessling-Resnick M. Manganese Transport Across the Pulmonary Epithelium. In: Costa L, Aschner M, editors. Manganese in Health and Disease: The Royal Society of Chemistry; 2014. p. 0.
100. Kim Y, Park S. Iron deficiency increases blood concentrations of neurotoxic metals in children. Korean Journal of Pediatrics. 2014;57(8):345–50.
101. Margrete Meltzer H, Lise Brantster A, Borch-Iohnsen B, Ellingsen DG, Alexander J, Thomassen Y, et al. Low iron stores are related to higher blood concentrations of manganese, cobalt and cadmium in non-smoking, Norwegian women in the HUNT 2 study. Environmental Research. 2010;110(5):497–504.
102. Brain JD, Heilig E, Donaghey TC, Knutson MD, Wessling-Resnick M, Molina RM. Effects of iron status on transpulmonary transport and tissue distribution of Mn and Fe. American Journal of Respiratory Cell and Molecular Biology. 2006;34(3):330–7.
103. Gandhi D, Bhandari S, Maity S, Mahapatra SK, Rajasekaran S. Activation of ERK/NF-kB Pathways Contributes to the Inflammatory Response in Epithelial Cells and Macrophages Following Manganese Exposure. Biological Trace Element Research. 2024:1–12.
104. Zhang L, Sang H, Liu Y, Li J. Manganese activates caspase-9-dependent apoptosis in human bronchial epithelial cells. Human & experimental toxicology. 2013;32(11):1155–63.
105. Tomoda K, Kimura H, Osaki S. Distribution of collagen fiber orientation in the human lung. The Anatomical Record. 2013;296(5):846–50.
106. Cavalcante FS, Ito S, Brewer K, Sakai H, Alencar AM, Almeida MP, et al. Mechanical interactions between collagen and proteoglycans: implications for the stability of lung tissue. Journal of applied physiology. 2005;98(2):672–9.
107. Djeska IS, Ceausu RA, Gaje PN, Cimpean AM, Mederle O, Nicodin A, et al. The reticular network contributes to the staging of idiopathic lung fibrosis. Archives of Biological Sciences. 2013;65(4):1599–604.
108. Bezerra FS, Lanzetti M, Nesi RT, Nagato AC, Silva CPe, Kennedy-Feitosa E, et al. Oxidative stress and inflammation in acute and chronic lung injuries. Antioxidants. 2023;12(3):548.
109. Choi J-Y, Kang M, Jung J-H, Kim WJ, Yang H-S, Lee K, et al. Exposure of lung fibroblasts to PM2. 5 and lead (Pb) induces fibrosis and apoptosis in alveolar epithelial cells via a paracrine effect. Ecotoxicology and Environmental Safety. 2024;288:117401.
110. Start R, McCulloch T, Silcocks P, Cotton D. Attitudes of senior pathologists towards the autopsy. The Journal of pathology. 1994;172(1):81–4.
111. Röllin HB, Nogueira CMCA. Manganese: Environmental Pollution and Health Effects. Encyclopedia of Environmental Health2011. p. 617–29.

112. Bredow S, Falgout MM, March TH, Yingling CM, Malkoski SP, Aden J, et al. Subchronic inhalation of soluble manganese induces expression of hypoxia-associated angiogenic genes in adult mouse lungs. Toxicology and Applied Pharmacology. 2007;221(2):148–57.
113. Date AR, Gray AL. Progress in plasma source mass spectrometry. Spectrochimica Acta Part B: Atomic Spectroscopy. 1983;38(1-2):29–37.
114. Date AR. An introduction to inductively coupled plasma source mass spectrometry. TrAC Trends in Analytical Chemistry. 1983;2(10):225–30.
115. Midelfart J, Aase S. The value of autopsy from a clinical point of view. Apmis. 1998;106(7-12):693–8.
116. Cavey T, Ropert M, Loréal O, Bendavid C, Peoc'h K. Metals: Common clinical applications in inductively coupled plasma mass spectrometry. Annales de Biologie Clinique. 2019;77(5):495–504.
117. Wehe CA, Bornhorst J, Holtkamp M, Sperling M, Galla HJ, Schwerdtle T, et al. Fast and low sample consuming quantification of manganese in cell nutrient solutions by flow injection ICP-QMS. Metallomics. 2011;3(12):1291–6.
118. Soyab T. Special stains used in histopathological techniques: A brief view. Indian Journal of Forensic Medicine and Toxicology. 2020;14(4):8632–6.
119. Mahapatra N, Babu NA, Behura SS, Rajesh E. A Brief Review on Haematoxylin: An Irreplaceable Tissue Stain. Indian Journal of Forensic Medicine & Toxicology. 2020;14(4):1221–5.
120. Sridharan D, Pracha N, Dougherty JA, Akhtar A, Alvi SB, Khan M. A one-stop protocol to assess myocardial fibrosis in frozen and paraffin sections. Methods and Protocols. 2022;5(1):13.
121. Suvarna KS, Layton C, Bancroft JD. Bancroft's theory and practice of histological techniques E-Book: Elsevier health sciences; 2018.
122. Seo PS, Park SD. Reticulum stain findings in various cutaneous granulomatous diseases. Korean Journal of Dermatology. 2006;44(8):925–30.
123. Boyko R, Darby S, Goldberg RC, Milin Z. Fulfilling broken promises. New Haven: Yale Law School and Yale School of Public Health. 2013.
124. Wieslander B, Ramos JG, Ax M, Petersson J, Ugander M. Supine, prone, right and left gravitational effects on human pulmonary circulation. Journal of Cardiovascular Magnetic Resonance. 2019;21(1).
125. Gosling JA, Harris PF, Humpherson JR, Whitmore I, Willan PL. Human Anatomy, Color Atlas and Textbook E-Book: Human Anatomy, Color Atlas and Textbook E-Book: Elsevier Health Sciences; 2016.
126. Tanvir EM, Whitfield KM, Ng JC, Shaw PN. Development and Validation of an ICP-MS Method and Its Application to Determine Multiple Trace Elements in Small Volumes of Whole Blood and Plasma. Journal of Analytical Toxicology. 2020;44(9):1036–46.
127. Zou Y, Yu S, Qiu L. Clinical application and research progress of inductively coupled plasma mass spectrometry technology. Chinese Journal of Laboratory Medicine. 2020;43(10):1039–43.
128. Li T, Shen K, Zhu Y, Min H, Li C, Liu S. Application progress of high resolution inductively coupled plasma mass spectrometry in determination of trace element in geological samples. Yejin Fenxi/Metallurgical Analysis. 2021;41(4):9–19.
129. Day SJ, Altman DG. Blinding in clinical trials and other studies. Bmj. 2000;321(7259):504.
130. Ashcroft T, Simpson JM, Timbrell V. Simple method of estimating severity of pulmonary fibrosis on a numerical scale. Journal of clinical pathology. 1988;41(4):467–70.
131. Mine Health and Safety Act, 29 (1996).
132. Krabbe K, Nielsen A, Krogh-Madsen R, Plomgaard P, Rasmussen P, Erikstrup C, et al. Brain-derived neurotrophic factor (BDNF) and type 2 diabetes. Diabetologia. 2007;50(2):431–8.
133. Moser M-B, Moser EI, Forrest E, Andersen P, Morris R. Spatial learning with a minislab in the dorsal hippocampus. Proceedings of the National Academy of Sciences. 1995;92(21):9697–701.
134. MCSA. Signed agreement: AGA and Harmony Johannesburg: Government Gazette; 2018.
135. Sá RC, Zeman KL, Bennett WD, Prisk GK, Darquenne C. Effect of posture on regional deposition of coarse particles in the healthy human lung. Journal of Aerosol Medicine and Pulmonary Drug Delivery. 2015;28(6):423–31.
136. Radstrom M, Loswick A, Bengtsson J. Respiratory effects of the kneeling prone position for low back surgery. European journal of anaesthesiology. 2004;21(4):279–83.
137. West JB. Respiratory physiology: the essentials: Lippincott Williams & Wilkins; 2012.
138. Brauer ACM. Ambient Atmospheric Particles in the Airways of Human Lungs. Ultrastructural Pathology. 2000;24(6):353–61.

139. Weibel ER, Cournand AF, Richards DW. Morphometry of the human lung: Springer; 1963.
140. Heyder J, Svartengren MU. Basic principles of particle behavior in the human respiratory tract. Lung biology in Health and Disease. 2001;162:21–46.
141. Schlesinger RB. Comparative deposition of inhaled aerosols in experimental animals and humans: a review. Journal of Toxicology and Environmental Health, Part A Current Issues. 1985;15(2):197–214.
142. Lucchini RG, Martin CJ, Doney BC. From manganism to manganese-induced parkinsonism: A conceptual model based on the evolution of exposure. NeuroMolecular Medicine. 2009;11(4):311–21.
143. Tyler NK, Plopper CG. Morphology of the distal conducting airways in rhesus monkey lungs. The Anatomical Record. 1985;211(3):295–303.
144. Dorman DC, Struve MF, Gross EA, Wong BA, Howroyd PC. Sub-chronic inhalation of high concentrations of manganese sulfate induces lower airway pathology in rhesus monkeys. Respiratory Research. 2005;6(1):121.
145. Heppleston A. The Pathological Anatomy of Simple Pneumokoniosis in Goal Workers. 1953.
146. Niewoehner DE, Kleinerman J, Rice DB. Pathologic changes in the peripheral airways of young cigarette smokers. New England Journal of Medicine. 1974;291(15):755–8.
147. Qi Y, Si H, Jin X, Guo Y, Xia J, He J, et al. Expression levels of key immune indicators and immune checkpoints in manganese-exposed rats. Ecotoxicology and Environmental Safety. 2024;272.
148. Qi Y, Si H, Jin X, Guo Y, Xia J, He J, et al. Changes in serum TIM-3 and complement C3 expression in workers due to Mn exposure. Frontiers in Public Health. 2023;11.
149. LeVan TD, Romberger DJ, Siahpush M, Grimm BL, Ramos AK, Johansson PL, et al. Relationship of systemic IL-10 levels with proinflammatory cytokine responsiveness and lung function in agriculture workers. Respiratory Research. 2018;19(1).
150. Field N, Murray J, Wong ML, Dowdeswell R, Dudumayo N, Rametsi L, et al. Missed opportunities in TB diagnosis: a TB process-based performance review tool to evaluate and improve clinical care. BMC Public Health. 2011;11(1):1.
151. Shin HJ, Choi MS, Ryoo NH, Nam KY, Park GY, Bae JH, et al. Manganese-mediated up-regulation of HIF-1α protein in Hep2 human laryngeal epithelial cells via activation of the family of MAPKs. Toxicology in Vitro. 2010;24(4):1208–14.
152. Weiss W. Asbestosis: a marker for the increased risk of lung cancer among workers exposed to asbestos. Chest. 1999;115(2):536–49.
153. Brown CH. A review of pulmonary fibrosis. US Pharmacist. 2015;40(7):HS12–HS6.
154. Pfau JC, Serve K, Woods L, Noonan C. Asbestos exposure and autoimmunity. Biological Effects of Fibrous and Particulate Substances2015. p. 181–94.
155. Blanc PD, Annesi-Maesano I, Balmes JR, Cummings KJ, Fishwick D, Miedinger D, et al. The occupational burden of nonmalignant respiratory diseases. An official American Thoracic Society and European Respiratory Society statement. American journal of respiratory and critical care medicine. 2019;199(11):1312–34.
156. Crossgrove JS, Yokel RA. Manganese distribution across the blood-brain barrier III: The divalent metal transporter-1 is not the major mechanism mediating brain manganese uptake. NeuroToxicology. 2004;25(3):451–60.
157. Alici NŞ, Öziş TN, Çeliker G, Aktürk TB. Welder's lung and brain MRI findings in manganese-exposed welders. Medicina del Lavoro. 2022;113(6).
158. Chen P, Chakraborty S, Mukhopadhyay S, Lee E, Paoliello MM, Bowman AB, et al. Manganese homeostasis in the nervous system. Journal of neurochemistry. 2015;134(4):601–10.
159. Gunter TE, Gerstner B, Gunter KK, Malecki J, Gelein R, Valentine WM, et al. Manganese transport via the transferrin mechanism. Neurotoxicology. 2013;34:118–27.
160. Steimle BL, Smith FM, Kosman DJ. The solute carriers ZIP8 and ZIP14 regulate manganese accumulation in brain microvascular endothelial cells and control brain manganese levels. Journal of Biological Chemistry. 2019;294(50):19197–208.
161. Tuschl K, Meyer E, Valdivia LE, Zhao N, Dadswell C, Abdul-Sada A, et al. Mutations in SLC39A14 disrupt manganese homeostasis and cause childhood-onset parkinsonism–dystonia. Nature communications. 2016;7(1):11601.
162. Aschner JL, Aschner M. Nutritional aspects of manganese homeostasis. Molecular aspects of medicine. 2005;26(4-5):353–62.

163. Racette B, McGee-Minnich L, Moerlein S, Mink J, Videen T, Perlmutter J. Welding-related parkinsonism: clinical features, treatment, and pathophysiology. Neurology. 2001;56(1):8–13.
164. No correction has been applied for transpiration that will occur after the pouch seal has been broken. See “Instructions for Use” for more information regarding transpiration.
165. Howe K, Clark MD, Torroja CF, Torrance J, Berthelot C, Muffato M, et al. The zebrafish reference genome sequence and its relationship to the human genome. Nature. 2013;496(7446):498–503.
166. No correction has been applied for transpiration that will occur after the pouch seal has been broken. See “Instructions for Use” for more information.
167. No correction has been applied for transpiration that will occur after the pouch seal has been broken. See “Instructions for Use” for more information.

ANNEXURE 1. Certificate of Standard Reference Material 1640A

National Institute of Standards & Technology

Certificate of Analysis

Standard Reference Material® 1640a

Trace Elements in Natural Water

This Standard Reference Material (SRM) is intended for use in evaluating methods used in the determination of trace elements in fresh water. SRM 1640a consists of acidified spring water with mass fractions and mass concentrations assigned for 29 elements, 22 of which were gravimetrically added. The solution contains nitric acid at a volume fraction of approximately 2 %. A unit of SRM 1640a consists of 250 mL of solution in a high-density polyethylene (HDPE) bottle sealed inside an aluminized Mylar pouch.

Certified Values and Uncertainties: The certified values for 22 elements in SRM 1640a are given expressed in mass fraction units and mass concentration units in Tables 1 and 2, respectively. A NIST certified value is a value in which NIST has the highest confidence in its accuracy, in that all known or suspected sources of bias have been fully investigated or taken into account [1].

Each certified mass fraction value given in Table 1 is the average of the value calculated from the gravimetric preparation and the value determined using either inductively-coupled plasma optical emission spectroscopy (ICP-OES) or inductively-coupled plasma mass spectrometry (ICP-MS), adjusted upward for transpiration that may occur over the certification period while the SRM bottle remains sealed inside the aluminized Mylar pouch. (164) The magnitude of the transpiration adjustment (0.11 %) is based upon the results of unpublished NIST studies of transpiration rates of similar HDPE bottles sealed inside similar aluminized Mylar pouches, and is such that the actual mass fraction is expected to be equal to the certified mass fraction value approximately halfway through the certification period. Each expanded uncertainty, U, in Table 1 is calculated as $U = ku_c$, where k is the coverage factor for the appropriate degrees of freedom (df) and a 95 % level of confidence (k and df are also given in Table 1) and u_c is the combined standard uncertainty calculated according to the ISO Guide [2]. The value of u_c is intended to represent, at the level of one standard deviation, the combined effect of uncertainty components associated with the gravimetric preparation, the ICP-OES or ICP-MS analysis, method bias [3], and the transpiration adjustment.

Each certified mass concentration value given in Table 2 is calculated from the corresponding certified mass fraction value in Table 1 through multiplication by the density of the SRM 1640a solution. Each expanded uncertainty, U, inTable 2 is calculated as $U = ku_c$, where k is the coverage factor for the appropriate degrees of freedom (df) and a95 % level of confidence (k and df are also given in Table 2) and u_c is the combined standard uncertainty calculated according to the ISO Guide [2]. The value of u_c is intended to represent, at the level of one standard deviation, the combined effect of uncertainty components associated with the certified mass fraction value and the solutiondensity.

Expiration of Certification: The certification of **SRM 1640a** is valid, within the measurement uncertainty specified, until **05 August 2020**, provided the SRM is handled and stored in accordance with instructions given in this certificate (see "Instructions for Use"). The certification is nullified if the SRM is damaged, contaminated, or otherwise modified.

Maintenance of SRM Certification: NIST will monitor this SRM over the period of its certification. If substantive technical changes occur that affect the certification before the expiration of this certificate, NIST will notify the purchaser. Registration (see attached sheet) will facilitate notification.

Coordination of the technical measurements leading to the certification of SRM 1640a was provided by
M.R. Winchester of the NIST Analytical Chemistry Division.

Stephen A. Wise, ChiefAnalytical Chemistry Division
Gaithersburg, MD 20899 Robert L.
Watters, Jr., Chief
Certificate Issue Date: 08 June 2010 Measurement
Services Division
See Certificate Revision History on Last Page

This SRM was prepared by T.A. Butler, L.L. Yu, and M.R. Winchester of the NIST Analytical Chemistry Division. The ICP-OES analyses were performed by T.A. Butler, J.L. Molloy, and M.R. Winchester of the NIST Analytical Chemistry Division. The ICP-MS analyses were performed by J.L. Molloy, T.A. Butler, L.L Yu, and M.R. Winchester of the NIST Analytical Chemistry Division.

Statistical consultation was provided by W.F. Guthrie of the NIST Statistical Engineering Division.

Support aspects involved in the issuance of this SRM were coordinated through the NIST Measurement Services Division.

Reference Values and Uncertainties: The reference values for seven elements in SRM 1640a are given expressed in mass fraction units and mass concentration units in Tables 3 and 4, respectively. Reference values are non-certified values that are best estimates of the true values. However, the values do not meet NIST criteria for certification and are provided with associated uncertainties that may not include all sources of uncertainty [1].

The reference mass fraction values and expanded uncertainties given in Table 3 are calculated using the same approach employed for the certified mass fraction values (see explanation above), including the use of the transpiration adjustment, except that each reference mass fraction value is based solely upon analysis using either ICP-OES or ICP-MS and uncertainty components are limited to those associated with the analysis and the transpiration adjustment. The reference mass concentration values and expanded uncertainties given in Table 4 are calculated using the same approach employed for the certified mass concentration values (see explanation above), except that they are calculated using the reference mass fraction values in place of the certified mass fraction values.

NOTICE AND WARNING TO USERS

CAUTION: This SRM is an acidic solution. All appropriate safety precautions, including use of gloves during handling, should be taken.

INSTRUCTIONS FOR USE

The SRM should be shaken before use to remix water that may have condensed on the inner surfaces of the bottle. To help prevent contamination, pipettes or other labware should **NOT** be inserted into the bottle. Instead, a portion of the solution should be decanted into another clean, dry container for use. Unused portions should not be returned to the SRM bottle.

The accuracy of trace element analysis is limited by contamination, especially at the microgram per kilogram (or microgram per liter) level. All apparatuses should be scrupulously clean, and only high-purity reagents should be employed. Sampling and manipulations, such as evaporations, should be done in a clean environment, such as a Class-100 clean hood.

The mass concentration values and uncertainties given in Tables 2 and 4 were calculated from the mass fraction values and uncertainties in Tables 1 and 3, respectively, taking into account the anticipated range of density values of the SRM solution in the temperature range 17 °C to 27 °C. Therefore, the mass concentration values and uncertainties given in the tables are valid when the SRM solution is used within a temperature range of 22 °C ± 5 °C. A more precise estimate of the mass concentration for a given temperature can be obtained by multiplying the mass fraction value by the accurately measured density of the solution at that temperature. The uncertainty associated with a mass concentration value calculated in this way can be estimated by combining the uncertainty components for the mass fraction value and the measured density following the ISO Guide [2].

Transpiration: The certified and reference values given in Tables 1 through 4 account for the effects of transpiration that may occur *prior to the first opening of the sealed pouch by the SRM user*. After the SRM bottle has been removed from the pouch, the rate of transpiration will rise, resulting in gradual increases in the mass fractions (and concentrations) of the elements. *It is the responsibility of the user of this SRM to account for this effect.* One approach is to weigh the SRM bottle both before and after each use. Mass loss observed during storage can be utilized to correct for transpiration. In order to minimize transpiration, the SRM bottle should be stored tightly closed and sealed inside an airtight container. The user should set a maximum shelf-life for a partially used SRM bottle commensurate with accuracy requirements.

PREPARATION OF MATERIAL

SRM 1640a was prepared at NIST using only high-purity reagents. An acid-cleaned HDPE tank of 2 kL capacity was filled with a known mass of commercially available spring water and enough concentrated nitric acid to adjust the acid volume fraction to approximately 2 %. After thorough mixing with a precleaned recirculating pump, a preliminary ICP-MS analysis was performed to determine the levels of the 29 elements of interest. The levels of the22 elements to be certified were gravimetrically adjusted to target values by additions of aliquots of known masses of the SRMs in the SRM 3100 series of single-element standard solutions. For each of these elements, the target value was approximately 80 % of the Maximum Contaminant Level (165) listed in either the National Primary Drinking Water Regulations or the National Secondary Drinking Water Regulations maintained by the United StatesEnvironmental Protection Agency (EPA) [4], or approximately the mass fraction that was present in SRM 1640 Trace Elements in Natural Water, whichever was less. After addition of the aliquots and thorough

mixing, the SRM solution was packaged in acid-cleaned HDPE bottles of 250 mL capacity and sealed inside aluminized Mylar pouches.

Table 1. Certified Values for Elements in SRM 1640a Expressed in Mass Fraction Units[a]

Element	Mass Fraction (µg/kg)			*k*	*df*
Aluminum	52.6	±	1.8	2.069	23
Antimony	5.064	±	0.045	2.365	7
Arsenic	8.010	±	0.067	1.980	120
Barium	150.60	±	0.74	1.984	98
Beryllium	3.002	±	0.027	2.060	25
Boron	300.7	±	3.1	2.365	7
Cadmium	3.961	±	0.072	2.365	7
Chromium	40.22	±	0.28	2.021	40
Cobalt	20.08	±	0.24	2.447	6
Copper	85.07	±	0.48	2.228	10
Iron	36.5	±	1.7	2.447	6
Lead	12.005	±	0.040	1.970	227
Manganese	40.07	±	0.35	2.201	11
Molybdenum	45.24	±	0.59	2.017	43
Nickel	25.12	±	0.12	2.026	37
Selenium	19.97	±	0.16	2.228	10
Silver	8.017	±	0.042	2.086	20
Strontium	125.03	±	0.86	2.179	12
Thallium	1.606	±	0.015	2.365	7
Uranium	25.15	±	0.26	2.145	14
Vanadium	14.93	±	0.21	2.447	6
Zinc	55.20	±	0.32	2.010	49

(a) Certified mass fraction values are the equally weighted means of results from gravimetry and ICP- OES or ICP-MS, adjusted upward for transpiration that may occur over the certification period while the SRM bottle remains sealed inside the aluminized Mylar pouch. (166) The magnitude of the transpiration adjustment (0.11 %) was selected so that the actual mass fractions are expected to be equal to the corresponding certified values approximately halfway through the certification period. The uncertainty listed with each value is an expanded uncertainty about the mean. The expanded uncertainty is calculated following the ISO Guide [2] as $U = ku_c$, where u_c is intended to represent, at the level of one standard deviation, the combined effect of uncertainty components associated with the gravimetric preparation, the ICP-OES or ICP-MS analysis, method bias [3], and the transpiration adjustment. The coverage factor (*k*) for each analyte is determined from the Student's *t*-distribution corresponding to the degrees of freedom (*df*) and a 95 % level of confidence.

Table 2. Certified Values for Elements in SRM 1640a Expressed in Mass Concentration Units[a]

Element	Mass Concentration [b] (µg/L)			*k*	*df*
Aluminum	53.0	±	1.8	2.064	24
Antimony	5.105	±	0.046	2.262	9
Arsenic	8.075	±	0.070	1.977	142
Barium	151.80	±	0.83	1.976	151
Beryllium	3.026	±	0.028	2.045	29
Boron	303.1	±	3.1	2.306	8
Cadmium	3.992	±	0.074	2.365	7
Chromium	40.54	±	0.30	2.008	51
Cobalt	20.24	±	0.24	2.365	7
Copper	85.75	±	0.51	2.120	16
Iron	36.8	±	1.8	2.447	6
Lead	12.101	±	0.050	1.965	517
Manganese	40.39	±	0.36	2.160	13

Molybdenum	45.60	±	0.61	2.013	46
Nickel	25.32	±	0.14	2.001	59
Selenium	20.13	±	0.17	2.160	13
Silver	8.081	±	0.046	2.040	31
Strontium	126.03	±	0.91	2.120	16
Thallium	1.619	±	0.016	2.306	8
Uranium	25.35	±	0.27	2.120	16
Vanadium	15.05	±	0.25	2.365	7
Zinc	55.64	±	0.35	1.995	68

[a] Certified mass concentration values are calculated from the certified mass fraction values in Table 1 through multiplication by the density of the SRM 1640a solution. The uncertainty listed with each value is an expanded uncertainty about the mean. The expanded uncertainty is calculatedfollowing the ISO Guide [2] as $U = ku_c$, where u_c is intended to represent, at the level of one standard deviation, the combined effect of uncertainty components associated with the certified mass fraction value and the solution density. The coverage factor (k) for each analyte is determinedfrom the Student's t-distribution corresponding to the degrees of freedom (df) and a 95 % level of confidence.

(b) The certified mass concentration values and expanded uncertainties are valid when the SRM solution is used within the temperature range (22 °C ± 5 °C).

(c) Table 3. Reference Values for Elements in SRM 1640a Expressed in Mass Fraction Units(a)

Element	Mass Fraction (mg/kg)			k	df
Calcium	5.570	±	0.016	2.120	16
Magnesium	1.0502	±	0.0034	2.262	9
Potassium	0.5753	±	0.0020	2.179	12
Silicon	5.169	±	0.017	2.074	22
Sodium	3.112	±	0.031	2.776	4
Lithium	0.4034	±	0.0092	2.776	4
Rubidium	1.188	±	0.011	1.961	3204

[a] Reference mass fraction values are the ICP-OES or ICP-MS values, adjusted upward for transpiration that may occur over the certification period while the SRM bottle remains sealed inside the aluminized Mylar pouch. (167) The magnitude of the transpiration adjustment (0.11 %) was selected so that the actual mass fractions are expected to be equal to the corresponding reference values approximately halfway through the certification period. The uncertainty listed with each value is an expanded uncertainty about the mean. The expanded uncertainty is calculated following the ISO Guide [2] as $U = ku_c$, where u_c is intended to represent, at the level of one standard deviation, the combined effect of uncertainty components associated with the ICP-OES or ICP-MS analysis and the transpiration adjustment. The coverage factor (k) for each analyte is determined from the Student's t-distributioncorresponding to the degrees of freedom (df) and a 95 % level of confidence.

Table 4. Reference Values for Elements in SRM 1640a Expressed in Mass Concentration Units[a]

Element	Mass Concentration [b] (mg/L)			*k*	*df*
Calcium	5.615	±	0.021	2.005	54
Magnesium	1.0586	±	0.0041	2.045	29
Potassium	0.5799	±	0.0023	2.040	31
Silicon	5.210	±	0.021	2.005	54
Sodium	3.137	±	0.031	2.571	5
	(µg/L)				
Lithium	0.4066	±	0.0094	2.776	4
Rubidium	1.198	±	0.011	1.961	3657

[a] Reference mass concentration values are calculated from the reference mass fraction values inTable 3 through multiplication by the density of the SRM 1640a solution. The uncertainty listed with each value is an expanded uncertainty about the mean. The expanded uncertainty is calculatedfollowing the ISO Guide [2] as $U = ku_c$, where u_c is intended to represent, at the level of one standard deviation, the combined effect of uncertainty components associated with the reference mass fraction value and the solution density. The coverage factor (*k*) for each analyte is determinedfrom the Student's *t*-distribution corresponding to the degrees of freedom (*df*) and a 95 % level of confidence.

[b] The reference mass concentration values and expanded uncertainties are valid when the SRM solution is used within the temperature range (22 °C ± 5 °C).

REFERENCES

[1] May, W.; Parris, R.; Beck II, C.; Fassett, J.; Greenberg, R.; Guenther, F.; Kramer, G.; Wise, S.; Gills, T.; Colbert, J.; Gettings, R.; MacDonald, B.; *Definition of Terms and Modes Used at NIST for Value-Assignment ofReference Materials for Chemical Measurements*; NIST Special Publication 260-136 (2000); available at http://ts.nist.gov/MeasurementServices/ReferenceMaterials/PUBLICATIONS.cfm (accessed Jun 2010).

[2] JCGM 100:2008; *Evaluation of Measurement Data — Guide to the Expression of Uncertainty in Measurement*(ISO GUM 1995 with Minor Corrections); Joint Committee for Guides in Metrology (2008); available at http://www.bipm.org/utils/common/documents/jcgm/JCGM_100_2008_E.pdf (accessed Jun 2010); see also Taylor, B.N.; Kuyatt, C.E.; *Guidelines for Evaluating and Expressing the Uncertainty of NIST Measurement Results*; NIST Technical Note 1297; U.S. Government Printing Office: Washington, DC (1994); available at http://www.nist.gov/physlab/pubs/index.cfm (accessed Jun 2010).

[3] Levenson, M.S.; Banks, D.L.; Eberhardt, K.R.; Gill, L.M.; Guthrie, W.F.; Liu, H.K.; Vangel, M.G.; Yen, J.H.; Zhang, N.F.; *An Approach to Combining Results From Multiple Methods Motivated by the ISO GUM*; J. Res. Natl. Inst. Stand. Technol., Vol, 105; p. 571 (2000).

[4] *Drinking Water Contaminants*, United States Environmental Protection Agency, available at http://www.epa.gov/safewater/contaminants/index.html#listsec (accessed Jun 2010).

Certificate Revision History: 08 June 2010 (This revision includes corrected lithium values in Tables 3 and 4 and minor editorial changes.);03 December 2009 (Original certificate date).

Users of this SRM should ensure that the Certificate of Analysis in their possession is current. This can be accomplished by contacting the SRM Program: telephone (301) 975-2200; fax (301) 926-4751; e-mail srminfo@nist.gov; or via the Internet at http://www.nist.gov/srm.

ANNEXURE 2. *Haematoxylin & Eosin, Masson Trichome, Reticulin, and Periodic Acid Schiff stains Protocols*

1. Haematoxylin and Eosin regressive staining procedure

The lung sections were dewaxed in xylene 1 & 2 for 5 minutes each. With agitation, the slides were hydrated through 100% ethanol for 30 seconds and 95% for 30 seconds, washed well in tap water, and stained in Gill's Haematoxylin for 20 minutes, washed well in water. The slides were differentiated with acid alcohol for 15 seconds, washed immediately in tap water, and examined under a light microscope to ensure that the cytoplasm and other tissue elements did not stain, except that only the nuclei would stain. After the differentiation, the sections will be blued in Scott's tap water substitute (TWS) for 30 seconds, washed well in tap water for 2 minutes (to remove the alkalinity of the Scott's TWS so as not to interfere with the 1% eosin Y stain, which is acidic in nature) and stained in 1% eosin Y for 5 minutes. The slides were rapidly washed in tap water, dehydrated through 95% and 100% ethanol, and cleared in xylene with agitation for 30 seconds. The slides were then placed in mounting xylene and mounted with DPX mounting media and cover slipped.

2. Masson's Trichrome staining procedure

The lung sections were dewaxed in xylene 1 & 2 for 5 minutes each. With agitation, the tissues were hydrated through 100% ethanol for 30 seconds and 95% for 30 seconds, rinsed in distilled water, and stained in Stable Iron Haematoxylin for 5 minutes, and washed well in water. The slides were then differentiated microscopically with acid alcohol for 15 seconds, washed well in tap water and stained with Ponceau Fuchsin for 10 minutes, rinsed with 1% acetic acid, treated with 1% phosphomolybdic acid for 2 and a half minutes, rinsed with 1% acetic acid, stained with light green stain for 2 and a half minutes, rinsed with 1% acetic acid and blot dried. Tissues were dehydrated by dipping the slides rapidly through 100% ethanol and cleared in xylene with agitation for 30 seconds. The slides were then placed in mounting xylene and mounted with DPX mounting media and cover slipped.

3. Reticulin Staining Procedure for Reticulin Fibres

The lung sections were dewaxed in xylene 1 & 2 for 5 minutes each. With agitation, the tissues were hydrated through 100% ethanol for 30 seconds and 95% for 30 seconds, rinsed in distilled water, and stained in 0.5% potassium permanganate

solution for 3-5 minutes to oxidize the reticulin fibres. Rinsed in distilled water. Treated with 3% potassium metabisulfite solution for 1-2 minutes to bleach and remove any residual colour from the potassium permanganate. Rinsed in distilled water. Placed sections in 2.5% ferric ammonium sulphate (iron alum) solution for 10 minutes. This step sensitized the tissue for silver impregnation. Rinsed thoroughly in distilled water. Prepared fresh ammoniacal silver solution (always follow lab safety protocols for handling silver solutions). Immersed slides in the silver solution for 1-2 minutes, monitoring under a microscope to avoid overstaining. Rinsed briefly in distilled water. Placed sections in 10% formalin solution for 5-10 minutes to reduce the silver ions and visualized the reticulin fibres as black structures. Rinsed in distilled water. Placed slides in 5% sodium thiosulfate solution for 3-5 minutes to remove any unbound silver and prevent non-specific staining. Rinsed in distilled water. Counterstained with Nuclear Fast Red or Light Green, if desired, to provide contrast. Rinsed in distilled water.

Tissues were dehydrated by dipping the slides rapidly through 100% ethanol and cleared in xylene with agitation for 30 seconds. The slides were then placed in mounting xylene and mounted with DPX mounting media and cover slipped.

4. Periodic Acid Shiff stain

The lung sections were dewaxed in xylene 1 & 2 for 5 minutes each. With agitation, the slides were hydrated through 100% ethanol for 30 seconds and 95% for 30 seconds, washed well in tap water, and rinsed in distilled water. Sections were then oxidized in 0.5–1% periodic acid solution for 5–10 minutes to convert glycol groups into aldehydes. After rinsing in distilled water, the slides were immersed in Schiff's reagent for 10–20 minutes, allowing the aldehydes to react and form a magenta-coloured complex. The slides were then washed in running tap water for 5–10 minutes to fully develop the colour. Haematoxylin, a nuclear counterstain, was applied, followed by bluing in tap water. Finally, the sections were dehydrated through graded alcohols, cleared in xylene, and mounted with a permanent mounting medium. PAS staining highlights glycogen, mucins, and basement membranes in magenta, while nuclei appear blue-purple.

ANNEXURE 3. *Histology Assessment Scoring Card*

Case Number: ……..

	H & E (Inflammation)				MT (Fibrosis)				RETIC (Fibrosis)			
LOBES	**No**	**Mild**	**Moderate**	**Severe**	**No**	**Mild**	**Moderate**	**Severe**	**No**	**Mild**	**Moderate**	**Severe**
UPPER	0	1	2	3	0	1	2	3	0	1	2	3
MIDDLE	0	1	2	3	0	1	2	3	0	1	2	3
LOWER	0	1	2	3	0	1	2	3	0	1	2	3

0: No< 10%>; 1: Mild = 11-30%; 2: Moderate = 31 – 60% and 3: Severe= 60%<

	UPPER LOBE	**MIDDLE LOBE**	**LOWER LOBE**
Pneumonia			
TB			
Silicosis			
Asbestos bodies			
Smokers macrophages			
Tumour			
Poorly preserved			

ADDITIONAL COMMENTS

Key: Where fibrosis/inflammation occurred in one lobe, it was described as focal. Where fibrosis/inflammation occurred in more than one lobe, it was described as diffuse.

ANNEXURE 4. Ethics Clearance Certificate (M210401)

UNIVERSITY OF THE WITWATERSRAND, JOHANNESBURG

R49 Ms JQ Mthombeni

HUMAN RESEARCH ETHICS COMMITTEE (MEDICAL)
CLEARANCE CERTIFICATE NO. M210401

NAME: **(Principal Investigator)**	Ms JQ Mthombeni
DEPARTMENT:	School of Public Health Medical School University
PROJECT TITLE:	*Quantification and mapping of manganese deposition and associated histopathological correlates in the lungs of deceased South African miners*
DATE CONSIDERED:	2021/04/30
DECISION:	Approved unconditionally
CONDITIONS:	
NOTE:	If contact information regarding student study participants is required, please contact the Registrar's office - <Nicoleen.Potgieter@wits.ac.za>
SUPERVISOR:	Professors G Nelson and B Racette; Dr N Vorajee
APPROVED BY:	Dr CB Penny, Chairperson, HREC (Medical)
DATE OF APPROVAL:	2021/09/16

This Clearance Certificate is valid for 5 years from the date of approval. An extension may be applied for.

DECLARATION OF INVESTIGATORS

To be completed in duplicate and **ONE COPY** returned to the Research Office secretariat on the 3rd floor, Phillip Tobias Building, Parktown, University of the Witwatersrand, Johannesburg.

I/we fully understand the conditions under which I am/we are authorized to carry out the above-mentioned research and I/we undertake to ensure compliance with these conditions. Should any departure be contemplated from the research protocol as approved, I/we undertake to submit details to the Committee. **I agree to submit a yearly progress report**. When a funder requires annual re-certification, the application date will be one year after the date when the study was initially reviewed. In this case, the study was initially reviewed in **April** and therefore reports and re-certification will be due in the month of **April** each year. Unreported changes to the study may invalidate the clearance given by the HREC (Medical).

Signature of Principal Investigator _____ Date _____

ANNEXURE 5. *NIOH Permission Letter*

NATIONAL INSTITUTE FOR OCCUPATIONAL HEALTH
Division of the National Health Laboratory Service

Pathology Division
25 Hospital Street, Constitution Hill, Johannesburg, 2000
Tel: +27 (0)11 712 6409 Fax: +27 (0)11 712 6450

9 December 2020

To whom it may concern

This letter serves to confirm that Ms Julian Mthombeni will be conducting research towards her pHD using materials and data in the Pathology Section NIOH. As head of the section, I grant her permission to conduct research on the hearts and lungs of deceased miners whose autopsy material is in our department, and I grant her permission to access the PathAut database for the purpose of her study, until such time as her PhD is completed.

Kind Regards,
Anita Gildenhuys
Head of Pathology Division
Histopathologist
National Institute of Occupational Health
Tel: 011 712 6409
AnitaG@nioh.ac.za | www.nioh.ac.za

NATIONAL INSTITUTE FOR OCCUPATIONAL HEALTH
Division of the National Health Laboratory Service

Practice number 5200296

ANNEXURE 6. *MBOD Permission Letter*

health

Department:
Health
REPUBLIC OF SOUTH AFRICA

16 August 2021

To whom it may concern

Re: Julian Mthombeni, student no. 678721

This letter serves to confirm that as part Ms Mthombeni's research towards her PhD, Medical Bureau for Occupational Diseases (MBOD) will give her controlled access tomedical records of deceased mineworkers. This will be provided through my office.

Kind Regards

Dr Nonhlanhla MtshaliDirector: MBOD

National Department of HealthCell: 0828524210

ANNEXURE 7. *Neuropathology study data: Permission letter*

UNIVERSITY OF THE WITWATERSRAND, JOHANNESBURG

Faculty of Health Sciences, 27 St Andrew's Road, Parktown 2193; Johannesburg; South Africa T +27 (0) 11 717 2543 www.wits.ac.za/publichealth

WITS School of Public Health

HUMAN RESEARCH ETHICS COMMITTEE UNIVERSITY OF THE WITWATERSRAND

Dear Committee members

7 April 2021

PERMISSION TO USE DATA – JULIAN MTHOMBENI (STUDENT NUMBER: 678721)

This is to confirm that Julian Mthombeni may use data collected for the *Neuropathology of Chronic Manganese Exposure* study (clearance certificate no. M081157) for her PhD. The principal investigators of the study, Gill Nelson and Brad Racette, are supervising the PhD.

Yours sincerely

Prof. Gill Nelson School of Public Health

gill.nelson@wits.ac.za

ANNEXURE 8. *Autopsy Consent Form*

NATIONAL INSTITUTE FOR OCCUPATIONAL HEALTH

25 Hospital Street, Constitution Hill, Johannesburg
PO Box 4788 Johannesburg 2000, South Africa
Tel: (011) 712 6400 • Fax: (011) 712 6450
Autopsy enquiries
(011) 712 6444 • (011) 712 6434 • (011) 7126465

CONSENT FOR A POST-MORTEM EXAMINATION

I _____

The *spouse/major child/ parent/ guardian/ major brother/ major sister/

(* Delete whichever is not applicable)

Of the late (name) _____

Age_____ **Sex**_____

Hereby consent to a post-mortem examination and the removal of such tissues as may be considered necessary for the purpose of the requirements of the Occupational Diseases in the Mines and Works Act (No.78 of 1973)* and for diagnostic, medical education, research and scientific purposes

Signature _____

Witness _____

Witness 2 _____

Place _____

Date _____ **Time** _____

NATIONAL HEALTH LABORATORY SERVICE
NATIONAL INSTITUTE FOR OCCUPATIONAL HEALTH

INFORMATION LEAFLET AND INFORMED CONSENT
for the next-of-kin of manganese miners

STUDY NUMBER: 08-1210

STUDY TITLE: Neuropathology of Chronic Manganese Exposure

SPONSORS: National Institute of Environmental Health Sciences, USA; Washington University, USA

INVESTIGATORS: Prof Gill Nelson, University of the Witwatersrand, South Africa
Prof Brad Racette, Washington University, USA
Prof Jill Murray, University of the Witwatersrand, South Africa

TELEPHONE NUMBER(S): Prof Gill Nelson 011 717 2138 / 082 338 9576

Good morning/afternoon. My name is _____(study nurse) and I am going to explain the purpose of this research and the procedures involved.

You are invited to consider providing permission for your relative[1] to participate in this research study. Participation is entirely voluntary.

1. Before providing permission, it is important that you read and understand the following explanation of the purpose of the study, the study procedures, and your right to refuse permission at any time. This information leaflet is to help you to decide if you would like to give permission. You should fully understand what is involved before you agree to take part in this study.
2. If you have any questions, do not hesitate to ask me.
3. You should not give permission unless you are satisfied about the procedures involved.
4. If you decide to give permission, you will be asked to sign this document to confirm that you understand the study. You will be given a copy to keep.

--- **To the next-of-kin**: *This consent form may contain words that you do not understand. Please ask the study doctor or the study nurse to explain any words or information that you do not clearly understand. You may take home* ***an unsigned copy of this consent*** *form to think about or discuss with family or friends* ***before making your decision.***

[1] **In this document, 'relative' may be father, son, brother, mother, daughter, sister, husband, wife**

PURPOSE OF THE STUDY:

- You have been contacted about this study because your relative was a manganese miner.
- The purpose of this study is to determine if there are any effects of long term, low dose manganese on the brain.

OCCUPATIONAL DISEASES IN MINES AND WORKS ACT:

According to the laws of South Africa (specified in the Occupational Diseases in Mines and Works Act of 1973), anyone who has been exposed to risk work while working on the mines or classified works has the right to have his or her lungs and heart examined after death, to determine the presence of compensable lung disease. It does not matter what the cause of death is.

The attached information leaflets provide more information about this autopsy service.

PARKINSON DISEASE

Parkinson Disease in a neurological condition, the cause of which remains unknown. Exposure to metals such as manganese may increase the risk of Parkinson's disease, but more research needs to be done to confirm this link. Understanding this relationship may bring us closer to a cure for Parkinson's disease and may make workplaces safer. An examination of brain tissue of people exposed to manganese is an extremely important way to help us learn more about the health effects of metals. If you consent to the removal and examination of your relative's brain after death, in addition to the hearts and lungs, you will be contributing to the understanding of Parkinson Disease. However, you will receive no compensation payment based on the outcome of the examination of the brain. This will be solely for the purposes of research, education, and the advancement of medical science.

LENGTH OF THE STUDY AND NUMBER OF PARTICIPANTS:

- The study will be performed only in South Africa.
- Approximately 80 participants will participate in this study (40 manganese miners and 40 non-manganese miners)
- The participants will be aged from 20 to 90 years old.

PROCEDURES:

- If you give permission, the heart, lungs and brain will be removed and sent to the National Institute for Occupational Health in Johannesburg. The brain will be sent to Washington University in America. Medical records from the occupational health clinic and records about the jobs done at the mine will be reviewed.
- In addition, a molar (back tooth), 1 cm of armpit hair, some toenail clippings, and a 2 cm piece of the sternum (breastbone) will also be removed to measure exposure to manganese.
- If you do not agree to the removal of the brain, and other tissues, the heart and lungs will still be examined by doctors at the National Institute for Occupational Health.

BENEFITS:

- There is no direct benefit to you if you give permission to have the brain removed.
- Nevertheless, the heart and lungs will be examined by doctors at the National Institute for Occupational Health in Johannesburg for the presence of compensable occupational disease. If any disease is found you MAY receive some financial compensation, depending on the extent of the disease and whether or not your relative was compensated for that disease while alive. You will receive no compensation payment based on the outcome of the examination of the brain.
- If you give permission for the removal of the brain, you will be contributing to the understanding of Parkinson's Disease.
- This will be solely for the purposes of research, education, and the advancement of medical science.

RIGHTS AS NEXT-OF-KIN:

- Participation in this study is entirely voluntary, and you can refuse permission to have the brain removed, without stating any reason.
- If you refuse permission, it will not prevent you from receiving compensation for any occupational lung disease.

FINANCIAL ARRANGEMENTS:

- The State will pay for the removal of the heart and lungs and related costs.
- The National Institute of Environmental Health Sciences and Washington University in the USA will pay for the removal of the brain and related costs.
- Neither you nor your family will be expected to pay for anything related to this study.

ETHICAL APPROVAL:

- This study protocol has been submitted to the University of the Witwatersrand, **Human Research Ethics Committee (HREC)** and written approval has been granted by that committee.
- This study is sponsored by the National Institute of Environmental Health Sciences and Washington University, USA.
  I do not have any financial or personal interests with this organisation that may bias my actions.

SOURCE OF ADDITIONAL INFORMATION:

Other doctors who are working on this study are:

- Dr Johan Mostert Tel. (053) 741 1420
- If you want any information regarding your **rights as a research participant, or have any complaints regarding this research study**, you may contact Prof Cleaton-Jones, Chairperson of the University of the Witwatersrand, Human Research Ethics Committee (HREC), which is an independent committee established to help protect the rights of research participants at (011) 717 2301.

CONFIDENTIALITY:

- All information, including hospital records, personal data and research data will be kept strictly confidential. Data that may be reported in scientific journals will not include any information that identifies your relative as a participant in this study.
- Any information uncovered regarding your relative's state of health as a result of participation in this study will be held in strict confidence.

INFORMED CONSENT

- I hereby confirm that I have been informed by the study doctor/nurse, about the nature, conduct, benefits and risks of study protocol no. 08-1210: The neuropathology of chronic manganese exposure.
- I have also received, read and understood the above written information (Participant Information Leaflet and Informed Consent) regarding the clinical study.
- I am aware that the results of the study, including personal details regarding my relative's sex, age, date of birth, initials and diagnosis will be anonymously processed into a study report.
- In view of the requirements of research, I agree that the data collected during this study can be processed in a computerised system by the National Institute for Environmental Sciences, Washington University, or on their behalf.
- I have had sufficient opportunity to ask questions and (of my own free will) consent to a post-mortem examination and the removal of such tissues (including the brain) as may be considered necessary for the purpose of the requirements of the Occupational Diseases in Mines and Works Act (No. 78 of 1973) and for diagnostic, medical education, research and scientific purposes.

NAME OF STUDY PATIENT:

_____

NEXT-OF-KIN:

Printed Name **Signature / Mark or Thumbprint** **Date and Time**

I, _____, herewith confirm that the above next-of-kin has been fully informed about the nature, conduct and potential benefits of the above study.

STUDY DOCTOR/NURSE:

Printed Name **Signature** **Date and Time**

TRANSLATOR / OTHER PERSON EXPLAINING INFORMEDCONSENT …….. (DESIGNATION):

Printed Name **Signature** **Date and Time**

WITNESS (If applicable):

Printed Name **Signature** **Date and Time**

VERBAL PARTICIPANT INFORMED CONSENT:

(Applicable when participants cannot read or write or are incapable of giving consent)

- I, the undersigned, _____, have read and have explained fully to the next-of-kin, named _____ , the participant information leaflet.
- The account I have given has explained both the potential benefits of the study. The next-of-kin understands these.

I hereby certify that, the next-of-kin has provided permission for his/her relative to participate in this study.

NEXT-OF-KIN:

Printed Name	**Mark or Thumbprint (if applicable)**	**Date and Time**

STUDY DOCTOR/NURSE:

Printed Name	**Signature**	**Date and Time**

TRANSLATOR / OTHER PERSON EXPLAINING INFORMED CONSENT: ……**(DESIGNATION)**

Printed Name	**Signature**	**Date and Time**

LEGALREPRESENTATIVE/FRIEND: ……**(RELATIONSHIP)**

Printed Name	**Signature / Mark or Thumbprint**	**Date and Time**

WITNESS:

Printed Name	**Signature**	**Date and Time**

NEUROPATHOLOGY OF CHRONIC MANGANESE EXPOSURE (MINERS STUDY)

FAMILY QUESTIONNAIRE

Part icipant no:

Date of birth: Place of Birth:

nearest tawn

Date of death: Place of death _____

Home, address, mine, name of hospital

Cause of death: _____

as far as is known

Known illnesses:

Any neurological symptoms of which the family was aware?

e.g. tremors, etc.

Place(s) where he grew up:

nearest town

Highest level of Education:

Age at which he first started working: _____ years

Job history

Year started	Year ended	Industry	Details	Name of company	Job

Information provided by:

mother, sister, uncle, etc.

Contact no: 1. 2.

MINERS STUDY: FAMILY QUESTIONNAIRE

Smoking

Participant no:

1. Was the deceased a **smoker** when he died?
2. Know

If yes

What did he smoke? Commercial cigarettes Yes

Hand rolled cigarettes Yes

Pipe Yes No

Other, specify_____

At what age did he start smoking? _____

How many (cigarettes/ pipes) did he smoke per day, on average?_____ _

Yes No Don't know

3. Was the deceased an **ex-smoker** when he died? Yes No Don't know

MINERS STUDY: FAMILY QUESTIONNAIRE

Alcohol

Participant no:

1. **In the past,** did the deceased ever drink alcohol regularly (3 or more drinks per week)?

Yes No

If yes

_____Years old

Did he regularly drink alcohol prior to his death (3 or more drinks per week)

Miners Study- Family Interview - Demo/Medical/Work History (12 Nov 2018)

MINERS STUDY: HAIR SAMPLE DATA COLLECTION

Participant Number:_____

Date: *Day Month Year (e.g. FEB)*

You will need:

- Nitrile Gloves
- Alcohol wipes
- Titanium-coated or ceramic scissors
- Sharpie permanent marker
- Ziploc bag

Instructions:

- Using a permanent marker (sharpie pen), label the Ziploc bag as "HAIR" and include the Participant Number and Date on the bag.
- Prior to cutting hair, clean titanium-coated/ceramic scissors with an alcohol wipe, and wipe again between each use.
- Wearing nitrile gloves, the worker should collect hair from the occipital region of the head (back of the head) using the titanium-coated or ceramic scissors. For participants with shorter hair, you may have to cut closer to the top or side.
- The hair should be cut as close to the proximal end of the hair (the scalp) as possible, ensuring hair is over a centimetre in length prior to cutting.
- Deposit the cut hair into the labelled Ziploc bag.
- If participant is bald, collect hair sample from other source (e.g. beard, under arm).

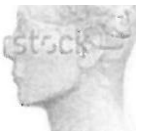

Occipital region

Please document the collection below:

Hair sample was collected **If No, why not?** **Participant is bald and has no other source of hair**

Not Collected

Other reason: _

_

Location of hair collection

Length of hair collected

(please tick appropriate box)

(please tick appropriate box}

Occipital lobe (Upper back of the neck)

Very short (less than 2 cm)

In the space below, please document any problems you encountered during sample collection:

Sample collected by: ____________________

(Name - Printed)

MINERS STUDY: NAIL SAMPLE DATA COLLECTION

Date:

Participant Number:

Day *Month* *Year*

(e.g. FEB)

You will need:

- A permanent marker (Sharpie Pen)
- Two small Ziploc bags
- Clean t itanium- coated na il clippers
- Alcohol wipe

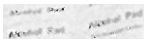

INSTRUCTIONS:

- Using a permanent marker (sharpie pen), label one Ziploc bag as **"BIG TOENAILS"** and one Ziploc bag as **"LITTLE TOENAILS,"** also incl ude the **Subject ID#** and **Date** on each of the bags.

7

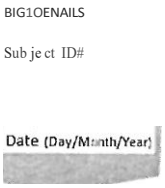

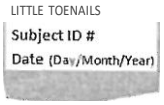

Using the clean, titanium-coated nail clippers...

- Cut a nail sample from each of the subject's big toenails letting the clippings fall into the Ziploc bag labelled **"BIG TOENAILS."**
- Cut nail samples from each of the subject's other eight toenails letting the clippings fall into the Ziploc bag labelled **"LITTLETOENAILS."**
- Clean the used nail clippers after each use with an alcohol wipe.

Please document the collection below:

Nail samples were collected **If No, why not?** **Nails are too short**

Not collected **Other reason:** ____

Nail Polish?

Yes, clipped nails have POLISH on them

NO, Clipped nails DO NOT have polish on them

In the space below, please document any problems you encountered during sample collection:

Sample collected by: _____

(Name- Printed)

NEUROPATHOLOGY OF CHRONIC MANGANESE EXPOSURE (MINERS STUDY)

AUTOPSY DETAILS

1. Participant number:

2. Date of death (dd/mm/yyyy):

3. Date of autopsy (dd/mm/yyyy):

4. Time of autopsy:

5. Place of autopsy:

6. Name of person performing autopsy,

@signature of person performing autopsy,

Name of person assisting with autopsy:

8. Signature of person assisting with autopsy:_____

9. Length of body: cm

10. Waist circumference (at umbilicus): _ _ _ cm

11. Build of body: small medium large

12. Organs removed: Heart Lungs Brain

Specimens collected: Nails Molar Bone Hair

13. Red Bucket numbers: Brain: Heart/lungs:

14. Formalin change:
Date (dd/mm/yyyy): _____

15. Shipment to NIOH:
Date (dd/mm/yyyy): _____

☐☐ h ☐☐

MINERS STUDY - autopsy details (9 Nov 2018)

Time: ☐☐ h ☐☐

NEUROPATHOLOGY OF CHRONIC MANGANESE EXPOSURE (MINERS STUDY)

Company Information/ Medical History

Participant Number:

Date of Birth: Sex:
Male Female _____ Education (highest number grade completed): Race:

Height: (39) Waist Circumference: (39)

Medical History:

Medications (most recent - what and when?)

Name:	Illness:

Chronic Illnesses/Diseases (List all illnesses/ diseases and the year diagnosed)

Name of Disease:	Year Diagnosed:

Operations: what and when?)

Name:	Body Part Operated on:	Year of Operation:

ANNEXURE 10. *Demographic and medical characteristics of manganese-exposed mineworkers.*

CASE NUMBER	AGE AT DEATH (YEARS)	YEAR OF DEATH	EMPLOYMENT IN MN MINING (YEARS)	CLINICAL CAUSE OF DEATH	AUTOPSY FINDINGS
1	52	2010	17.7	Natural causes	Bronchopneumonia
2	62	2014	31.7	Natural causes	Slight asbestosis
3	59	2010	10	Hyperglycaemia	Tuberculosis is absent
4	57	2010	31.5	Natural causes	Non-Hodgkin lymphoma, slight asbestosis
5	54	2011	23.2	Natural causes, diabetes	Severe atherosclerotic heart disease
6	48	2012	31.2	Natural causes	Hodgkins lymphoma, nocardia pneumonia, Cytomegalovirus pneumonia
7	58	2016	31.3	Natural causes	Moderate tuberculosis, bronchopneumonia, slight asbestosis
8	71	2010	12.5	Natural causes	Moderate asbestosis and plague, moderate emphysema
9	40	2010	13.8	Natural, varicella	Intra-alveolar oedema
10	54	2013	27.7	Unnatural, wound right temporal area with possible depressed fracture	Bronchopneumonia
11	64	2018	31	Natural causes	Pulmonary oedema
12	57	2012	33	Natural causes	Severe mixed dust fibrosis, moderate emphysema, pulmonary infarction
13	61	2012	39.7	Natural, Cancer of the oral cavity	Focal cryptococcal pneumonia
14	33	2017	4.4	Natural causes	Pneumonia
15	55	2012	19.6	Natural causes	Pneumocystis pneumonia
16	39	2012	7	Natural causes	Suppurative pneumonia, PTB not present

ANNEXURE 11. *Demographic and medical data of manganese-unexposed mineworkers*

CASE NUMBER	AGE AT DEATH	YEAR OF DEATH	YEARS IN PT	CLINICAL CAUSE OF DEATH	AUTOPSY FINDINGS
1	53	2014	3.8	Natural causes	Shock lung
2	55	2014	26.7	Natural causes	Pulmonary tuberculosis was not present
3	45	2016	22.9	Natural causes	Bronchopneumonia
4	39	2016	10.7	Natural causes	Pulmonary tuberculosis was not present
5	49	2016	16.8	Unnatural causes	Pulmonary tuberculosis was not present
6	45	2016	17.4	Unnatural causes	Pulmonary tuberculosis was not present
7	52	2016	14.8	Natural causes	Pulmonary tuberculosis was not present
8	58	2016	32.1	Natural, Cerebral vascular accident. Chronic illness	Fungal bronchopneumonia
9	53	2016	26.1	Natural, Bowel obstruction septicaemia	Pulmonary tuberculosis was not present
10	46	2016	25.4	Unnatural, Carbon monoxide poisoning	Pulmonary oedema
11	51	2016	30.5	Natural, Myocardial infarction	Pulmonary tuberculosis was not present
12	46	2016	23.2	Natural	Pulmonary tuberculosis was not present
13	59	2016	17.5	Not stated (under investigation)	Bronchopneumonia
14	56	2016	7.8	Natural causes	Bronchopneumonia
15	61	2016	19	Unnatural causes	Pulmonary tuberculosis was not present
16	53	2016	21.7	Natural causes	Bronchopneumonia
17	58	2016	24.5	Unnatural causes	Pulmonary tuberculosis was not present
18	52	2016	26.9	Natural, Cirrhosis upper gastrointestinal bleed	Pulmonary tuberculosis was not present

19	56	2016	30.7	Unnatural, Blunt force, multiple injuries	Pulmonary Haemorrhage
20	52	2016	6.2	Natural causes	Pulmonary Tuberculosis was not present
21	58	2016	24.3	Natural causes	Aspiration pneumonia, Bronchopneumonia
22	61	2016	29.2	Natural, Myocardial infarction	Bronchopneumonia, severe coronary artery atheroma and ischaemic fibrosis
23	52	2017	32.3	Natural causes	Pulmonary Tuberculosis was not present
24	45	2017	9.1	Natural causes	Aspiration pneumonia
25	52	2017	21.7	Natural causes	Pulmonary Tuberculosis was not present
26	49	2017	22	Unnatural causes	Pulmonary oedema
27	47	2017	16.6	Natural causes	Suppurative pneumonia
28	52	2017	25.9	Natural causes	Pulmonary Tuberculosis was not present
29	58	2017	21	Natural causes	Tuberculosis is absent
30	51	2018	24.5	Natural causes	Pulmonary Tuberculosis was not present
31	52	2018	16	Natural causes	Bronchopneumonia
32	48	2018	17.8	Unnatural causes	Pulmonary Tuberculosis was not present
33	68	2018	13	Natural causes	Lobar pneumonia suppurative pneumonia
34	48	2018	13.9	Natural, Acute myocardial infarction, Renal failure, HIV	Pulmonary Tuberculosis was not present
35	60	2018	14.8	Natural, Lower respiratory infection, Chronic obstructive lung diseases, Hyperglycaemia	Lobar pneumonia
36	59	2018	31.8	Natural, Cerebral accident, Septicaemia, Retroviral Disease	Pulmonary Tuberculosis was not present. Severe coronary atheroma
37	61	2019	10.9	Natural, Chronic obstructive pulmonary disease	Moderate emphysema, coronary artery disease

38	61	2019	29	Natural causes	Pulmonary Tuberculosis was not present
39	61	2019	8.9	Unnatural causes	Pulmonary Tuberculosis was not present
40	57	2020	17.9	Natural causes	Pulmonary Tuberculosis was not present
41	56	2020	26	Natural causes	Pulmonary Tuberculosis was not present
42	58	2020	39.9	Natural, Acute myocardial infarction	Coronary artery disease
43	60	2020	35.3	Natural, Hepatocellular carcinoma, multi-organ failure	Bronchopneumonia, pulmonary oedema
44	53	2020	27.8	Natural, Multi-organ failure	Bronchopneumonia, Pulmonary oedema
45	57	2018	25.5	Natural causes	Pulmonary Tuberculosis was not present
46	48	2020	21.2	Unnatural causes-blunt force injury to chest as a result of mining accident	Pulmonary Tuberculosis not present
47	45	2020	10	Natural, Acute heart failure, coronary artery atherosclerosis, hypertension	Coronary and hypertensive heart disease
48	35	2020	12.2	Natural, HIV disease, cryptococcal pneumonitis	Cryptococcal pneumonitis

ANNEXURE 12. *Turnitin Report.*

I have reviewed the report and am satisfied with the similarity index
Prof. Gill Nelson

QUANTIFICATION AND MAPPING OF MANGANESE DEPOSITION AND ASSOCIATED HISTOPATHOLOGICAL CORRELATES IN THE LUNGS OF DECEASED MINEWORKERS IN SOUTH AFRICA

ORIGINALITY REPORT

16%	12%	13%	4%
SIMILARITY INDEX	INTERNET SOURCES	PUBLICATIONS	STUDENT PAPERS

PRIMARY SOURCES

1	www.igw.uni-jena.de Internet Source	1%
2	wiredspace.wits.ac.za Internet Source	<1%
3	www.uspaquatic.library.usp.ac.fj Internet Source	<1%
4	epawebapp.epa.ie Internet Source	<1%
5	www.epa.gov Internet Source	<1%
6	speciation.net Internet Source	<1%
7	www.science.gov Internet Source	<1%
8	link.springer.com Internet Source	<1%